## Unraveling the role of Mxr2 in regulating CVT pathway and nonselective macroautophagy pathway in Saccharomyces cerevisiae

Thesis submitted for the degree of

DOCTPR OF PHILOSOPHY

BY

**ARPAN CHATTERJEE** 

(17LBPH09)



Department of Biochemistry School of Life Sciences University of Hyderabad Hyderabad -500046, India



#### **Department of Biochemistry**

School of Life Sciences, University of Hyderabad,

Hyderabad-500046, Telangana, India

#### **DECLARATION**

I, Arpan Chatterjee, hereby declare that the work presented in this thesis entitled 'Unraveling the role of Mxr2 in regulating CVT pathway and nonselective macro-autophagy pathway in Saccharomyces cerevisiae' is entirely original and was carried out by me in the Department of Biochemistry, University of Hyderabad, under the guidance and supervision of Prof. Naresh babu V. Sepuri. I further declare that this work has not been submitted earlier in part or full for the award of degree or diploma from any other university or institution.

S. V. Daeur Prof. Naresh Babu V. Sepuri

NARESH BOSEPURI, Ph.D Dept. of Biochemistry School of Life Science

University of Hyderabad Date: Hyddrospy-500-046. T.S.

Place: Department of Biochemistry,

University of Hyderabad

Alpan Chatterice.
Arpan Chatteriee 10/09/2024

Student



#### **Department of Biochemistry**

School of Life Sciences,

University of Hyderabad,

Hyderabad-500046, Telangana, India

#### **CERTIFICATE**

This is to certify that, this thesis entitled 'Unraveling the role of Mxr2 in regulating CVT pathway and nonselective macro-autophagy pathway in Saccharomyces cerevisiae' submitted to the University of Hyderabad by Mr. Arpan Chatterjee, bearing the Reg No. 17LBPH09 for the degree of Doctor of Philosophy in Biochemistry, is based on the studies carried out by him under my supervision. To the best of my knowledge, this work has not been submitted earlier for the award of degree or diploma from any other university or institution.

S√. Nouw | — Prof. Naresh Babu V. Sepuri

Supervisor

Professor
Dept. of Biochemistry
School of Life Science
University of Hyderabad
Hyderabad-500 046. T.S.

Dean

**School of Life Sciences** 

Department of Biochemistry

S.v. Souin

अध्यक्ष / Head जीवरसायनविभाग / Department of Biochemistry जीवविज्ञान रांकाय / School of Life Sciences हैदराबाद विश्वविद्यालय / University of Hyderabad हैदराबाद / Hyderabad-500046. INDIA

जीव विज्ञान संकाय / School of Life Sciences हैदराबाद विश्वविद्यालय / University of Hyderabad हैदराबाद / Hyderabad-500 046.



## Department of Biochemistry School of Life Sciences,

University of Hyderabad,

Hyderabad-500046, Telangana, India

#### CERTIFICATE

This is to certify that the thesis entitled "Unraveling the role of Mxr2 in regulating CVT pathway and nonselective macro-autophagy pathway in Saccharomyces cerevisiae" submitted by Mr. Arpan Chatterjee, bearing the Reg No. 17LBPH09, in partial fulfillment of the requirements for the Doctor of Philosophy in Biochemistry, is genuine work done by him under my supervision.

This thesis is free from plagiarism and has not previously been submitted in part or whole for the award of degree or diploma from this or any other University or Institution. Furthermore, prior to submitting the thesis/monograph for adjunction, the student had the following publication(s) and proof for it in the form of reprints in the relevant field of this study.

Arpan Chatterjee, Naresh Babu V. Sepuri. Methionine sulfoxide reductase 2 regulates Cvt autophagic pathway by altering the stability of Atg19 and Ape1 in Saccharomyces cerevisiae. Journal of Biological Chemistry, 2024.

The student has attended following conferences during his Ph.D. program:

- 1. Presented a poster entitled "Methionine sulfoxide reductase 2 regulates Cvt autophagic pathway by altering the stability of Atg19 and Ape1 in Saccharomyces cerevisiae" in Cell Symposia: Multifaceted Mitochondria 2022 on 6<sup>th</sup>-8<sup>th</sup> November 2022, held in Seville, Spain.
- 2. Presented a poster entitled "Methionine sulfoxide reductase 2 regulates Cvt autophagic pathway by altering the stability of Atg19 and Ape1 in Saccharomyces cerevisiae" in the

International Conference on Virus Evolution, Infection and Disease Control on 15th-17th December 2022 organized by University of Hyderabad.

- 3. Presented a poster entitled "Methionine sulfoxide reductase 2 regulates Cvt autophagic pathway by altering the stability of Atg19 and Ape1 in Saccharomyces cerevisiae" in 42nd Mahabaleshwar Seminars: Mitochondria Network Meeting on 13th-15th February, organized by Indian Institutes of Science Education and Research, Pune.
- 4. Participated in the XI International Conference on Biology of Yeasts and Filamentous Fungi held on 27th -29th November 2019, organized by the University of Hyderabad and Centre for DNA Fingerprinting and Diagnostics, Hyderabad.

Further, the student has passed the following courses towards fulfilment of coursework requirement for Ph.D.

Course code	Name	Credits	Pass/fail
BC 801	Research methodology/Analytical techniques	4	Pass
BC 802	Research Ethics, Biosafety, Data Analysis and Biostatistics	4	Pass
BC 803	Scientific Writing and Research Proposal	4	Pass

Supervisor

NARESH B SEPURI, Ph.D. Professor

Dept. of Biochemistry School of Life Science University of Hyderabad Hyderabad-500 046. T.S. S.V. Now

10/09/24

जीव विSchool of Cheel of Life Sciences

**Department of Biochemistry** 

राबाद विश्वविद्यालय / Uni हैदराबाद / Hyderabad-500

अध्यक्ष / Head जीवरसायनविभाग / Department of Biochemistry जीवविज्ञान रांकाय / School of Life Sciences हैदराबाद विश्वविद्यालय / University of Hyderabad हैदराबाद / Hyderabad-500046. INDIA

#### **ACKNOWLEDGEMENTS**

First and foremost, I would like to express my sincere gratitude to my supervisor **Prof. Naresh Babu V. Sepuri**. You are the best Ph.D. guide anyone can ask for and I am a true and big fan of yours, sir. Your knowledge, enthusiasm and passion for science and ability to think out of the box fascinate me and helped me grow every day to be a better researcher. I will be forever grateful for your guidance and patience. Thank you so much sir for trusting me and giving so much freedom to think and work. You have been a constant source of motivation and inspiration during this Ph.D. tenure and will be in my entire lifetime. Whenever I found a dead end in some experiments with misleading and confusing results, you always found some valuable information in those and opened up a new direction (but very rarely you also said 'I don't know'). Thank you so much sir for being available and helping me whenever I was in some crisis, whether it was personal or professional. Your ideals and morals and your way of taking both success and failure on a lighter note will always motivate me to be a better version of me every day.

I would like to thank my doctoral committee member **Prof. K.V.A. Ramaiah** and **Prof. Krishnaveni Mishra** for their invaluable suggestions and encouragement. I would like to thank specially Krishnaveni ma'am for being so generous in providing various plasmids and strains that were extremely helpful for my work.

I feel very lucky to share my time in the lab with some great scientific minds and lovely people. Thank you so much **Amita di** and **Arun Bhaiya**, for being there in my initial days to help and guide me. I have learned mostly all scientific techniques from you. Moreover, I also learned how to plan and execute experiments and how to think about different scientific topics from you people only. You people are some of the best scientific brains, I have come across. Thank you for all your care and affection. Thank you so much, **Vandana** and **Priyanka**, for being so nice and lovely friends and lab mates. Thank you for helping me in every possible way whether it is lab work or admin work. Thank you Vandana for showing up and helping with formalities for the fellowship upgrade. Your calls to e-gov people to revoke my room rent were very helpful. Thank you, Priyanka, for all your help, whether it is filling out my fellowship continuation forms or taking care of my CSIR documents. My fellowship activation would have been impossible without your help. **Niroj**, my workbench neighbour, thank you for all your help, respect, and support. Legpulling of pushpa with you was blissful. **Pushpa**, thank

you for all your help and support in yeast work. After Amita di, you helped me a lot in yeast works, whether it was preparing YNB media powders or sorting out things for yeast work. Your help was important for my work. Ankur, thank you for always being there to help me whether in the lab or outside the lab, talking to you in the lab was an absolute stress-buster. Lahari, thank you so much for your help and support at the end to finish off my work. Without your help, it would have been impossible to finish the work timely. Dheeraj, thank you for all your help, respect and care. Laughing on memes and sharing them with you was instrumental in decompressing the pressure situations. Nanditha, Dahlia, Shivani, Vaani and Manusha, thank you for being such supportive labmates and for providing an amazing working environment. Thank you Narsimha sir and Venkat sir for making our lab life easy. I would also like to thank my seniors Ramana sir, Yerranna sir, Srinivas sir, Fareed sir, Aritra da, Usha madam, Noble sir and Prasad bhaiya for their help and guidance during my initial days.

I would like to thank all my friends here at this university, **Supriya**, **Saumashish**, **my brother Ayon**, **Abhishek** and **Prodosh da**. I don't feel my existence without you people and friendship with you people is one of the best things that happened in my life. I am blessed to have such nice friends and human beings around me. I would like to thank Supriya and Saumashish, they are like brothers from different mothers. Thank you for being there with me every time, listening to me and supporting me when I was at my lowest point. Thank you for supporting and caring for me always unconditionally. Special thanks to Supriya for helping me in qPCR work and analysis to finish my work. Thank you, Ayon (Dada) for always being there right beside me for the help and support in each possible way. I am always grateful for your love and care and am blessed to have you as my brother.

I would like to thank **Sriparna** for being there with me with all her unwavering love, care and support. Thank you for believing in me, when I doubted myself. When I was at my lowest, you absorbed all the negativity from me and showered immense positivity and hope, which kept me motivated and sane so that I could finish this Ph.D. journey. I feel blessed and super lucky to have you in my life.

I would like to express my deepest gratitude to my parents, **Krishna Chatterjee (Maa)** and **Arup Chatterjee (Baba)** for being the backbone throughout my entire journey. You trusted, supported and showered your blessings on me every single day, unconditionally. Thank you for being so understanding and patient throughout this time and keeping all my desires and wishes

above yours, so that I can achieve my dreams. Nothing would have been possible without your selfless and unconditional love.

I want to acknowledge **S. B. Chary** and all the **non-teaching staff** of the Department of Biochemistry and School of Life Sciences for their help.

I want to thank CSIR for my financial support through JRF and SRF.

Finally, I thank almighty God for her blessing throughout.

ARPAN CHATTERJEE

#### **TABLE OF CONTENTS**

#### **Chapter 1: Introduction**

1.1. M	fitochondria	2
1.2. R	eactive Oxygen Species, Oxidative Stress and damage to biomolecules	3
1.3. A	nti-oxidant defence mechanism	5
1.3.1.	Superoxide Dismutases	5
1.3.2.	Catalases	5
1.3.3.	Peroxidases	5
1.3.4.	Thioredoxin System.	5
1.3.5.	Glutaredoxin System	6
1.4. M	Methionine oxidation and Role of Methionine Sulfoxide Reductases	6
1.5. A	utophagy	7
1.6. C	ytoplasm to Vacuole (Cvt) pathway	8
1.7. N	Ion-selective Macroautophagy	9
1.7.1.	Autophagy induction and phagophore nucleation	9
1.7.2.	Expansion of phagophore	11
1.7.3.	Docking and fusion of the matured autophagosome with vacuole	12
1.7.4.	Vesicle Breakdown and Recycling of the Resulting Macromolecules	12
1.8.	Mitophagy	12
1.9.	Transcriptional control of Non-selective Macroautophagy	13
1.10.	Protein acetylation	14
1.11.	Iron-Sulfur Cluster Biogenesis	16
1.12.	Retrograde Signaling	17
1.13.	Rationale and Objective	18
Chapt Ape1	ter 2: Mxr2 regulates Cvt autophagic pathway by altering the stability of	`Atg19 and
2.1. B	ACKGROUND	24
2.2. M	MATERIALS AND METHODS	21
2.2.1.	Yeast strains and plasmids	21
2.2.2.	Media and Growth conditions	26
2.2.3.	Whole cell lysate preparation and Immunoblotting	27
2.2.4.	Coimmunoprecipitation	28

2.2.5. Cycloheximide Chase Assay.	28
2.2.6. RNA extraction, cDNA synthesis, and qRT-PCR	28
2.2.7. Leucine aminopeptidase (LAP) Assay	29
2.3. RESULTS	29
2.3.1. Mxr2 interacts with Ape1 and Atg19 of the Cvt pathway	29
2.3.2. Mxr2 protects Ape1 and Atg19 proteins from oxidative stress and pren	nature
degradation	31
2.3.3. Amino acid methionine 17 in Ape1 is required for interaction with Mxr2	34
2.3.4. M17L mutation confers increased stability to Ape1	37
2.3.5. mxr2Δ strain exhibits decreased LAP activity	39
2.3.6. Mxr2 helps in maintaining the stoichiometry of Ape1 and Atg19 in Cvt pathway	40
2.4. CONCLUSION.	43
Chapter 3: Mxr2 controls the bulk autophagy pathway by regulating Atg8 transcrithrough the Mxr2-Mge1-Dep1 axis	ption
3.1. BACKGROUND.	46
3.2. MATERIALS AND METHODS	47
3.2.1. Media and Growth conditions	47
3.2.2. Yeast strains and plasmids	48
3.2.3. Whole cell extract preparation and Western blot Analysis	52
3.2.4. Cycloheximide Chase Assay	52
3.2.5. Mitochondrial Fractionation.	53
3.2.6. RNA extraction and quantitative real-time PCR (qRT-PCR)	53
3.2.7. Coimmunoprecipitation Assay	55
3.2.8. Statistical Analysis.	53
3.3. RESULTS.	54
3.3.1. The <i>mxr2</i> △ strain exhibits a markedly reduced autophagy flux	54
3.3.2. ATG8 gene is transcriptionally downregulated in the <i>mxr2∆</i> strain	56
3.3.3. Stress-induced repositioning of Mxr2 into mitochondria is essential for the progre	ession
of autophagy	59
3.3.4. The <i>mxr2</i> △ strain stabilizes the Ume6 and deacetylase complex proteins	63
3.3.5. Dep1 relays the signal from mitochondria to the Rpd3-Sin3 complex	67
3.3.6. Improved iron sulfur cluster biogenesis rescues the autophagic defect in the n	nxr2∆
strain	70

3.3.7. Mge1 connects iron-sulfur cluster machinery with Rpd3-Sin3	deacetylase complex
required for autophagy progression via Dep1	73
3.4. CONCLUSION	76
Chapter 4: Discussion	
4.1. Discussion for Chapter 2.	79
4.2. Discussion for Chapter 3.	81
4.3. Importance of the study	85
References	87
Publications	111

## **CHAPTER 1**

## Introduction

#### 1.1. Mitochondria

Mitochondria are double membrane-bound organelles (mitochondrion, singular) found in almost all eukaryotic cells. Mitochondria are popularly known as the 'powerhouse of the cell' as their main function is to produce adenosine triphosphate (ATP) through aerobic metabolism, which is used as the energy source for cellular activities. Later other studies have revealed that, other than energy production, mitochondria play a major role in cellular signaling networks like calcium signaling, and apoptosis; metabolic pathways like fatty acid metabolism, amino acid metabolism, iron-sulfur cluster biosynthesis, and many other stress responses. Mitochondrial size varies from 0.5-1 μM in diameter and 0.75 to 3 μM<sup>2</sup> in cross-section. Mitochondrial size and shape vary with the physiological and metabolic conditions of the cell. The double membrane structure of the mitochondria of the mitochondria divides it into 4 different compartments- outer membrane (OM), intermembrane space (IMS), inner membrane (IM), and matrix. The outer membrane of the mitochondria is highly permeable towards low molecular weight molecules due to the presence of porin, which allows them for free diffusion into the IMS region. The IMS region is a closed lumen encircled by outer and inner membranes, and it contains the proteins, involved in protein transport, lipid homeostasis and apoptosis. The inner membrane is impenetrable and only allows proteins through the transporter complex. The inner membrane also carries the respiratory chain complexes for energy production. The inner membrane forms finger-like invaginations, known as cristae, and thus enhances the inner membrane surface to maximize the energy production. The matrix region is the central luminal region of the mitochondria which is tightly enclosed by the inner membrane and this is the site for most of the mitochondrial metabolic pathways like fatty acid oxidation, urea cycle, and citric acid cycle etc.

Yeast mitochondria contain more than 1000 proteins among them only eight proteins are transcribed from mitochondrial DNA. Among those eight proteins, seven proteins are associated with respiratory chain complexes (Cob1 from Complex III; Cox1, Cox2, and Cox3 from Complex IV; Atp6, Atp8, and Atp9 from Complex V) and one protein from small ribosomal subunit, Var1. Most of the mitochondrial proteins are encoded by nuclear DNA and synthesized in cytoplasmic ribosomes, so these proteins are imported within mitochondria via the mitochondrial protein import pathways. There are 5 different mitochondrial protein import pathways all of them is dependent on the translocase complex present in the outer membrane (TOM complex) and among them, the protein import pathway using pre-sequence is the major

pathway used to import mitochondrial matrix proteins and some inner membrane proteins. In this pathway, precursor proteins carry a presequence and are recognized by the TOM complex, which helps it to pass through the TIM complex (Translocase of Inner membrane). The import via the TIM complex is driven via the Tim23 associated import motor consisting of the PAM complex, HSP70 chaperone protein Ssc1, and nucleotide exchange factor Mge1. During import through the TIM complex, the presequence region is cleaved by mitochondrial processing protease (MPP), and further proteolytic processing is done by other cleaving proteases if needed.

## 1.2. Reactive Oxygen Species, Oxidative Stress and damage to biomolecules

Reactive oxygen species (ROS) are highly reactive compounds generated from oxygen (O<sub>2</sub>), water (H<sub>2</sub>O) or hydrogen peroxide (H<sub>2</sub>O<sub>2</sub>). As most of them contain one or more free electrons in their outer shell, they are unstable in nature and can extract one electron form a stable molecule to gain stability. This makes the newly affected molecule unstable and thus starts a sequence of reactions and ultimately leads to cellular damage. This some of the most important ROS are hydroxyl radicals, singlet oxygen, superoxides, peroxides etc. Hydroxyl radicals are generated by the Fenton reactions between ferrous compounds and hydrogen peroxide and it is the most reactive ROS, which can oxidize both in organic and inorganic substrates [1,2]. The reduction of oxygen leads to the production of superoxides, by an enzymatic or non-enzymatic electron transfer reaction, which mostly occurs in mitochondria. The enzymes involved in the formation of superoxides are cyclooxygenase, lipooxygenase, xanthine oxidase and NADPHdependent oxidase [3,4]. Peroxyl radicals are generated by the protonation of superoxides and are involved in fatty acid oxidation [5]. Hydrogen peroxide is produced via a dismutation reaction carried out by superoxide dismutase. It can cross the biological membranes to cause oxidative damage [6]. Singlet oxygen is highly reactive and unstable form of molecular oxygen, a very toxic ROS molecule [7]. It is generated via the stimulation of eosinophils and neutrophils [8,9], catalyzed by dioxygenases lipoxygenases and lactoperoxidase [10-12]. This ROS molecule can do serious DNA damage and even tissue damage [9,13]. Cellular organelles involved in the production of ROS are mitochondria peroxisomes, endoplasmic reticulum etc. Mitochondria produces around 70% of the total cellular ROS during oxidative phosphorylation. The main sites of ROS generation in mitochondria are complex I and complex III [14]. In peroxisomes, β-oxidation of the fatty acids is the main source of ROS production [15]. In endoplasmic reticulum, cytochrome p-450 enzymes, thiol oxidase and diamine oxidase produce ROS and contribute to oxidative stress [16,17].

At a low level, ROS molecules are used in different biological functions, such as various cellsignaling pathways, as a protective measure against pathogenic organisms, and in redox regulations [18,19]. But uncontrolled and high concentrations lead to oxidative stress and damage different biomolecules including DNA, RNA, proteins, and lipids [20-22]. ROS can damage DNA molecules by reacting with every constituent i.e., DNA bases, phosphate groups, sugar molecules etc. Hydroxy radicals extricate the hydrogen atoms from the base and produce modified adducts of purine (8-hydroxy deoxy adenosine, 8-hydroxydeoxy guanosine etc.), pyrimidine bases (uracil glycol thymine glycol, 5-hydroxy deoxycytidine, 5-hydroxydeoxy uridine etc.) and sugars molecules (erythrose, glycolic acid etc.), DNA -protein crosslinks or even DNA breaks [23]. The level of 8-hydroxydeoxy guanosine or 8-oxo G is a biomarker to understand the oxidation of DNA molecules. Mitochondrial DNA is much more sensitive to oxidative stress because of lack of a protective membrane around it and the vicinity of the DNA with the site of ROS source. RNA molecules are more prone to ROS-mediated attack as they are single-stranded, get less protection from proteins than DNA and lacks repair mechanisms [24]. RNA damage has been found to be more present in different pathological conditions like Parkinson's and Alzheimer's disease, atherosclerosis etc. [25-27]. Membrane lipids and specifically phospholipids are more prone for oxidation by free radicals, which causes lipid peroxidation and leads to, the deactivation of membrane-bound proteins and reduced membrane fluidity [28]. At the start of lipid peroxidation one free radical extracts a hydrogen atom from a fatty acid's methylene group and produces a lipid radical, which then forms lipid peroxyl radical using molecular oxygen. These radicals attack further lipids and start a chain of oxidative reactions [29]. Almost all ROS molecules can cause protein oxidation [30]. ROS oxidizes different amino acids in the proteins and forms different oxidized products of the amino acids causing protein cross-links, which ultimately results in denaturation and dysfunction in different enzymes like enzymes and transport receptors [31].

Oxidative stress can be formed either due to excess production of ROS or a dysfunction in antioxidant pathways. Oxidative stress has been reported to cause different clinical conditions like cardiovascular [32], neurodegenerative [33], digestive [34] diseases, cancer [35] and even aging [36].

#### 1.3. Anti-oxidant defence mechanism

To protect cellular components from such fatal oxidative insults, cells have evolved with diversified antioxidant mechanisms involving enzymatic and nonenzymatic techniques. Among different defence mechanisms, some of them directly work upon ROS molecules and detoxify them, while the other act upon the oxidatively damaged biomolecules specifically proteins, to repair them. The anti-oxidant defence mechanisms found in yeast is explained below-

- **1.3.1. Superoxide Dismutases-** Superoxide dismutases or SODs catalyze the enzymatic conversion of superoxide ions to hydrogen peroxide and require metal ions in their active site [37,38]. *S. cerevisiae* contains two SOD enzymes namely Sod1, which reside in the cytosol and requires copper and zinc molecules in their active site whereas Sod2 has been found in the mitochondrial matrix which requires manganese ion [38]. A small pool of Sod1 has been also found in the mitochondrial IMS region, thus enabling both SODs to quench mitochondrial ROS [39]. Sod1 has been found to defend cells against environmental exposure to oxidants, while Sod2 is essential for cells to deal with ROS generated within the cellular environment [40-45].
- 1.3.2. Catalases Catalases reduce hydrogen peroxide utilizing the reduction properties of the haem group attached to it. S. cerevisiae possesses two catalase enzymes, one is peroxisomal Cta1 and another is cytosolic Ctt1 [46]. Cta1 is involved in the quenching of  $\beta$ -oxidation mediated ROS, where the function of Ctt1 is unclear [47].
- **1.3.3. Peroxidases** These enzymes reduce both organic and inorganic peroxides into alcohol using their active cysteine thiol groups, unlike SOD or catalase which employ metal-associated co-factors. Depending on the type of electron donor for the thiol group, peroxidases are of Two types, namely glutathione peroxidases (GPXs), which require GSH and the other is TRX peroxidases or peroxiredoxin, which require TRX as their electron donor. Yeast cells possess three GPXs; Gpx1, Gpx2 and Gpx3. They can all reduce soluble and lipid hydroperoxides with Gpx3 having the highest activity [48-51]. Peroxiredoxins (PRXs) use TRX as the electron donor to reduce peroxides [52,53]. *S. cerevisiae* has five different PRXs present in different locations within the cell; Tsa1, Tsa2, Ahp1 in cytosol; Prx1 in the mitochondria; Dot5 in the nucleus.
- **1.3.4.** Thioredoxin System- Thioredoxins (TRXs) are small proteins that catalyze the reduction of thiols groups present in proteins utilizing two conserved cysteine residues present

in their active site. The thioredoxins system includes TRXs and TRX reductases, which participate in the reduction reaction of oxidized TRXs using NADPH [54]. *S. cerevisiae* possesses 3 TRX proteins, among which Trx1 and Trx2 are cytosolic whereas Trx3 is mitochondrial. On the other hand, this yeast strain contains only 2 thioredoxin reductases, one is Trr1, found in cytosol and the other one is Trr2, found in mitochondria.

**1.3.5. Glutaredoxin System-** Like thioredoxins glutaredoxins are also small oxidoreductase proteins that catalyze disulphide reductions via using active cysteine residues in its active site. But unlike thioredoxins, here GSH molecules are used as hydrogen donors [54-56]. After getting oxidized (GSSG), glutathione gets reduced (GSH) by glutathione reductase with the help of NADPH. *S. cerevisiae* possesses 2 GRX enzymes Grx1 and Grx2 [57]. Though both proteins are mainly cytosolic, a pool of Grx2 is present in mitochondria also [58]. Grx1 protects the cell from both hydroperoxides and superoxides, whereas Grx2 can protect only against hydroperoxides [59].

#### 1.4. Methionine oxidation and Role of Methionine Sulfoxide Reductases

Sulfur-containing amino acids such as cysteine and methionine are the prime targets of ROS molecules [60,61]. Oxidation of thiol groups in the cysteine produces disulphides, whereas oxidation of methionine leads to the formation of either reversible methionine sulfoxide (Met-SO) or irreversible methionine sulfenic acid (Met-SO2) [61]. These modifications bring major structural changes in the three-dimensional conformation of the protein leading to the inactivation of the enzymes or even accelerating the degradation of the protein due to less stability.

Methionine sulfoxide reductases (MSRs) are the enzymes that reduce oxidized methionine sulfoxides to their native form, thus restoring structural and functional alteration in the proteins that happened due to oxidation [62,63]. These enzymes are conserved from bacteria to humans [64]. After a reduction cycle of sulfoxides, MSRs get oxidized and are unable to reduce any more sulfoxides, unless they are reactivated by thioredoxin and thioredoxin reductases [65,66]. Based on their structural conformation methionine sulfoxides are of 2 types- R or S form. Based on the enantiomeric form of sulphoxide they reduce, Msrs are segregated into A and B families, where Msrs of the A family takes care of Met-(S)-SO and Msrs of the B family look after Met-(R)-SO (9 jbc). There are three MSR enzymes in *S. cerevisiae*, fRMsr, Mxr1, and Mxr2; Mxr1 corresponds to the A family, whereas fRMsr and Mxr2 belong to the B family [67]. Mxr1 can reduce both free sulfoxides and those that are embedded within the protein, whereas Mxr2 can

reduce only protein-bound sulfoxides and fRMsr reduces only free methionine sulfoxides [68,69]. If we see the localization of the MSRs in yeast, Mxr1, and fRMsr are present in cytosol whereas Mxr2 is present in mitochondria [67]. Our earlier studies have shown that Mxr2 is more important than Mxr1 in combating against oxidative stress, as  $mxr2\Delta$  cells exhibited much more sensitivity than  $mxr1\Delta$  cells towards oxidative stress [70]. Mge1, the nucleotide exchange factor for mitochondrial Hsp70, was the first identified physiological substrate for the Mxr2 [70]. Later studies have also shown the presence of Mxr2 in cytoplasm and identified Fes1 as the substrate for both Mxr2 and Mxr1 [71]. Though few physiological substrates have been identified, the molecular signaling circuits, Msrs are involved, are largely unexplored. For mammalian cells also both A and B families of MSRs are present. There is only one member in A family, known as MsrA which is present in cytosol, mitochondria, and nucleus. But there are 4 different members in the B family, namely MsrB1 found in the nucleus and cytosol; MsrB2 in mitochondria; MsrB3A in endoplasmic reticulum and MsrB3B in mitochondria.

Enzymatic reaction Mechanism of MSR- Msrs interact with oxidized methionine sulfoxides to reduce them to methionines. The catalytic mechanism was first elucidated on MsrA enzymes. It was later found that both MsrA and MsrB follow a canonical process where three cysteine residues from the enzymes participate in the reduction reaction [72]. The first cysteine makes a nucleophilic attack on the sulfoxide moiety to form an unstable intermediate that breaks down to form sulfenic acid at the first cysteine, releasing a reduced methionine. The other two cysteines reduce the sulfenic acid at first cysteine residue by exchanging multiple thiol-disulfide reactions using the thioredoxin system and NADPH [65,73-76].

#### 1.5. Autophagy

Autophagy is a physiological stress-responsive recycling process of cellular components, which helps cells to adapt and survive under various stress condition including starvation and other physiological stress conditions. In this process damaged cellular components or even damaged organelles are engulfed and digested inside vacuole (for yeast) or lysosome (higher eukaryotes). Autophagy process initiates with the formation of a double membrane, which matures to form autophagosome, after engulfing damaged components or organelles. Autophagosomes further fuses with either vacuole or lysosome to pour the cargo materials of the vesicle for degradation by the resident hydrolases [77].

In yeast, based on the type of cargo engulfed within the vesicle, autophagy pathways are divided into two categories- selective and non-selective. In non-selective autophagy, a random

part of the cytoplasm is sequestered, whereas specific proteins or organelles are engulfed in selective autophagy[78]. Non-selective autophagy is mainly induced by the inactivation of kinase target of rapamycin complex 1 (TORC1) during nutrient limitation, whereas selective autophagy can occur even in high TORC1 activity. Selective autophagy is mostly dependent on master adapter protein of selective autophagy, Atg11 [79]. Selectivity in this process is based on the specificity of interaction between Atg11 and the receptor protein present on the surface of the organelles (e.g., Atg32 on the mitochondria, for mitophagy) [80] . The selective autophagy pathways found in yeast are Cvt pathway, Mitophagy (Mitochondria), ribophagy (Ribosome), nucleophagy (Nucleus), lipophagy (Lipid molecules), reticulophagy (Endoplasmic reticulum) etc,

#### 1.6. Cytoplasm to Vacuole (Cvt) pathway

Cytoplasm to vacuole targeting (Cvt) pathway is a well-characterized selective autophagy pathway, which is responsible for the delivery of vacuolar hydrolases from the cytoplasm to the vacuolar lumen both under vegetative growth condition (via Cvt vesicles) and nutrient starvation condition (via autophagosomes) [81,82]. Cvt vesicles are specialized autophagosomes, which specifically enclose Cvt cargos and are much smaller (~ 150 nm) than autophagosomes, which develop during nutrient starvation (300 nm- 900nm) [81-83].

The vacuolar hydrolases that are transported via the Cvt pathway are Leucine aminopeptidase (Ape1), α-mannosidase (Ams1) and Aspartyl aminopeptidase (Ape4), where, Ape1, being the major cargo, acts as the core of the Cvt vesicle. Ape1 is synthesized in the cytosol as a zymogen form with a 45 amino-acid long N-terminal propeptide, which interacts with the propeptide of other Ape1 molecules and readily forms a homo-dodecamer structure, which further congregates into Ape1 complex that shapes Cvt vesicle core [84,85]. After Ape1 complex formation, the first α-helical region of Ape1 propeptide interacts with the coiled-coil region of receptor protein, Atg19 and forms a heterotrimer with an Ape1 molecule, which stops further Ape1 assembly and allows Atg19 to localize onto Ape1 complex surface, and this structure is known as the Cvt complex [86-91]. Ams1 and Ape4, the other two cargo of this pathway, also associate with the Cvt complex via distinct interactions with Atg19 [92-95].

The C-terminal region of Atg19 in the Cvt complex interacts with the master adaptor protein of selective autophagy, Atg11, which helps the Cvt complex to reach the phagophore assembly site (PAS), with the help of actin cytoskeleton and Arp2/3 actin binding complex. Atg11 helps to tether the Cvt complex with the actin cytoskeleton, and the Arp2/3 complex motors the

progression of the complex to PAS through actin [79,88,96,97]. After reaching PAS, Atg19 interacts via its WXXL motif with the β2 of Atg8 to form a β sheet structure, and this interaction tethers the Cvt complex with the phagophore and aids in phagophore expansion around the Cvt complex [98,99]. Vps53 tethering (VFT) complex also assists in the localization of the Cvt complex and Atg19 in PAS [100]. Once properly localized at PAS, VFT complex, Vps45, QSNAREs (Tlg1 and Tlg2) and autophagy machinery drive CVT vesicle formation [101].

After vesicle formation, Atg8 molecules attached to the phosphatidylethanolamine residues on the outer surface of the Cvt vesicle are cleaved off by ATG4, and finally the vesicle docks and fuses with the vacuole where its inner single membrane compartment is liberated in the vacuolar lumen [102]. Atg15 in the vacuolar lumen acts as a lipase that degrades the inner membrane, which releases Cvt vesicle cargo into the lumen [103,104]. In the lumen, Pep4 cleaves the propeptide of the Ape1, resulting in the formation iApe1 which further gets processed by Prb2 for maturation and activation of the Ape1 enzyme [105]. At the same time, the other cargo hydrolases do not require processing as they do not have any propeptide (105).

#### 1.7. Non-selective Macroautophagy

Non-selective autophagy is an evolutionarily conserved cellular recycling process, which degrades different biomolecules, dysfunctional components, and even damaged organelles into reusable simpler forms. In vegetative condition, basal level of autophagy has been noted and used for the turnover of some proteins and organelles. But in different stress conditions like oxidative stress, heat shock or nutrient starvation conditions, autophagy is induced to deal with these conditions [106]. Autophagy is involved in diverse physiological functions like cellular growth and development, immunity responses and MHC presentations etc. [106,107].

After induction, autophagy starts with the nucleation of a double membrane phagophore, which engulfs damaged cellular components and eventually matures into an autophagosome [108]. Autophagosome fuses with the lysosome (vacuole for yeast), leading to degradation of the engulfed component and consequent release into simpler biomolecules [109]. More than 40 Atg proteins are involved in different steps of autophagy in yeast. Different stages of this dynamic process are explained below, emphasizing the pathway induced by nitrogen starvation condition.

#### 1.7.1. Autophagy induction and phagophore nucleation-

Role of Atg1 kinase complex -

TORC1 (target of rapamycin complex I) kinase phosphorylates Atg13 protein in nutrient-available conditions. Phosphorylated Atg13 cannot interact with Atg1 and Atg17 proteins due to their low affinity for them in phosphorylated conditions. Under nutrient limitation conditions, the TORC1 complex is inhibited and the Atg13 protein gets dephosphorylated. Hypophosphorylated Atg13 protein interacts with Atg1 and thus mediates the interaction between Atg1 and the scaffold complex consisting of Atg17-Atg29-Atg31 [110]. Interaction with Atg13 and the scaffold complex generates a ternary complex and activates the kinase activity of Atg1. Activated Atg1 kinase complex recruits other Atg proteins at the phagophore assembly site (PAS) and phosphorylates downstream target proteins [111,112].

#### Role of class III phosphatidylinositol 3-kinase complex-

Phagophore is the precursor form of the autophagosome, which lengthens by gaining huge amounts of membrane lipid to generate autophagosome. In the phagophore nucleation step, a small bunch of proteins mobilize towards PAS, which promotes further assembly of Atg protein for phagophore expansion. Recruitment of class III phosphatidylinositol 3-kinase (PtdIns3K) is an essential event during nucleation. This complex helps in membrane acquisition and consists of a serine/threonine kinase Vps34 and some auxiliary proteins. Vps34 forms two different complexes in yeast namely, complex I and complex II, each of which consists of three common protein subunits, Vps34, Vps15, Vps30, and either Atg14 (complex I) or Vps38 (complex II) [113,114]. Vps34 complex is involved in autophagy, Cvt pathway, and vacuolar transport of carboxypeptidase Y (CPY). Vps15 is necessary for membrane attachment and activation of Vps34 [115]. Atg14 and Vps38 provide substrate specificity to the complex as it has been shown deletion of Atg14 inhibits autophagy and Cvt pathway, whereas deletion of Vps38 hinders CPY's vacuolar delivery. The role of this complex is to produce phosphatidylinositol-3-phosphate so that phosphatidyl-inositol-3-phosphate binding proteins can be recruited, which will further recruit other downstream proteins involved in autophagy [116]. Atg20 and Atg24 are two such proteins, which interact with Atg17 and are thought to be part of the Atg1 kinase complex [117]. Along with Atg20 and Atg24, Atg18 and Atg21 also binds with phosphatidyl-inositol-3-phosphate. Atg18 is required for appropriate movement of Atg9 but, Atg21's function is still unknown [118,119]. Along with Atg9, this complex is also involved in recruiting Atg8 and Atg12 [120].

#### 1.7.2. Expansion of phagophore-

Role of Ubiquitin-like conjugation system- There are two essential protein conjugation systems for phagophore expansion, involving two major proteins Atg12 and Atg8 [121]. During the formation and expansion of phagophores, the Atg12 complex is located on the phagophore surface and serves as the E3 ubiquitin ligase enzyme for the Atg8 conjugation system [122]. Unlike Atg12, Atg8 is distributed symmetrically in two different surfaces of the autophagosome. Atg8 proteins present in the outer surface of the autophagosome are cleaved off, while those present in the inner surface are degraded when delivered and processed in the vacuole [123-125]. The Atg8 complex helps in autophagosome membrane expansion by driving membrane tethering and fusion.

The Atg12 complex is comprised of Atg12, Atg5, and Atg16. The conjugation reaction of Atg12 with Atg5 via an isopeptide bond is carried out by Atg7 and Atg10 proteins, where Atg7 acts as an E1 or Ubiquitin activating enzyme and Atg10 as E2 or Ubiquitin-conjugating enzyme [126-128]. Atg5 non-covalently interacts with Atg16, which further assembles to generate a multimeric complex of 350 kDa [129].

The Atg8 protein in the second complex is conjugated with the phosphatidylethanolamine (PE) residues of the phagophore membrane [130]. At first, Atg4, a cysteine protease cleaves Arg117 at the C-terminal part of Atg8 and exposes a Glycine residue (DD). Via this glycine residue, Atg8 at first covalently interacts with E1 enzyme Atg7, then transferred to E2 enzyme, Atg3 and ultimately to PE residue of the phagophore membrane via E3 enzyme, Atg12 complex. Atg8 protein conjugation is a reversible process, as the proteins present on the outer membrane of the autophagosome is cleaved of Atg4 for further rounds of association [102,131].

Role of Atg9 for membrane provision- A continuous supply of membrane lipid is required at the PAS site for phagophore expansion and autophagosome formation. This job is meticulously done by Atg9 [132,133], which is the only transmembrane Atg protein. and 0unlike other Atg proteins, which concentrate only close to PAS region, punctate structures of Atg9 have been observed in PAS regions and also in other cytosolic regions [134]. The shuttling of Atg9 from other cytosolic regions to PAS region is thought to be the mechanism, by which membrane component is trafficked from the membrane donor region to the PAS region. This shuttling of Atg9 involves several Atg proteins like Atg11, Atg23 and Atg27. Atg23 and Atg27 along with Atg9 produce a structure involved in membrane acquisition [135,136]. Along with Atg proteins, the Actin cytoskeleton and Arp2 protein in the Arp2/3 complex of Actin, physically

interacts with Atg9 and controls the Atg9 shuttling [137]. So, in Atg9 shuttling, adaptor protein Atg11 helps Atg19 to attach to actin, and the Arp complex pushes the Atg9 complexed with membrane to the PAS region [132,137,138].

#### 1.7.3. Docking and fusion of the matured autophagosome with vacuole-

After formation and maturation, autophagosomes are destined to fuse with vacuole, using the machinery involved in homotypic vacuole fusion. This machinery is composed of SNARE proteins Ykt6, Vam7, Vam3 and Vti1, the NSF Sec18, the α-SNAP Sec17, class C Vps/HOPS complex and the Rab GTPase Ypt7. Another two protein, which is involved in this fusion process are Mon1 and Ccz1 [139]. The atg12-Atg5-Atg16 complex on the outer face prevents premature docking of the autophagosome. After fusion, the inner vesicle with a single membrane layer is discharged in vacuolar lumen.

#### 1.7.4. Vesicle Breakdown and Recycling of the Resulting Macromolecules-

After delivery to the vacuolar lumen, the single membrane of the released vesicle is digested by Atg15. Atg15 contains a lipase active-site motif and is a putative lipase [103,104]. The multivesicular body (MVB) pathway targets Atg15 to the vacuolar lumen [140]. After digestion of the membrane, the autophagosomal content is released into the vacuolar lumen. Vacuolar hydrolases, Prb1 and Pep4 and the acidic pH of the vacuole degrade the cargo components released into the lumen. Once degraded, the products must be freed to cytosol for recycling. Atg22, a known amino acid efflux protein in the vacuolar membrane, releases leucine and other amino acids in the cytosol [141]. Other than Atg22, Avt3 and Avt4 also act as the vacuolar permeases, which are involved in the efflux of recycled components [142].

#### 1.8. Mitophagy

During oxidative phosphorylation within the mitochondria, along with ATP molecules, reactive oxygen species (ROS) molecules are also produced, which damage mitochondria. Damaged mitochondria further produce more ROS, which damages different biomolecules and organelles and leads to various pathological conditions [143]. To maintain mitochondrial homeostasis, these damaged mitochondria should be eliminated from the cells, where mitophagy play a vital role.

In the absence of mitophagic stimuli, polymerase-associated factor 1 (Paf1) complex and Rpd3-Sin3 deacetylase complex inhibits transcriptional expression of Atg32, which is mitochondrial membrane protein and acts as a receptor for mitophagy [144-146]. Moreover, phosphorylation

of Atg32 is blocked by Ppg1 and Far complex. Upon mitophagic stimuli, Atg32 gets upregulated and then phosphorylated at Ser114 and Ser119 by CK2 with the dissociation of the Far complex [147]. Moreover, Yme1 also cleaves Atg32 at its C-terminal end [148]. Phosphorylated Atg32 interacts with Atg11, which recruits the damaged mitochondria to the PAS. In the PAS, autophagy machinery expands the isolation membrane around the surface of the damaged mitochondria, which helps it to get engulfed within autophagosome vesicle.

#### 1.9. Transcriptional control of Non-selective Macroautophagy

Autophagy is a highly synchronized process, which involves more than 40 Atg proteins. Though basal autophagy is needed for turnover of the biomolecules which could not get degraded via proteasome or other degradation machineries in the cell, but it is mainly induced, when cells are exposed to stress conditions. So, the expression or the activity autophagy regulatory proteins should be tightly regulated, to avoid autophagy activation in favourable conditions and less activation in stressed conditions. So eukaryotic cells have evolved different mechanisms for precise regulation of autophagy in different level like transcriptional, post-transcriptional, translational, and posttranslational etc. Transcriptional regulation of autophagy is done by different transcription factors and histone modifications; post-transcriptional regulations are executed by regulating the localization and turnover of mRNAs and by controlling ribosome binding proteins; whereas the post-translational regulations include protein modifications like acetylation, phosphorylation, glycosylation, ubiquitination, and protein-protein interactions etc. Here to our interest, transcriptional control of autophagy is further discussed.

Transcriptional regulation of autophagy is one of the most crucial regulatory circuits, which helps cells to persist in various stress conditions. Several ATG genes and other factors are upregulated during autophagy induction. Studies have shown that, under cycloheximide conditions, where protein synthesis is blocked, if autophagy is induced, it generates tiny autophagosomes. This result indicates that protein synthesis is essential for the formation of autophagosome and autophagy progression but not for autophagy induction [149]. Among ATG genes, Atg8 and Atg14 show maximum upregulation. Atg8 shows at least 8-fold upregulation during autophagy induction [123,124]. Atg8 knockout mutant [149,150] or cells with mutant Atg8, having defective fusion properties [151] also exhibit tiny autophagosomes. On the other hand, the ATG14 gene is upregulated up to 14 folds, once autophagy is induced, via the Gln3 transcription factor [152]. Other than ATG8 and ATG14, to a lower extent other ATG genes like

ATG1, ATG3, ATG4, ATG5, ATG7, ATG12 and ATG13 also get upregulated [153]. The molecular network regulating ATG8 gene transcript level is further explained elaborately.

#### Transcriptional regulation of ATG8 gene during autophagy induction-

Transcriptional regulation of ATG8 is very crucial for optimal autophagic activity. Though the Ume6 repressor mainly controls the transcriptional expression of Atg8, other transcriptional regulators like Pho23, Rph1 and Msn2-Msn4 were also found to regulate *ATG8* expression [154-158]. Availability of nutrients is sensed by Tor and Sch9 kinases which phosphorylate and retain Rim15 kinase in cytoplasm so that it cannot phosphorylate nuclear localized Ume6 [159,160]. Unphosphorylated Ume6 binds with the ATG8 promoter and represses its expression with the help of histone deacetylase Rpd3 and co-repressor Sin3 [154,155,161]. However, under nitrogen starvation, Tor and Sch9 kinases become inactive and cannot phosphorylate Rim15 anymore [155,161]. Moreover, Tps2 dephosphorylates the phosphorylated residue of Rim15 [162]. Dephosphorylated Rim15 enters the nucleus and undergoes autophosphorylation [159]. Hyperphosphorylated Rim15 phosphorylate Ume6 and disarray the association with Sin3 and Rpd3 thus ATG8 gene expression reinstates [161,162].

#### 1.10. Protein acetylation

Protein acetylation is one of the most important post-translational modifications, along with phosphorylation, ubiquitination, etc. Acetylation of histones is well-reported and is known to regulate transcriptional expression of genes, DNA silencing, DNA repair, and cell cycle [163,164]. However recent discoveries have identified many non-histone proteins that get acetylated and their acetylation plays a significant role in cellular signaling [165-168]. In protein acetylation, an acetyl group is transferred from acetyl-CoA to a protein's \(\varepsilon\)-amino group of lysine residues, catalyzed via lysine deacetylases (KATs), which employ either an aspartate or glutamate residue in their active site. In these reactions at first, a ternary intermediate of KAT- acetyl CoA – lysine residue formed, followed by deprotonation by the aspartate or glutamate residue and the nucleophilic attack on the carbonyl residue of acetyl-CoA [169-171]. The level of protein acetylation in the cells is also controlled by histone deacetylase complexes (HDACs), which remove protein acetylation by degrading the amide linkage between lysine residues and the acetyl group.

Based on their localization, KATs are of two types: A-type, found in the nucleus, or B-type, found in cytoplasm [172]. In *S. cerevisiae*, only one B-type KAT is present, known as Hat1

[173]. On the other hand, there are 6 candidates in the A-type KATs, namely Gcn5, Esa1, Sas3, Sas2, Elp3 and Rtt109 [174]. HDACs on the other side, are of three types, class I, class II and class III HDACs. Class I and II HDACs form similar types of catalytic domains, whereas class III HDACs, also known as sirtuins, depend on NAD<sup>+</sup> for their activity. Class I HDACs are Rpd3, Hos1, and Hos2; Hda1 and Hos3 are classified as class II; whereas class III candidates are Sir2, Hst2, Hst1, Hst4, and Hst3 [175,176].

#### Role of Protein acetylation in cellular physiology

Histone acetylation- The entire length of DNA is orderly assembled around histone proteins to form the chromatin structure. This stringent packaging of DNA in one way prevents the exposure of DNA to mutagens, but in the other way, it prevents DNA access from DNA modifying enzymes (167). Acetylation of the specific lysine residues in the histone proteins in one way neutralizes the positive charge of the lysine and thus loosens the tight packaging of the DNA, and on the other way marks the lysine residues for the chromatin structure modifying reactions by bromodomain-containing proteins. Acetylation of histones modifies chromatin structure, thus affecting gene expression and regulating different molecular signaling. [164,177]

#### Acetylation of non-histone proteins-

Acetylation of non-histone proteins regulates various physiological processes. These processes range from RNA metabolism, membrane trafficking, cell cycle progression, metabolic pathways, and regulation of cytoskeleton dynamics [166,178]. Acetylation modifies activity of different enzyme subunits like Pck1 and Sip2, thus regulating gluconeogenesis and replicative lifespan, respectively [167,179]. The Rsc4p subunit of the RSC chromatin remodeling complex and Swi2 subunit of the SWI/SNF complex is acetylated and regulated by Gcn5 [180,181]. Along with other proteins, different subunits of acetylase complexes also gets acetylated. In NuA4 complex, the catalytic subunit Esa1 undergoes autoacetylation [182] and also acetylates Yng2 subunit [183]. Rtt109 also undergoes autoacetylation and regulates itself [169]. Gcn5 also catalyzes different subunits of the SAGA complex [184]. Several mitochondrial proteins are also reported to be regulated by the acetylation. One of the prime examples is the Pda1 subunit of PDH1 enzyme complex [185].

Role of Rpd3 deacetylase complexes - Rpd3 deacetylase complexes are one of the most important groups of lysine deacetylases, which is conserved from unicellular yeast to human [186]. Normally Rpd3 is associated in 3 different protein complexes namely Rpd3L, Rpd3S

and Rpd3μ. Rpd3L is involved in different ribosome biogenesis, and in response to different abiotic stresses like heat [187,188]. On the other hand, Rpd3S is involved in maintaining chromatin integrity [189], while Rpd3μ complex helps the cell to deal with oxidative stress [190]. RPD3L complex is composed of around 10 protein subunits, Rpd3, Sin3, Pho23, Dep1, Rxt2, Rxt3, Sds3, Ume1, Sap30, Cti3. Rpd3S complex is composed of Rpd3, Sin3, Ume1, Eaf3, Rco1. Rpd3μ complex is composed of Rpd3, Snt2, Ecm5 [190].

Role of Ume6 Acetylation- Ume6 is a transcription factor that regulates gene expression of early meiotic genes in yeast like Ime2, Spo11 and Spo13 and [191]. Ume6 represses these genes during mitosis but during the onset of meiosis, proteolytic destruction of Ume6 ensures optimal meiotic induction [192,193]. During repression, the Ume6 protein binds with URS1 element present upstream of the target gene and then recruits Rpd3 and Sin3, the deacetylase complex subunits, thus causing hypoacetylation of the histone H3 and H4, resulting in target gene repression [194,195]. Proteolytic degradation of Ume6 protein is executed in two different steps. In the first step, where the meiotic condition has been induced, Ume6 is acetylated by Gcn5 acetylase at specific sites, which induces its partial degradation. To prevent Ume6 degradation in vegetative conditions, the HDAC, Rpd3 complex removes undesirable acetylation from Gcn5. Upon meiotic entry, complete degradation of Ume6 happens by ubiquitination-mediated proteasomal destruction.

DNA binding region within the C-terminal region of the Ume6 possesses 6 cysteine residues and can bind two Zn<sup>2+</sup> ions, thus it is named the Cys<sub>6</sub>Zn<sub>2</sub> motif. Within this motif, there are 5 different lysine clusters, among which acetylation at Cluster 1 and 3 is important for Ume6-mediated regulation [196,197]. Acetylation at cluster 1 marks it for degradation to relieve the repression [196]. Moreover, acetylation at cluster 3 prevents Ume6 from binding with the target gene promoter [197]. Thus, the first level of Ume6-mediated gene repression is withdrawn. Upon meiotic entry, Ume6 is phosphorylated by two kinases, Rim11 and Mck1[198,199]. Phosphorylated ume6 interacts with meiotic gene transcriptional activator Ime1 [200]. This interaction activates Cdc20, which in turn activates APC/C ubiquitin ligase for ubiquitination-mediated degradation of Ume6 [193].

#### 1.11. Iron-Sulfur Cluster Biogenesis

The iron-sulfur cluster biogenesis is a critically regulated multistep process, involving different cellular compartments. All biosynthesis and steps for insertion of clusters within mitochondrial proteins occur in mitochondria using Fe/S cluster assembly (ISC) machinery consisting of 18

proteins. Cytosolic Fe/S protein assembly (CIA) machinery helps in further biosynthetic rearrangement, transferring and incorporation of the clusters in the cytosolic and nuclear proteins. The basic constituents needed for this biosynthesis are cysteine, iron and electrons. Iron-sulfur clusters containing proteins are involved in diverse physiological processes like protein translation, DNA replication, biosynthetic enzymes and defence mechanisms [201-203].

At the very beginning, a [2Fe-2S] cluster is started to synthesize by early ISC machinery, comprised of scaffold protein Isu1; cysteine desulfurase complex Nfs1-Isd11-Acp1, which provides sulfide; NADPH-Arh1 which provide electrons from electron transport chains; ferredoxin Yah1 and regulatory protein Yfh1, that donate iron. The [2Fe-2S] cluster biosynthesized upon scaffold protein Isu1 is then transferred to a glutaredoxin molecule Grx5. This reaction is accomplished by an Hsp70 chaperone Ssq1, co-chaperone Jac1 and the nucleotide exchange factor Mge1. This [2Fe-2S] cluster is either incorporated into the target protein within mitochondria or delivered to late ISC machinery for synthesis of the [4Fe-4S] cluster. The late ISC machinery is mainly composed of 3 proteins, Isa1, Isa2, and Iba57. Trafficking and incorporation of the [4Fe-4S] clusters are further done by Nfu1, Ind1 and Bol proteins. The iron-sulfur clusters are also transported out of the mitochondria for insertion in the different proteins localized in the cytosol and nucleus [201-203].

#### 1.12. Retrograde Signaling

Earlier we have discussed that mostly all of the mitochondrial protein are encoded because during evolution, most of the genetic material has been transferred from mitochondria to nucleus. this phenomenon necessitates a stable communication between mitochondria and nucleus to harmonize the protein expression and import and to convey the information about mitochondrial dysfunction to nucleus to counterbalance the crisis. Retrograde signaling is a communication circuit between mitochondria and nucleus along with various other organelle, which helps cells to adapt with the changes in mitochondrial functionality. This signaling is conserved from yeast to human and best understood in yeast, where it is mainly regulated by Rtg1-Rtg3 transcription factor complex [204].

The major event in this signalling is translocation of Rtg1-Rtg3 complex to the nucleus from cytoplasm. Both transcription factors are of basic helix loop helix leucine zipper type, which forms and hetero dimer. This complex binds to a specific sequence (GTCAC) in the target DNA via Rtg3 and upregulate specific set of genes required for the metabolic reprogramming

[205,206]. In the uninduced condition, cytoplasmic protein Mks1 forms a complex with 14-3-3 proteins Bmh1/2. This complex keeps Rtg3 in hyperphosphorylated state, where it cannot interact with Rtg1 leading to silence of the target genes [207]. During mitochondrial distress, the signal is sensed by Rtg2, which prevents binding of Mks1 with 14-3-3 proteins, which leads to partial dephosphorylation of Rtg3 [208]. Moreover, Mks1 is ubiquitinated and marked for degradation by E3 ubiquitin ligase, Grr1 [209]. Partially phosphorylated Rtg3 now make complex with Rtg1 in cytoplasm and this complex is then translocate to nucleus to upregulated downstream genes, like CIT2, DLD3 and other genes involved in the TCA cycle.

#### 1.13. Rationale and Objective

In this work, we have tried to find the role of Msrs, specifically Mxr2 in cellular physiology of *Saccharomyces cerevisiae*. A high-throughput study suggested that, Mxr2 may interact with two proteins of Cvt autophagic pathway, Atg19 and Ape1 [210]. Here we have attempted to check the role of Mxr2 in Cvt pathway. Later we also tried to search if Mxr2 controls nonselective macro autophagy and whether the status of mitochondrial physiology can regulate the autophagy machinery. To achieve these goals, this work is divided into two major objectives-

- 1. To study the role of Mxr2 in regulating Cvt autophagic pathway
- 2. To study the role of Mxr2 in controlling nonselective macro autophagy.

### **CHAPTER 2**

# Mxr2 regulates Cvt autophagic pathway by altering the stability of Atg19 and Ape1

#### 2.1. BACKGROUND

Sulfur-containing amino acids, cysteine, and methionine are more vulnerable to oxidative damage. Under oxidative stress conditions, Methionine residues in the cell either free or embedded in the protein, get oxidized and form either reversible methionine sulfoxides or irreversible methionine sulfone [61]. This oxidation of methionine residues results in detrimental consequences within the cell, ultimately leading to cell death. Methionine sulfoxide reductases reduce oxidized methionine sulfoxide molecules to their native form to restore the physiological equilibrium within the cell. Loss or reduction in Msrs' activity has been implicated in many diseases, including pulmonary, vascular, ocular, aging, and neurological disorders [211-215]. The known physiological consequences of dysfunctional Msrs are mitochondrial dysfunction, decreased cytochrome C biosynthesis, and metal resistance in yeast [67,216]. Given the dynamic nature of ROS levels, the importance of redox homeostasis, the alacrity at which the cells reactivate Msrs, the number of diseases associated with dysfunctional Msrs, and the plethora of proteins that harbor methionine, more studies are required to identify the substrates of Msrs rapidly and to unravel the ramifications of Msrs role that impinge on the structural and functional stability of proteins.

Cytoplasm to vacuole targeting (Cvt) pathway is a well-characterized selective autophagy pathway in yeast that delivers vacuolar hydrolases from the cytoplasm to the vacuolar lumen [81,82,217]. Cvt pathway has been extensively studied to identify the molecular players regulating it and as a model system to delineate selective autophagy pathways. However, little is known about the stability and turnover rate of the proteins orchestrating the intricate Cvt pathway under normal, oxidative, and nutrient stress conditions.

Our earlier study published identified the first substrate for Mxr2, Mge1, the nucleotide exchange factor for mitochondrial Hsp70 [70,218]. Recently, it has been shown that cytosolic Hsp40 may also be a probable substrate of Mxr2. Since Mxr2 is present in the cytosol and mitochondria, we wished to identify other cytosolic substrates of Mxr2. A high-throughput yeast interactome study predicted that, Ape1 and Atg19 proteins of the Cvt pathway might interact with Mxr2. This study demonstrates Ape1 and Atg19 as potential substrates of Mxr2 and tries to uncover the role of Mxr2 in the regulation of Cvt pathway.

#### 2.2. MATERIALS AND METHODS

#### 2.2.1. Yeast strains and plasmids

The yeast strains used in this study are derived from the parent strain BY4741 and are listed in Table 1. Genomic deletion of the MXR2 gene was achieved by replacing the ORF of the MXR2 gene with HIS3MX6 cassette by PCR-based homologous recombination using NB1164/NB1165 primers, as indicated [219]. For generating the plasmid constructs, the coding regions of the genes were amplified either from yeast genomic DNA or mentioned. All the plasmids and the primers are listed in Tables 2 and 3, respectively. To generate p425TEF Mxr2-FLAG, the coding region of MXR2 was amplified using primers NB815/NB1048, where the reverse primer NB1048 has the 3× flag sequence embedded within it. The PCR product was then digested with BamHI/XhoI and ligated with digested p425TEF (pNB356) empty vector to create pNB904. MXR2- FLAG fragment from pNB904 was then subcloned into BamHI/SalI sites of yeast two-hybrid vector pGBD- C1(pNB415) to generate pNB901. For constructing yeast two-hybrid vectors pGAD-APE1, pGAD-ATG19, and pGBD- MXR1, the coding regions of APE1, ATG19, and MXR1 genes were amplified using NB1364/NB1365, NB1362/NB1363, and NB 1678/NB1679, respectively and digested with ClaI/SalI, BamHI/SalI, and EcoRI/BamHI enzymes, respectively. Double- digested DNA fragments were ligated to the respective site of pGAD-C1 (pNB422) and pGBD-C1 to generate pNB902, pNB903, and pNB912, respectively. For producing the over- expressing constructs of APE1 and ATG19 with HA tag, DNA fragments of both genes were amplified using NB1404/ NB1405 and NB1362/NB1399 primers, respectively, where both reverse primers (NB1405 and NB1399) have the HA tag sequence embedded within them. The amplified DNA fragments were then digested with HindIII/SalI and BamHI/XhoI enzymes, respectively, and then ultimately ligated to respective sites of p426 (pNB356) to generate pNB906 and pNB907. To create \( \Delta 45 \) deletion mutation of the first 45 amino acids in the APE1 gene, the requisite DNA fragment was amplified using NB1563/NB1365 and ligated to ClaI/SalI sites of pGAD-C1 to generate pNB908. For creating further point mutations in APE1 genes, at first APE1 coding region was amplified with NB1645/NB1365 and NB 1633/NB1365 primers to create M1L single and M1L/M17L double mutation, respectively. After digesting the amplified fragments with ClaI/SalI, DNA frag- ments were then ligated to respective sites of pGAD-C1 to generate pNB911 and pNB909. For generating M17 single mutant, pNB909 was used as a template and amplified with NB1364/NB1365 primers and after digestion with ClaI/SalI, ligated to the same sites in pGAD-C1 vector to generate pNB910. For expressing wt and M17L APE1 from the pRS315 CEN vector, 5' UTR of the gene (380 bp) was amplified with NB1406/NB1674 primers and the coding region of the gene along with 3' UTR (729 bp) was amplified with either NB1499/NB1511 (for wt *APEI*) or NB1675/NB1511 (for M17L *APEI*) primers. The 5' UTR and the gene along with 3' UTR fragments were then digested with NotI/SpeI and SpeI/ApeI and then ligated to NotI/ApaI site of the pRS315 (pNB399) to generate pNB913 and pNB914. For the construction of pRS313 ATG19-HA, 5' UTR of the gene (700 bp) and the DNA fragment having *ATG19* coding region along with HA tag were amplified using NB1400/NB1401 and NB1362/NB1399 primers, respectively. The amplified products after digestion with NotI/BamHI (5' UTR) and BamHI/XhoI (gene sequence with HA tag) were then ligated to NotI/XhoI digested pRS313(pNB398) to generate pNB915.

**Table 1. Strains** 

Strain	Genotype	Reference
YNB105	BY4741; MATa his $3\Delta 1$ ; leu $2\Delta 0$ ; met $15\Delta 0$ ; ura $3\Delta$	Euroscarf
YNB117	BY4741; <i>mxr2∆</i> :: <i>KANMX</i>	Euroscarf
YNB114	BY4741; <i>mxr1∆::KANMX</i>	Euroscarf
YNB 339	PJ469-A	[220]
YNB 483	BY4741; atg19∆::KANMX	Euroscarf
YNB 484	BY4741; <i>ape1∆::KANMX</i>	Euroscarf
YNB 514	BY4741; ape1Δ::KANMX mxr2Δ::HIS3	This study

**Table 2. Plasmids** 

Plasmid no.	Plasmid Name	Source/Reference
pNB478	pFA6a-HisMX6	[221]
pNB415	pGBD-C1	[220]

pNB422	pGAD-C1	[220]
pNB901	pGBD-C1 MXR2-Flag	This study
pNB902	pGAD-C1 <i>APE1</i>	This study
pNB903	pGAD-C1 ATG19	This study
pNB908	pGAD-C1 <i>APE1</i> Δ45	This study
pNB909	pGAD-C1 APE1 DM (M1L,M17L)	This study
pNB910	pGAD-C1 APEI M17L	This study
pNB911	pGAD-C1 APEI MIL	This study
pNB912	pGBD-C1 MXR1	This study
pNB356	p425 TEF	[222]
pNB357	p426 TEF	[222]
pNB904	p425TEF MXR2-Flag	This study
pNB905	p426TEF APEI-HA	This study
pNB906	p426TEF <i>ATG19-HA</i>	This study
pNB270	p426TEF MXR2-Flag	[70]
pNB399	pRS315	[223]
pNB398	pRS313	[223]
pNB913	pRS315 APEI	This study
pNB914	pRS315 APEI M17L	This study
pNB915	pRS313 <i>ATG19</i>	This study

**Table 3. Primers** 

Primer name	Sequence (5'-3')	Restriction site
NB815 MXR2 fwd	ATCGGGATCCATGAATAAGTGGAGCAGGC	BamHI
NB1048 MXR2 FLAG rev	GTTTAAACCTCGAGTTACTTGTCATCGTCATCCT TGTAATCGATGTCATGATCTTTATAATCACCGTCAT GGTCTTTGTAGTCGGGCCCGTCGACATCCTTCTTGA GGTTTAAAGACGC	XhoI
NB1101 FLAG	ACATGTCGACTTACTTGTCATCGTCATCCTTGTAAT CGATG	SalI
NB1164 Mxr2 deletion fwd	CCGATGATAGTTTAAATAAAGGGAGAAAGGAAGC AATATCAAAAACGGATCCCCGGGTTAATTAA	
NB1165 Mxr2 deletion rev	GTACGTATGCATACACACATATATATATATATATATATAT	
NB1362 ATG19 fwd	CTAGGATCCATGAACAACTCAAAGACTAACC	BamHI
NB1363 ATG19 rev	ATGGTCGACGAGTTCTTCCCAAGTCAG	SalI
NB1364 APE1 fwd1	CCCATCGATATGGAGGAACAACGTGAAATAC	ClaI
NB1365 APE1 rev	ATGGTCGACCAACTCGCCGAATTCATC	SalI
NB1399 ATG19 HA rev	ATGCTCGAGCTAAGCATAATCTGGAACATCATATG GATAGTCGACGAGTTCTTCCCAAGTCAG	XhoI

NB1400 ATG19 5' UTR fwd	CTAGCGGCCGCTGAGAAGCAATTGTGA	NotI
NB1401 ATG19 5' UTR rev		
NB1404 APE1 fwd2	CTAAAGCTTATGGAGGAACAACGTGAAATAC	HindIII
NB1405 APE1 HA rev	ATGGTCGACCTAAGCATAATCTGGAACATCATATG GATAAGATCTCAACTCGCCGAATTCATC	SalI
NB1406 APE1 5' UTR fwd	CTAGCGGCCGCGTCAGCTTCTACTTTAG	NotI
NB1499 APE1 fwd3	CCCACTAGTATGGAGGAACAACGTGAAATAC	SpeI
NB1511 APE1 3' UTR rev	ATGGGGCCCCTTATTGCTTATTTGGCCC	ApaI
NB1563 APE1 Δ45 rev	CCCATCGATATGGAGCACAATTATGAGGATATTG	ClaI
NB1633 APE1 DM fwd	CCCATCGATCTGGAGGAACAACGTGAAATACTGGA ACAATTGAAGAAAACTCTGCAGCTGCTAAC	ClaI
NB1645 APE1 M1L fwd	CCCATCGATCTGGAGGAACAACGTGAAATAC	ClaI
NB1674 APE1 5' UTR rev	ATGACTAGTTCTTTTTTTTTTAATTTTGTTGGTTGTC	SpeI
NB1675 APE1 M17L fwd	CCCACTAGTATGGAGGAACAACGTGAAATACTGGA ACAATTG AAGAAAACTCTGCAGCTGCTAAC	SpeI
NB1678 MXR1 fwd	CTAGAATTCATGTCGTCGCTTATTTCAAAAACC	EcoRI

NB1679 MXR1 rev	ATGGGATCCCATTTCTCTCAGATAATGAGTA	BamHI
NB758 ACT1 RT fwd	GAAATCACCGCTTTGGCTCC	
NB759 ACT1 RT rev	GTGGTGAACGATAGATGGACCA	
NB1621 APE1 RT fwd	CGTCAACCACCTCTACAA	
NB1622 APE1 RT rev	TGGCCATATGACCGTTAG	
NB1623 ATG19 RT F P	TTACAGGCATCCCAAGAG	
NB1624 ATG19 RT R. P	TGTCGTCACCGTCATAAG	

#### 2.2.2. Media and Growth conditions

Yeast cells of the mid-log phase ( $A_{600}$  = approximately 0.8–1) were used for all experiments, where strains were grown at 30 °C either in synthetic medium with dextrose [0.67% yeast nitrogen base (Becton Dickinson, 291940), 2% dextrose (Himedia, GRM077), and supplemented auxotrophic amino acids and vitamins as needed, pH 5.5] as described previously [224] or in synthetic minimal medium, where specific auxotrophic nutrient needed for plasmid DNA selection in the experiment was not supplemented. To induce autophagic condition, where APE1 expression increases, cells grown up to mid-log phase were incubated in nitrogen starvation medium [0.17% yeast nitrogen base having neither ammonium sulfate nor amino acids (Becton Dickinson, 233520), and 2% dextrose]. For imparting oxidative stress, cells from mid-log phase were treated with 2 mM H<sub>2</sub>O<sub>2</sub> for 2 h at 30 °C. Yeast cell were transformed with plasmids using lithium acetate and single-stranded carrier DNA, as described [225]. For yeast two hybrid analysis, transformants

carrying yeast two hybrid constructs were grown, serially diluted, and spotted on selection plates and then incubated at 30 °C for 2 to 3 days, as described [226].

# 2.2.3. Whole cell lysate preparation and Immunoblotting

Yeast cells of  $A_{600nm}$  3.0 were harvested and washed with water to prepare whole cell lysate. The washed cells were then resuspended in freshly prepared 200  $\mu$ l lysis buffer [1.85 M NaOH (Himedia, MB095), 7.4% β-mercaptoethanol (Sigma- Aldrich, M3148)] and incubated on ice for 10 min. An equal volume of 50% trichloroacetic acid (Himedia, GRM6274) was then added to the cell suspension, mixed and incubated on ice for another 10 min. After incubation, the cell suspension was centrifuged at 13,000 R.P.M for 2 min at 4°C. The protein pellet was then washed with 500 µl 1M Tris (Sigma-Aldrich, T6066) solution (not pH adjusted), without resuspending the pellet, by centrifugation at the same speed. The pellet was resuspended in 30  $\mu$ l 1× Laemmli buffer and heated at 95 °C for 5 min. The protein samples were centrifuged at 13,000 RPM for 5 min after cooling down to collect the supernatant. Ten microliters of the supernatant, equivalent to 1 A<sub>600nm</sub> cells, were then analyzed via SDS-PAGE. After electrophoresis, Western blot was performed following standard protocols. Immunoblotting was done with standard procedures with anti-FLAG antibody (Sigma-Aldrich, F3165, 1:2000), anti-HA antibody (Proteintech, 66006-2-Ig, 1:5000), anti-Pgk1 serum (kind gift from Prof. Debkumar Pain, New Jersey Medical School, Rutgers University), anti- Apel antibody (kind gift from Dr Claudine Kraft, Institute for Biochemistry and Molecular Biology, University of Freiburg), Horseradish peroxidase-conjugated anti-rabbit polyclonal antibody (Jackson Laboratories, 111-035-144, 1:25,000), anti-mouse polyclonal antibody (Jackson Laboratories, 115-035-146, 1:25,000). Immunoblotting signals enhanced by enhanced chemiluminescence reagents (Advansta WesternBright, K-12045- D20) were detected in the Chemidoc imaging facility (Bio-Rad). Immunoblot images were quantified using Fiji software (http://imagej.net), followed by statistical analysis using GraphPad Prism8.

#### 2.2.4. Coimmunoprecipitation

Cells, harvested for co-IP assay, were washed, and then resuspended in NP-40 lysis buffer [50 mM Tris–HCl buffer pH8, 150 mM NaCl (Himedia, GRM031), 2 mM EDTA

(Amresco, 0105), 2 mM MgCl<sub>2</sub> (SRL, 69396), 1% NP-40 (Sigma-Aldrich, I8896),  $1\times$  Protease inhibitor cocktail (Roche, 04693132001)]. Resuspended cells were then lysed with glass beads using the bead-beating method. The cell lysate was centrifuged at 12,000 R.P.M. for 12 min to remove the cell debris and supernatant with soluble protein fraction was collected. After protein estimation with Lowry reagents, 1 mg of the supernatant was incubated with 10  $\mu$ l of Protein A/G PLUS-Agarose beads (Santacruz Biotechnology, SC-2003) in an end-over-end rotator at 4 °C for 2 h, for pre-clearing step. The precleared supernatant was then incubated with anti-FLAG antibody at the same condition for overnight incubation. For binding of the antibody with the beads, 30  $\mu$ l of protein A/G beads were added to the mix and again incubated at the same condition for 4 h. After incubation, beads were collected and washed three times with the lysis buffer and then analyzed *via* SDS-PAGE, followed by immunoblotting with anti-FLAG, anti-HA, and anti-APE1 antibodies.

#### 2.2.5. Cycloheximide Chase Assay

For the cycloheximide chase assay, strains were grown up to mid-log phase either in synthetic complete medium or synthetic minimal medium, as required, and then harvested. Harvested cells were then subjected to cycloheximide [Sigma- Aldrich, C7698] treatment (50 or  $100 \mu g/ml$ ) for different durations (0, 10, 30, 60, and 120 min). After each time point, cells were harvested and subjected to whole cell lysate preparation followed by the analysis of the protein degradation profile by immunoblotting with anti-Ape1 antibody.

#### 2.2.6. RNA extraction, cDNA synthesis, and qRT-PCR

For RNA extraction, cells were harvested after growing up to mid-log phase. Total RNA was extracted using the hot acid phenol method described in [227]. To remove DNA contamination, extracted RNA was subjected to DNase digestion, where 3  $\mu$ g of RNA was incubated with 1 Unit of DNase I (Thermo Fisher Scientific, EN0521) at 37 °C for 2 h followed by DNase inactivation by incubating the mix with EDTA at 65°C for 2 min. DNase treated RNA was subjected to complementary DNA (cDNA) synthesis using Verso cDNA Synthesis Kit (Thermo Fisher Scientific, AB1453A) as per kit protocol, where 1  $\mu$ g of RNA was used and incubated at 42°C for 35 min followed by inactivation

at 95 °C for 2 min, along with the kit reagents. One  $\mu$ g of cDNA was diluted to a final concentration of 40 ng/ $\mu$ l, and 1  $\mu$ l of cDNA was analyzed via qRT-PCR in a final volume of 10  $\mu$ l reaction mix with the PowerUp SYBR Green PCR Master mix (Applied Biosystems, A25742) using a Quanstudio 3 Real-Time PCR System.

#### 2.2.7. Leucine aminopeptidase (LAP) assay

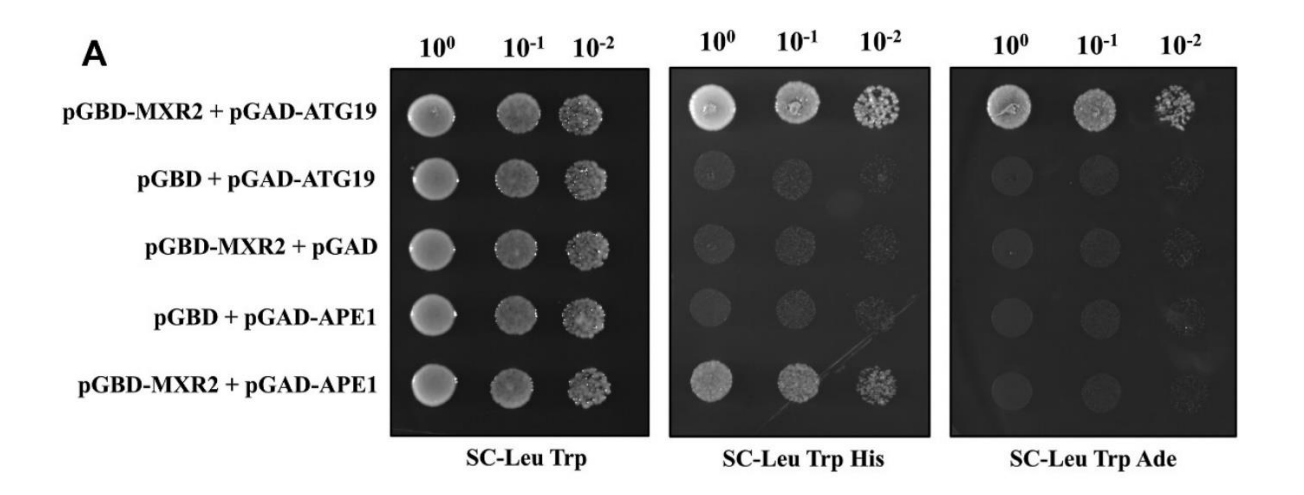
For LAP activity assay, the respective strains were grown in minimal medium up to midlog phase and harvested. Cell lysates were prepared using lysis buffer previously described for performing co-immunoprecipitation. Fifty micrograms of cell lysate were used for each reaction. A total volume of 500  $\mu$ l of reaction mixture was prepared consisting of 400  $\mu$ l of 75 mM Tris–HCl pH-7.5, 50  $\mu$ l 20 mM leucine para nitroanilide (Sigma-Aldrich, L9125) and 50  $\mu$ g of cell lysate and incubated at 30 °C for 15, 30, and 45 mins time points. After incubation, spectrophotometric analysis was performed at 405 nm and  $\mu$ mol of product formed/mg of cell lysate was calculated according to the equation mentioned in Figure 5B.

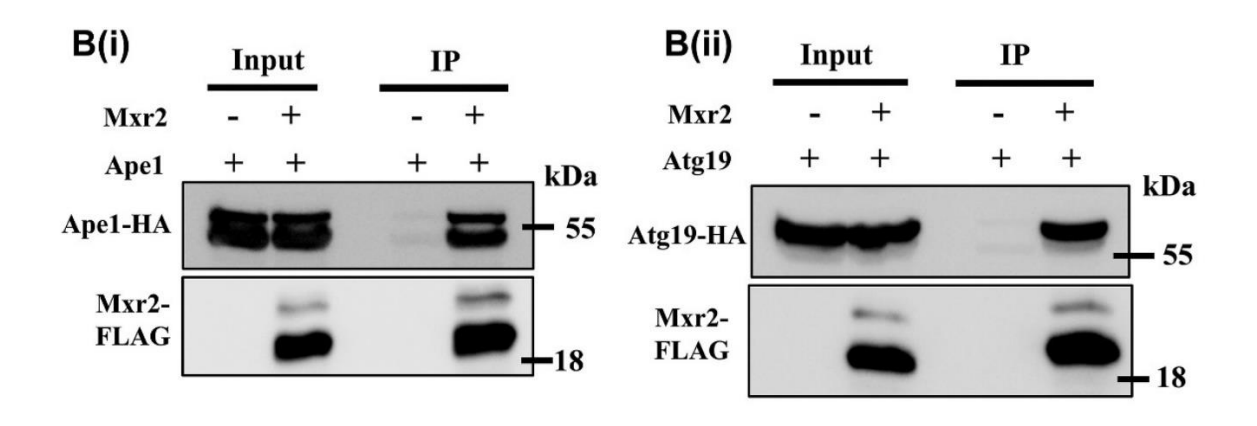
#### 2.3. RESULTS

# 2.3.1. Mxr2 interacts with Ape1 and Atg19 of the Cvt pathway

To identify potential cytosolic substrates of Mxr2, we studied the high throughput data of yeast interactome. The data predicted Atg19 and Ape1 of the Cvt pathway to be probable substrates of Mxr2 [210]. To validate this finding, a yeast two-hybrid assay was performed as described in the materials and methods. We find that Mxr2 strongly interacts with Atg19 and weakly with Ape1 as transformants carrying *MXR2* with *APE1* constructs cannot grow on the SC- Leu-Trp-Ade medium plate (Fig. 1A). To further confirm these interactions, we overexpressed *MXR2* with a 3x FLAG tag from the p426 vector and *ATG19* or *APE1* with a hemagglutinin (HA) tag from the p425 vector under the TEF1 promoter in *mxr2*\$\Delta\$ strain. Next, immunoprecipitation with FLAG antibody was carried out after growing the above strains as described in the materials and methods. Immunoprecipitation results showed that Atg19 and Ape1 proteins interact with Mxr2 *in vivo*. To confirm the specificity of Mxr2 interaction with Atg19 and Ape1, we included Mxr1, which acts on S-methionine sulfoxide in the yeast two-hybrid assay. Unlike Mxr2,

Mxr1 does not interact with Atg19 or Ape1 (Fig. 1C). Based on yeast two-hybrid and immunoprecipitation results, we show that Mxr2 interacts specifically with Atg19 and Ape1, which are crucial components of the Cvt pathway.





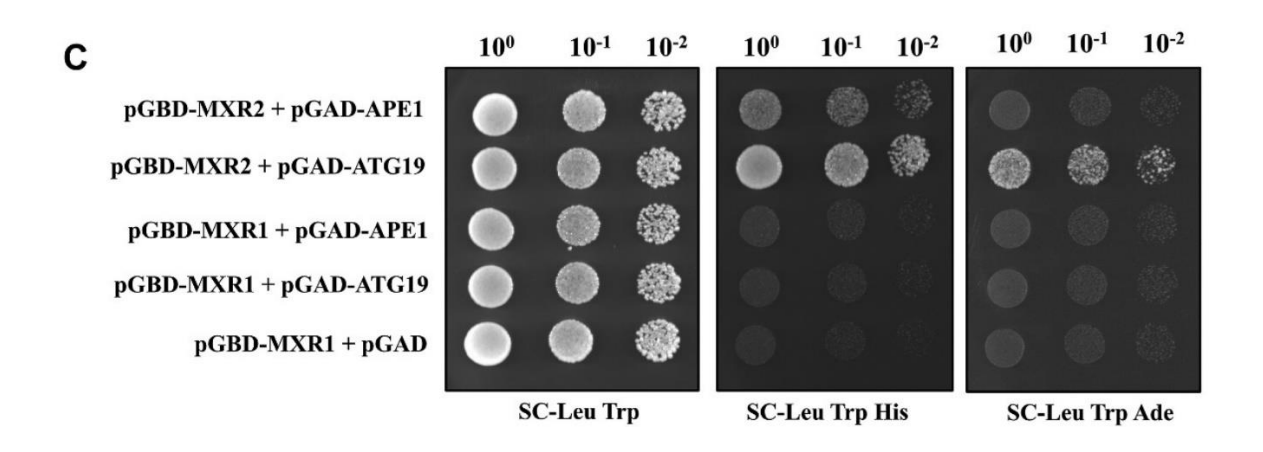


Figure 1. Mxr2 interacts with the Cvt pathway proteins, Atg19 and Ape1. A, yeast two-hybrid assay was performed between Mxr2 and Atg19 or Ape1. The PJ69-4A strain was transformed with pGBD-C1 (expressing MXR2) and pGAD-C1 (expressing APE1 or ATG19) plasmids. Transformants were then grown in the presence and absence of histidine and adenine at 30 °C for 2 days. B(i), coimmunoprecipitation assay between Mxr2 and Ape1 (ii) co-immunoprecipitation assay between Mxr2 and Atg19.  $mxr2\Delta$  cells expressing Mxr2-FLAG and either Ape1-HA or Atg19-HA were grown in a minimal medium lacking leucine and uracil up to the mid-log phase.  $mxr2\Delta$  cells not expressing Mxr2 were kept as the negative control.

# 2.3.2. Mxr2 protects Ape1 and Atg19 proteins from oxidative stress and premature degradation

To gain insights into the physiological role of Mxr2 in the context of the Cvt pathway, we initially looked at whether Mxr2 affects prApe1 maturation. To investigate this, an Ape1 maturation assay was performed in wt,  $mxr2\Delta$ , and  $atg19\Delta$  strains under normal and nitrogen starvation conditions as described in the materials and methods. Strains were grown to the mid-log phase before being exposed to nitrogen starvation for 0 or 4 h. Next, cells were lysed, and lysates resolved on SDS-PAGE, Western transferred and immunoblotted with anti-Ape1 antibody. Immunoblotting results showed two distinct bands of molecular weights, 62 kDa and 50 kDa, corresponding to the prApe1 and mature Ape1 (mApe1) in the wt control strain (Fig. 2Ai). As expected, the expression of Ape1 increased upon nitrogen starvation in the wt strain (Fig. 2Ai) [228]. In the absence of Atg19, maturation of Ape1 is abolished in control and nitrogen-starved cells (Fig. 2Ai).

Intriguingly, the deletion of MXR2 does not affect the maturation process of Ape1. However, the Ape1 protein level is significantly reduced compared to wt cells in control and nitrogen-starved cells (Fig. 2Ai). As we observed the interaction of Mxr2 and ATG19 along with Ape1, we also looked at the expression of HA-tagged Atg19 in wt and  $mxr2\Delta$  strains (Fig. 2Aii). As speculated, the protein expression of HA-Atg19 from the pRS313 vector shows a modest decrease in  $mxr2\Delta$  than the wt strain (Fig. 2Aii).

The apparent decrease in protein levels of Ape1 and Atg19 could be a cascading effect of a decline in their transcription. To determine if this is true, we examined the transcript levels of APE1 and ATG19 after isolating total RNA from wt and  $mxr2\Delta$  strains. Quantitative reverse transcription PCR (qRT- PCR) results revealed no significant difference in the mRNA levels of both genes in *the mxr2* $\Delta$  strain compared to the wt strain (Fig. 2B).

Considering the above results, we hypothesized that Mxr2 protects Ape1 and Atg19 from oxidative stress and degradation. To test this hypothesis, the turnover rate of Apel was monitored in wt and  $mxr2\Delta$  strains. Cells were grown to the mid-log phase before treating them with cycloheximide for 2 h to stop the translation of new proteins. Temporal protein degradation monitoring was done by regularly harvesting cells during cycloheximide treatment. Western blotting was carried out on harvested cells as described in the material and methods. The blots were probed with Ape1 and Pgk1 antibodies, the latter as a loading control (Fig. 2C). At zero time points, the Ape1 protein levels in both strains appear comparable (Fig. 2C). However, at the end of 2 h, the  $mxr2\Delta$  strain significantly deviates from the wt strain as the Ape1 protein undergoes almost 60% degradation compared to 20 to 25% in the wt strain (Fig. 2C). Our results demonstrate that in the absence of Mxr2, the Apel protein is susceptible to premature degradation. To ensure that the protective function of Mxr2 on Ape1 is not a generic function of all MSRs, we monitored the steadystate levels of Ape1 in wt and  $mxr1\Delta$  strains under nitrogen starvation, as described earlier. In contrast to the decreased level of Ape1 in *mxr2∆* strain compared to WT strain under nitrogen starvation duress (Fig. 2Ai), there is no change in Ape1 level in  $mxr1\Delta$  strain (Fig. 2D). This result underscores the specificity of Mxr2 action on Ape1.

Our previous study [105] found excess ROS in the *mxr2∆* strain compared to the wt strain. If the ROS-triggered anti- oxidant function of Mxr2 is driving its protective function on Ape1 and Atg19, increased oxidative stress should also affect the stability of these proteins. To ascertain if this assumption is accurate, we first treated wt strain expressing HA-Atg19 with 2 mM H<sub>2</sub>O<sub>2</sub> for 2 h to induce the production of ROS. After that, we checked for the protein levels of Ape1 and HA-Atg19 by Western blotting (Fig. 2E). H<sub>2</sub>O<sub>2</sub> treatment led to a sig- nificant reduction in the steady-state level of both proteins (Fig. 2E). The above results suggest that Mxr2 protects Ape1 and Atg19 from oxidative stress and premature degradation.

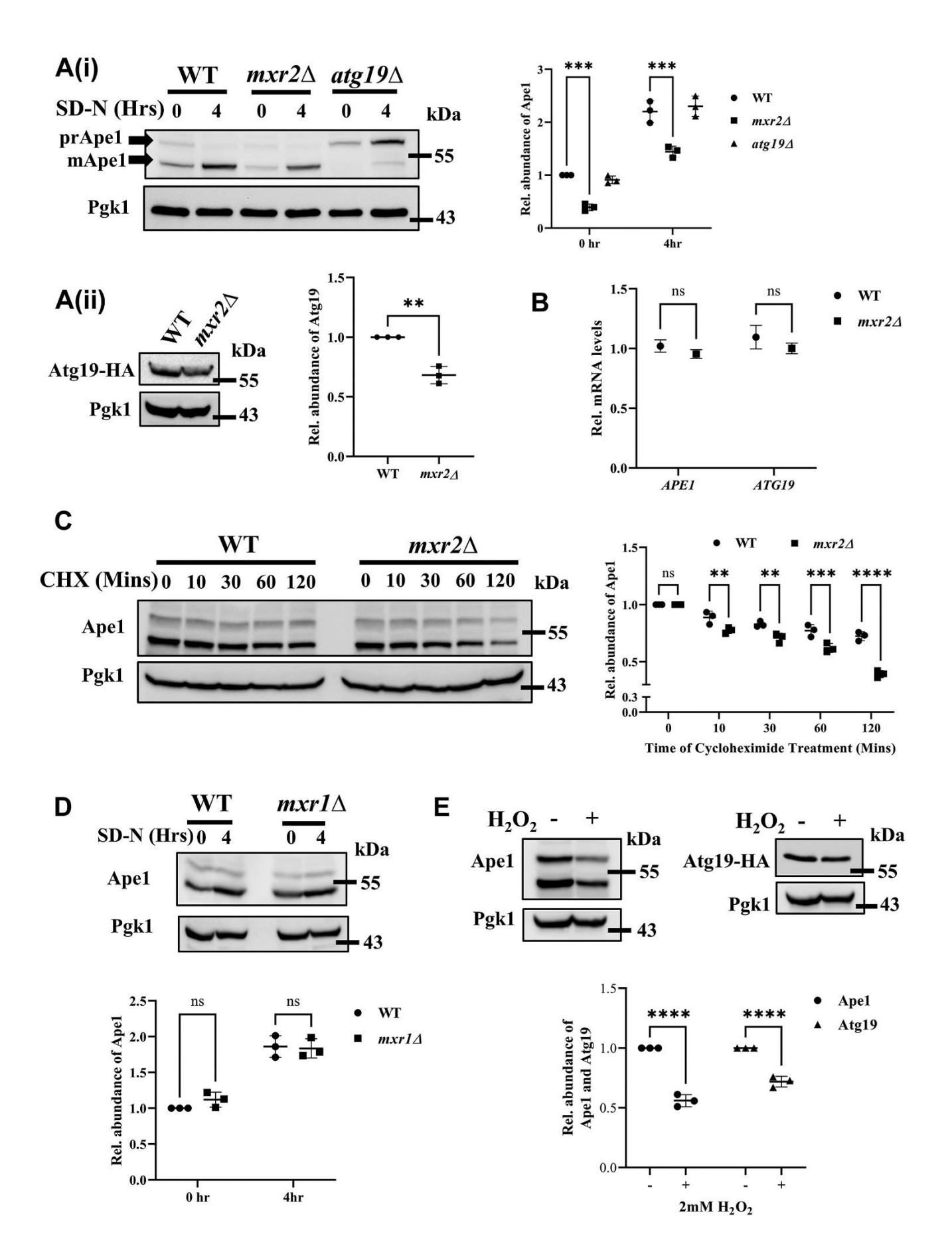


Figure 2. Mxr2 protects Ape1 and Atg19 proteins from oxidative stress-mediated degradation. A, analysis of the steady-state level of (i) the Ape1 protein in wt, mxr2Δ, and  $atg19\Delta$  and (ii) the Atg19 protein in wt and  $mxr2\Delta$  strains. For (i) wt,  $mxr2\Delta$ , and  $atg19\Delta$  strains were grown and then either left untreated or exposed to nitrogen starvation for 4 h, whereas for (ii) wt and mxr2Δ strains transformed with Atq19-HA CEN constructs and grown up to mid- log phase. Harvested cells were analyzed via Western blotting using either anti-Ape1 antibody (i) or anti-HA antibody (ii). B, APE1 and ATG19 transcript levels were checked in wt and mxr2Δ strains via qRT-PCR analysis. C, cycloheximide chase assay. wt and mxr2\Delta strains were grown up to midlog phase and treated with 50 µg of cycloheximide for 2 h, and then the Ape1 turnover profile was checked via Western blotting with anti-Ape1 antibody. D, wt and  $mxr1\Delta$  strains were grown and left untreated or exposed to nitrogen starvation for 4 h. The steady-state level of Ape1 protein was checked in these conditions via Western blotting. E, degradation of the Ape1 protein under oxidative stress. wt strain was treated with 2 mM H<sub>2</sub>O<sub>2</sub> for 2 h. Treated and untreated cells were analyzed for steady-state levels of Ape1 and Atg19 via Western blot. To monitor the Atg19 steady-state level, wt strain transformed with the CEN construct of Atq19-HA was used. The data shown are the mean ± SD of three biologically independent experiments and full-length blots are represented in supporting information 1. Statistical analysis was done using an unpaired Student's t test for (B), whereas for (A) and from (C-E), it was done using a two-way ANOVA test. \*\*\*\*p < 0.0001, \*\*\*p < 0.001, \*\*p < 0.01 and \*p < 0.05. ns, nonsignificant. HA, hemagglutinin; gRT-PCR; quantitative reverse transcription PCR.

# 2.3.3. Amino acid methionine 17 in Ape1 is required for interaction with Mxr2

Yeast Ape1 exists in two intracellular protein pools, prApe1 and mApe1. The N-terminal 45 amino acid propeptide is cleaved by Pep4 protease in the vacuole to generate a 55 kDa intermediate form (iApe1) before being finally converted into the 50 kDa mature form (mApe1) by proteinase B (PRB1) [229]. Yeast two-hybrid (Fig. 1A) and immunoprecipitation (Fig. 1Bi) assays show that Mxr2 can interact with prApe1. To determine if Mxr2 can also interact with vacuolar processed Ape1 by yeast two-hybrid, we first amplified the Ape1 without the propeptide resembling the iApe1 (Ape1⊿ 2–45aa) and cloned it into the pGAD-C1 vector as described in the materials and methods. Yeast two-hybrid was performed, and we observe that Mxr2 interacts with full-length Ape1 (prApe1) (Fig. 3A), as observed above (Fig. 1A); however, it fails to interact with iApe1 implying that the propeptide is essential for Mxr2 to interact with Ape1.

Mxr2 binds to oxidized methionine residues in the proteins to reduce them [230]. Our earlier study [70] showed that Mxr2 interacts with Mge1 in a manner that is dependent on methionine 155, as substitution of methionine with leucine at 155 in Mge1 abolishes the interaction. Ape1 contains a total of six methionine residues, of which two are present in the propeptide (M1 and M17), and the remaining four are present in the mature peptide (M277, M312, M420, and M478). Since mApe1 does not interact with the Mxr2, we

hypothesized that the association of Mxr2 with prApe1 may depend on M1 or M17 or both residues in Ape1. Site-directed mutagenesis generated three prApe1 constructs in the pGAD-C1 vector where M1, M17, or both (DM) were substituted with leucine for yeast two-hybrid studies. Both wt prApe1 and prApe1 M1L interact with Mxr2 (Fig. 3B). Strikingly, neither prApe1 M17L nor prApe1 M1L M17L exhibited any interaction with Mxr2 (Fig. 3B). To further confirm this result, we performed coimmunoprecipitation. First, we constructed plasmids that expressed *APE1* wt or *APE1* M17L mutant under its native promoter. Next, *the ape1*\Delta strain was transformed with wt *APE1* or *APE1* M17L plasmid and the plasmid expressing FLAG-MXR2 under the TEF1 promoter. Coimmunoprecipitation was carried out using the FLAG antibody as described in the materials and methods (Fig. 3C). WT Ape1 coprecipitates with FLAG-Mxr2, whereas the M17L mutant does not. Significantly, only the premature form of Ape1, not the mature form, precipitates with FLAG-Mxr2. These results reinforce the pivotal role of M17 in prApe1 interaction with Mxr2.

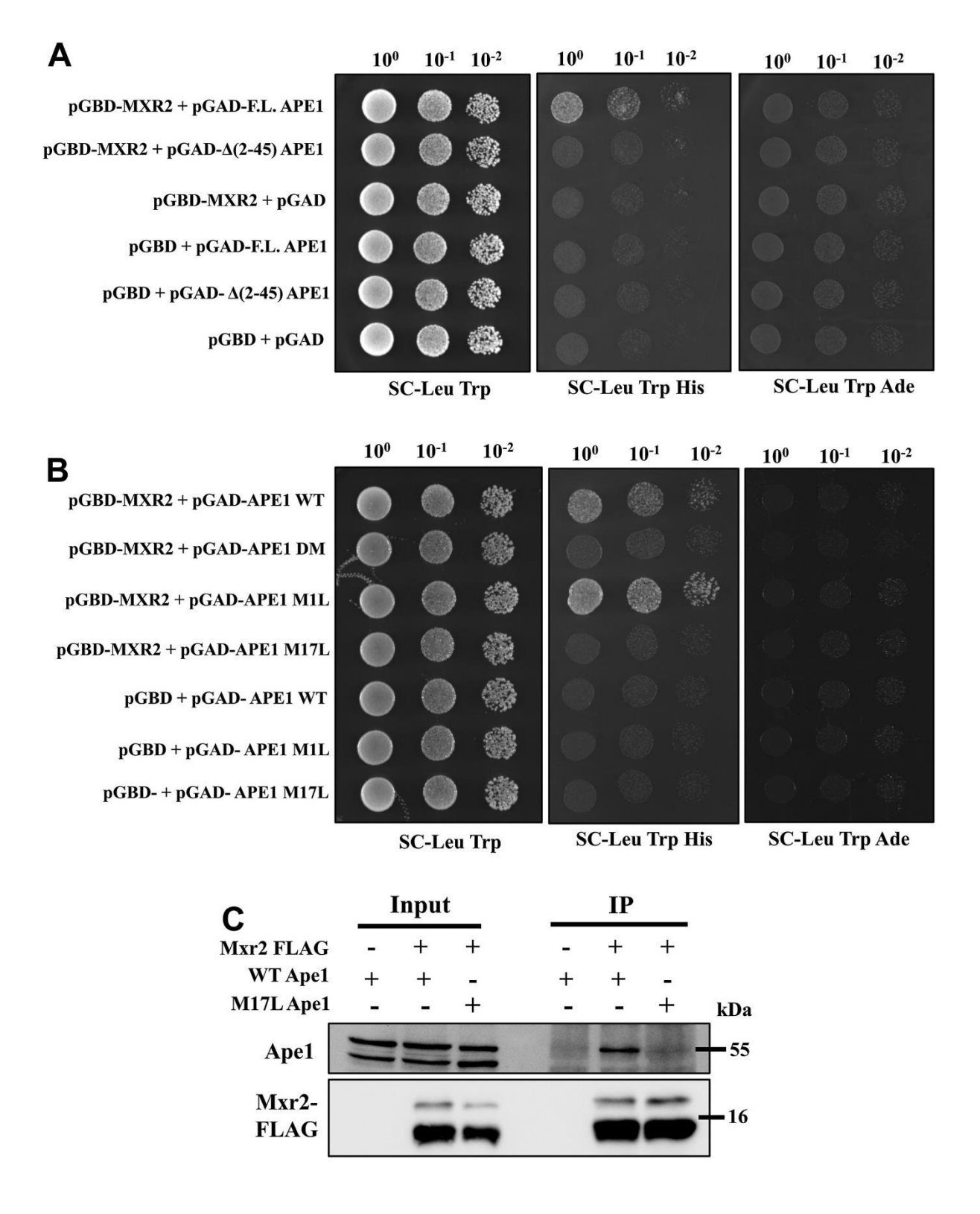
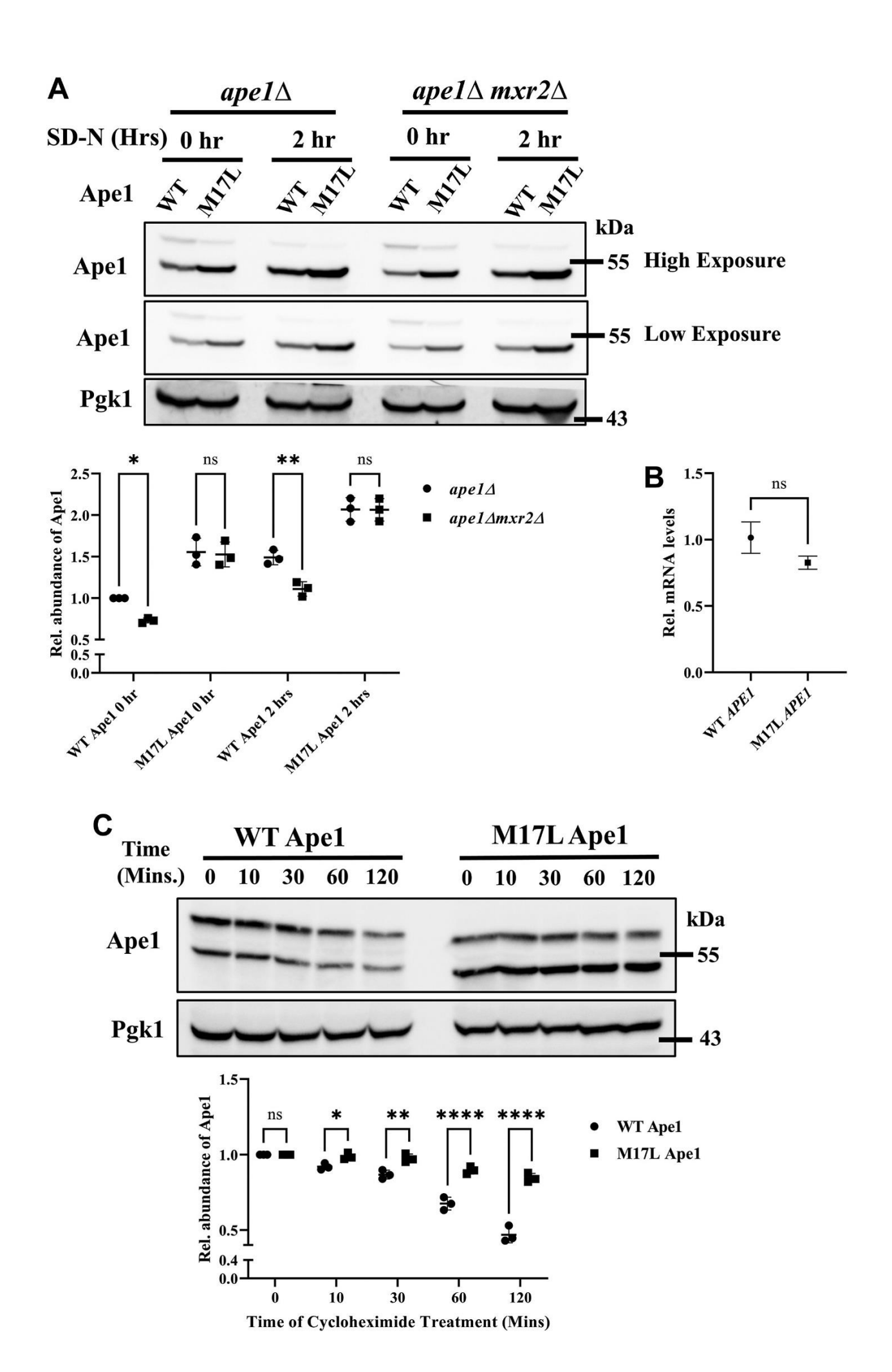


Figure 3. Mxr2 interacts exclusively with M17 residue of Ape1. A, yeast two-hybrid experiment between Mxr2 and either full-length or  $\Delta$  (2–45aa) Ape1 constructs was carried out. The PJ69-4A strain was transformed with yeast two-hybrid vector constructs expressing indicated proteins. B, yeast two-hybrid experiment between Mxr2 and different methionine mutant constructs (M1L; M17L; M1L, M17L) of Ape1. C, coimmunoprecipitation assay between Mxr2 and wt or M17L mutant Ape1.  $mxr2\Delta ape1\Delta$  cells expressing Mxr2-FLAG and either wt or M17L Ape1 were grown up to the mid-log phase. The  $mxr2\Delta ape1\Delta$  cells transformed with wt Ape1 alone were

used as a negative control. The anti-FLAG antibody was used to precipitate the Ape1 protein. Immunopre- cipitated proteins were then detected *via* Western blots using anti-Ape1 and anti-FLAG antibodies. Spotting assay and the immunoprecipitation experiments were conducted twice.

### 2.3.4. M17L mutation confers increased stability to Ape1

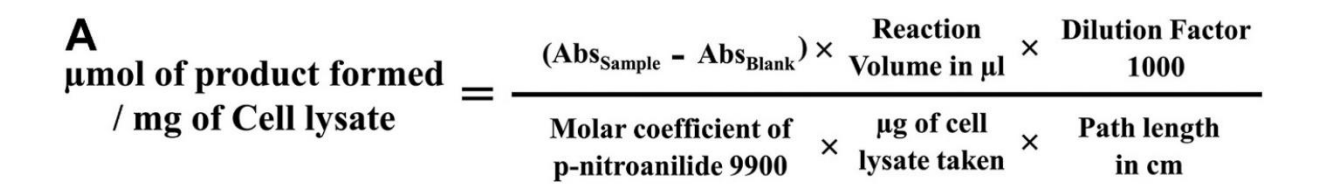
Oxidative stress triggers methionine oxidation in proteins, making them dysfunctional and vulnerable to degradation. Mxr2 has the innate ability to recognize oxidized methionine within proteins, bind, and reduce it. Counterintuitively, we speculated what would happen if the methionine is mutated into an amino acid that cannot be oxidized. The protein will probably be insensitive to oxidative stress and become stable, and Mxr2 will not interact with the protein. If this is true, we reasoned that Ape1 M17L should resist oxidative stress and be highly stable. We expressed wt or M17L Ape1 protein from a pRS315 vector in apel $\Delta$  and apel $\Delta$ mxr2 $\Delta$  strains to validate this thinking. The steadystate level of Ape1 protein was assessed as described earlier by immunoblotting with Ape1 antibody after exposure to 0 or 2 h of nitrogen starvation. Similar to earlier results (Fig. 2Ai), the steady-state level of wt Apelis reduced in the  $apel\Delta mxr2\Delta$  strain in comparison to the apel∆ strain (Fig. 4A), reinforcing the impact Mxr2 has on the stability of Apel. Consistent with our reasoning, the Apel M17L mutant is highly stable as it is present at a significantly higher concentration than wt Ape1 with or without nitrogen starvation and in both strains (Fig. 4A). Deletion of MXR2 does not affect the stability of Ape1 M17L (Fig. 4A). Ape1 M17L appears immune to oxidative stress and degradation. To rule out the possibility of increased expression of Apel M17L compared to wt Apel, we isolated total RNA from cells expressing wt and Ape1 M17L and measured their transcription levels. The transcription of both genes is comparable, and no significant difference is observed (Fig. 4B). To verify that Ape1 M17L is less prone to turnover and thereby more stable, we performed the cycloheximide chase assay on  $apel\Delta$  cells expressing either wt or M17L mutant Ape1. We observe nearly 45 to 50% wt Ape1 protein degradation at the end of 2 h (Fig. 4C). Significantly and in contrast, Apel M17L is robust by displaying a mere 10% degradation (Fig. 4C).



**Figure 4. M17L mutant Ape1 resists degradation.** *A*,  $ape1\Delta$  and  $ape1\Delta mxr2\Delta$  strains expressing either wt or M17L mutant Ape1 were grown up to mid- log phase and further exposed to nitrogen starvation for 2 h or left untreated. Harvested cells were lysed and analyzed via Western blot. *B*, wt and M17L mutant Ape1 expressing cells were assessed to check the transcript level of Ape1. *C*, cells harboring wt and M17L Ape1 were grown and subjected to cycloheximide treatment for five different time points for up to 2 h. Harvested cells were analyzed via Western blot. Data is represented as mean  $\pm$  SD of three independent experiments. Statistical analysis was done using an unpaired Student's t test for ( $taurred{B}$ ), whereas for ( $taurred{A}$  and  $taurred{C}$ ), it was done using a two-way ANOVA test. \*\*\*\* $taurred{P}$  < 0.0001, \*\*\* $taurred{P}$  < 0.01 and \* $taurred{P}$  < 0.05. ns, nonsignificant.

# 2.3.5. *mxr2* strain exhibits decreased LAP activity

Apel is a vacuolar resident leucine aminopeptidase (LAP), which cleaves N-terminal leucine residues. The enzyme is a member of the M18 class of zinc metalloproteases [231-233]. Saccharomyces cerevisiae has four leucine aminopeptidases: Lap1/Ape2, Lap2, Lap3, and Lap4/Ape1 [233]. As the deletion of MXR2 affected the stability of Ape1, we reasoned that it may additionally affect its activity. To check this, we carried out the LAP activity assay. As the yeast cell harbors redundant LAPs, we measured the LAP activity in three strains, wt,  $mxr2\Delta$ , and  $ape1\Delta$  strains. Generally, leucine- $\beta$ -naphthylamide or leucine-para-nitroanilide are used as substrates to assess the LAP activity. Both substrates generate fluorescent products after the reaction, which can be monitored in a spectrophotometer. Trumbly J. R. et al. showed that leucine-para-naphthylamide is the preferred substrate for Ape1 as it exhibits more activity with this substrate over the others [233,234]. Hence, we used leucine-para-naphthylamide as the substrate in our assays, as described in the materials and methods. Cell lysates from the above three strains were used to perform the aminopeptidase assay, where  $\mu$ mol of product formed/mg of cell lysate was measured as described (Fig. 5A). The amount of product formed in the  $mxr2\Delta$  strain is comparable to that in *the apel∆* strain; however, it is significantly lower than the wt strain (Fig. 5B). These results imply that the Ape1 enzyme molecules in  $mxr2\Delta$  are oxidatively modified and less active.



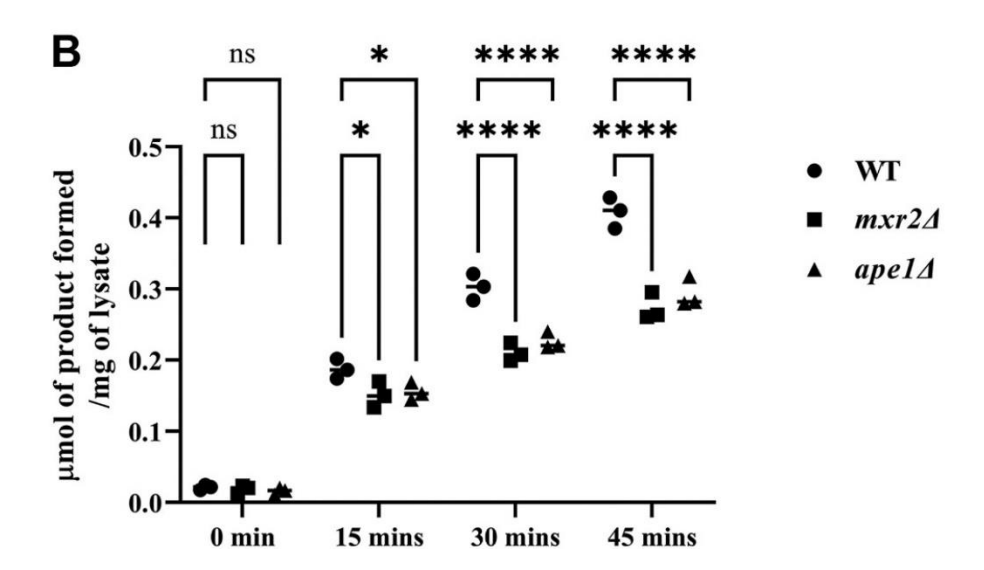


**Figure 5. Leucine aminopeptidase activity decreases in** *mxr2*Δ **strain.** *A*, equation to estimate amount (μmol) of product formed/mg of lysate in leucine aminopeptidase assay. *B*, wt, mxr2Δ and ape1Δ cells were grown up to log phase, and cells lysates were prepared to check the leucine aminopeptidase activity of the cells. Fifty micrograms lysate from each strain was then incubated with leucine p-nitroanilide substrate for up to 45 min as described under methods. Samples were analyzed in a spectrophotometer by measuring their absorbance at 405 nm, and μmol of product formed was calculated for the three strains. Data are represented as mean ± SD of three independent experiments. Statistical analysis was done using a two-way ANOVA test. \*\*\*\*p <0.0001, \*\*\*p < 0.001, \*\*p < 0.01 and \*p < 0.05. ns, nonsignificant.

# 2.3.6. Mxr2 helps in maintaining the stoichiometry of Ape1 and Atg19 in Cvt pathway

After the Ape1 complex formation, Atg19 interacts with Ape1, facilitating communication and association with other Atg proteins, including Atg8 and Atg11, to form Cvt vesicles. Considering the above information, we inquired whether overexpression of Atg19 alone or with Mxr2 can rescue the unstable phenotype of Ape1 in *the mxr2* $\Delta$  strain. HA-tagged *ATG19* plasmid alone or with FLAG-tagged *MXR2* plasmid were overexpressed in wt and *mxr2* $\Delta$  strains. The strains were grown until the mid-log phase before being exposed to nitrogen starvation for 4 h. As described earlier, cells were harvested, Western blotted, and

probed with Ape1, HA, FLAG, and Pgk1 (loading control) antibodies (Fig. 6). Intriguingly, instead of rescuing the instability phenotype of Ape1, over-expression of Atg19 exacerbates the phenotype in not only *the mxr2* $\Delta$  strain but also destabilizes Ape1 in the wt strain (Fig. 6). This could be due to imbalanced stoichiometry of both the protein in the system. This effect is observed under normal physiological and nitrogen starvation conditions (Fig. 6). Interestingly, additional overexpression of Mxr2 does not improve the stability of Ape1 in wt or  $mxr2\Delta$  strain under physiological conditions (Fig. 6). Strikingly, under nitrogen stress, Mxr2 overexpression restores the steady-state level of Ape1 in wt and  $mxr2\Delta$  strains to that observed in wt cells transformed with an empty vector (Fig. 6). Moreover, Ape1 in *the mxr2* $\Delta$  strain exhibits increased stability in the presence of Mxr2 overexpression (Fig. 6). We conclude that Mxr2 acts as a shield protecting Ape1 and Atg19 from premature degradation during oxidative stress and thus maintains their stoichiometry for proper functioning of the Cvt pathway.

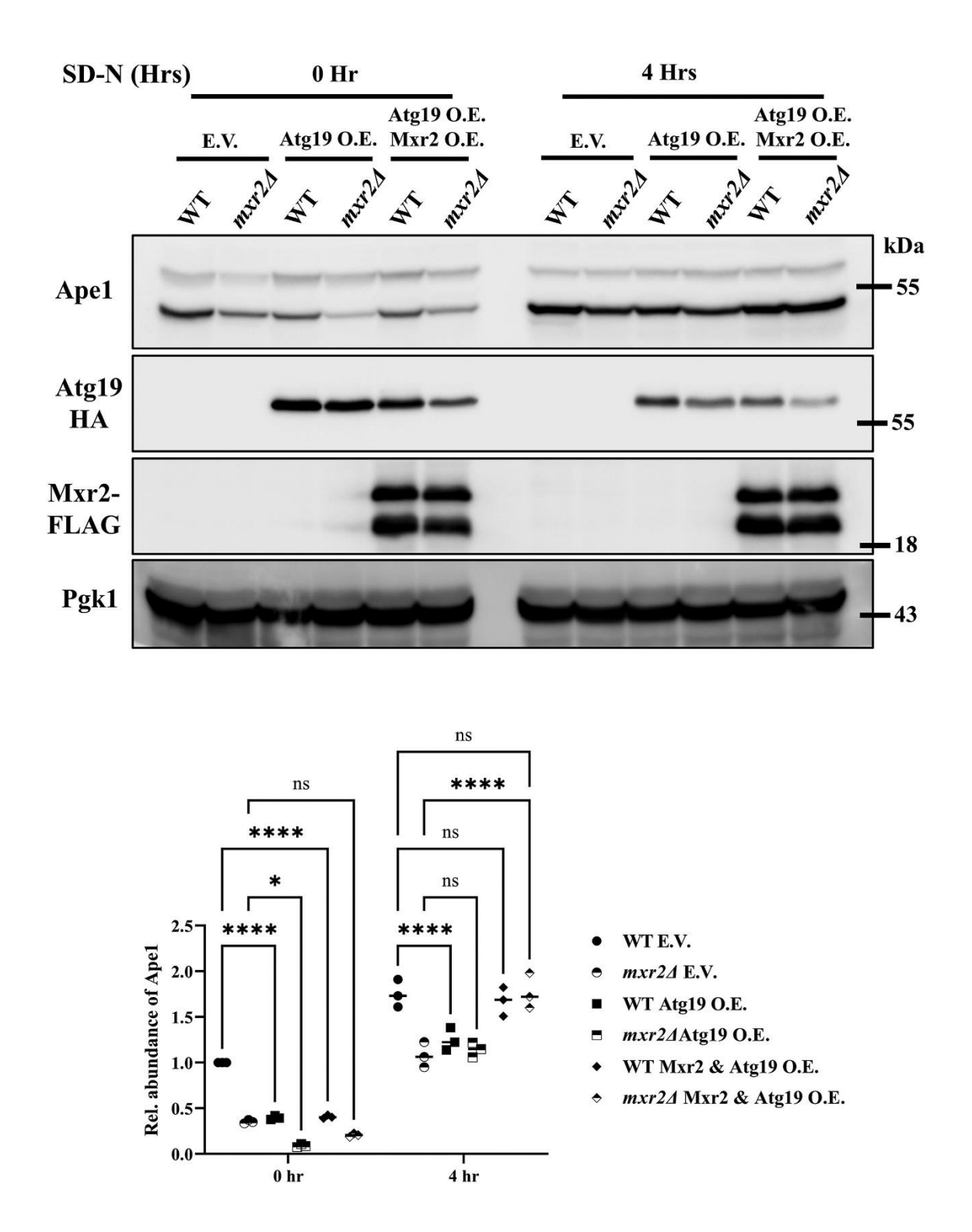


Figure 6. Mxr2 maintains stoichiometry of Atg19 and Ape1 in the Cvt pathway. wt and  $mxr2\Delta$  cells carrying empty vectors or expressing either HA- Atg19 alone or with Flag-Mxr2 were grown up to the mid-log phase. Next, cells were exposed to nitrogen starvation for four hours to induce oxidative stress or left untreated. Cells were harvested, lysed, and analyzed via immunoblotting with Ape1, HA, and FLAG antibodies. The data are represented as mean  $\pm$  SD of three independent experiments and f Statistical analysis was done using a two-way ANOVA test. \*\*\*\*p < 0.0001, \*\*\*p < 0.001, \*\*\*p < 0.01 and \*p < 0.05. ns, nonsignificant. Cvt, cytoplasm to vacuole targeting; HA, hemagglutinin.

# 2.4. CONCLUSION

In this chapter, we conclude that Mxr2 physically interacts with both Atg19 and Ape1, using yeast two-hybrid assay and the co-immunoprecipitation method and regulates the Cvt pathway. We showed that Mxr2 protects Ape1 and Ag19 from oxidative stress, as  $\Delta mxr2$  strain showed less physiological abundance and less stability in cycloheximide chase assay. Further, we also showed that Mxr2 interacts with Ape1 via M17 residue in the Ape1, which is vulnerable to oxidative damage and reduces the methionine residue, if oxidized and mutating the residue renders Ape1 protein more stable and less vulnerable towards oxidative stress. Leucine aminopeptidase activity assay showed the  $\Delta mxr2$  strain exhibits significantly reduced leucine aminopeptidase activity, which is comparable with  $\Delta ape1$  strain. At last, it has been demonstrated that, Mxr2 protects both proteins and maintains their stoichiometry within the cell for smooth running of the Cvt pathway, and thus regulates this specific autophagy pathway. The overview of this study is summarized in the following schematic diagram (Fig. 7)

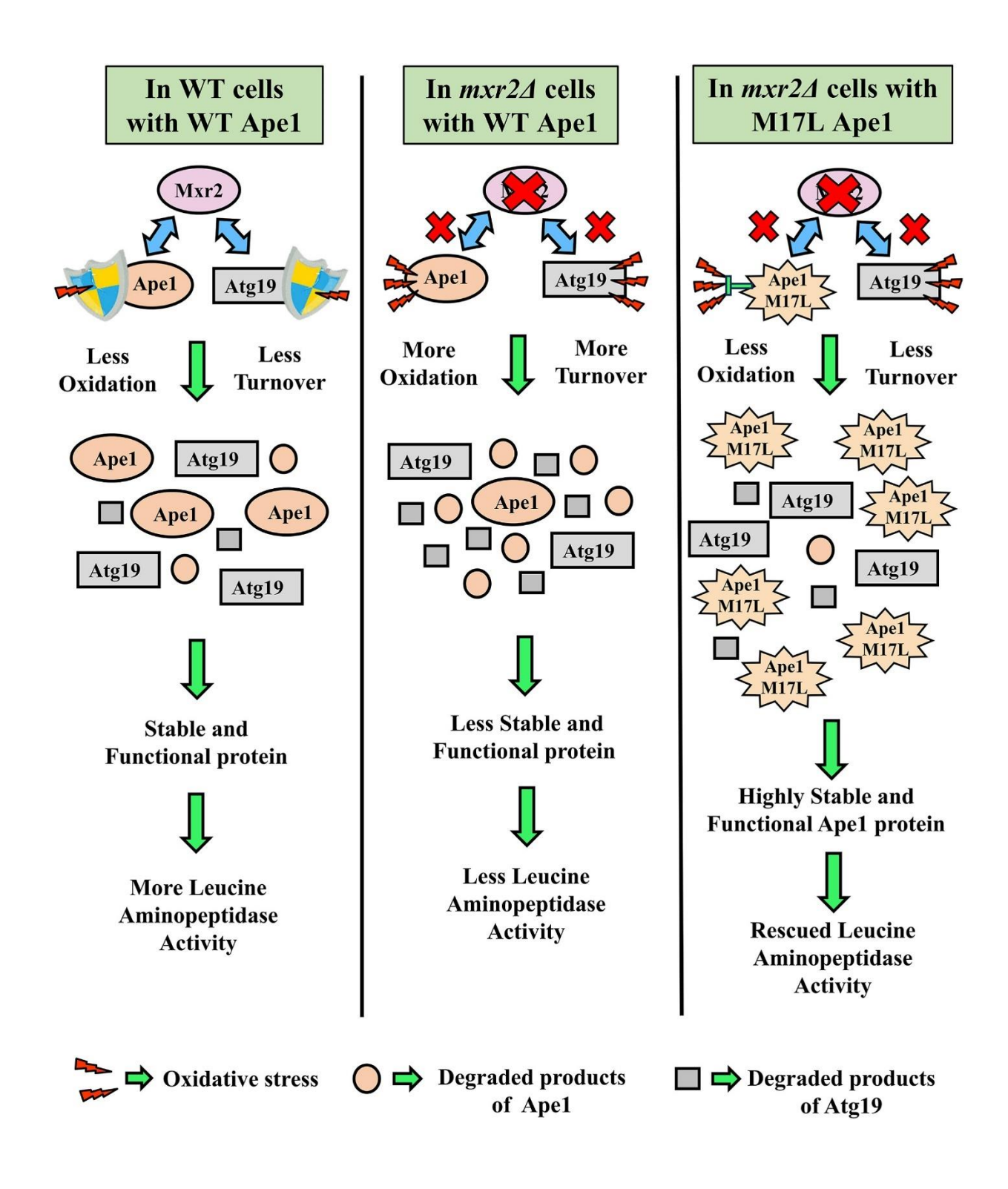


Figure 7. Schematic diagram depicting the role of Mxr2 in the Cvt pathway. (*Left panel*) In wt cells, Mxr2 interacts and protects Ape1 and Atg19 from oxidative stress, thereby preventing premature turnover. (*Middle panel*) Excess ROS in  $mxr2\Delta$  cells destabilizes Ape1 and Atg19 proteins. Destabilized proteins tend to degrade faster, and in this context, leading to decreased leucine aminopeptidase activity. (*Right* panel) M17L mutation confers oxidative stress resistance to the Ape1 protein. Stable and oxidative stress-resistant Ape1 M17L protein rescues the decreased leucine aminopeptidase activity phenotype of the  $mxr2\Delta$  strain. Cvt, cytoplasm to vacuole targeting; ROS, reactive oxygen species.

# **CHAPTER 3**

Mxr2 controls the bulk autophagy pathway by regulating Atg8 transcription through the Mxr2-Mge1-Dep1 axis

#### 3.1. BACKGROUND

Cells are continually exposed to oxidative insults, which can lead to structural and functional changes in biomolecules, leading to various clinical conditions' onset [235-237]. Cells have evolved various enzymatic and non-enzymatic mechanisms to combat oxidative stress. Among these are methionine sulfoxide reductases (MSRs), which are crucial role in reducing oxidized methionine sulfoxide residues back to their native form [62,63,238]. The impairment of MSR enzymatic activity is linked to harmful physiological defects in yeast, and various human pathophysiological conditions [67,211,213,215,239]. In yeast, studies have demonstrated that MSRs protect nucleotide exchange factors for cytosolic and mitochondrial Hsp70 [70,71]. Additionally, research has shown that one specific autophagy pathway in yeast, the Cvt pathway, is regulated by the MSR known as Mxr2 [226]. Despite evidence that MSRs safeguard specific physiological substrates, the broader physiological impact of their functional loss and their associations with diverse physiological events remain largely unexplored.

Non-selective autophagy is a highly conserved cellular recycling process that breaks down various biomolecules, dysfunctional components, and damaged organelles into simpler forms that can be reused [106]. In yeast, more than 40 Atg proteins participate in various stages of autophagy. Autophagic dysregulation leads to severe consequences, and hence, cellular autophagic activity is tightly regulated, primarily through stringent transcriptional control of ATG genes [145,240]. Although extensive research has focused on understanding the transcriptional regulation of ATG genes, many molecular factors remain to be elucidated.

Among the ATG proteins whose transcriptional expression undergoes significant changes before and after autophagy induction, Atg8 stands out as a prominent candidate. Atg8, a ubiquitin-like protein, integrates into the phagophore membrane, a crucial step for its expansion and the formation of autophagosomes [241,242]. Therefore, the transcriptional regulation of ATG8 is pivotal for maintaining optimal autophagic activity. While the Ume6 repressor predominantly controls Atg8 transcriptional expression, other regulators such as Pho23, Rph1, and Msn2-Msn4 have also been identified as modulators of Atg8 expression [154-156,158]. In addition to its role in autophagy, Ume6 also plays a critical role in the transcriptional regulation of meiotic genes, where the acetylation status of Ume6 proteins is crucial for this regulation [196,197,243]. Although the significance of acetylation in ATG proteins has been studied

extensively, the role of Ume6 acetylation in autophagy progression has not received sufficient attention.

Autophagy plays a critical role in maintaining mitochondrial quality control. During stress conditions, dysfunctional mitochondria are eliminated through either mitophagy or non-selective autophagy. Numerous studies have highlighted that cells deficient in autophagy exhibit significant impairments in mitochondrial function, including lower oxygen consumption rates, growth defects in non-fermentable medium, reduced activities of respiratory complexes, decreased membrane potential, and increased levels of mitochondrial DNA mutations and reactive oxygen species [244]. Under stress, when cells transition from glycolysis to respiratory growth, autophagy facilitates the recycling of iron necessary for mitochondrial activity during respiration. Mutants lacking functional autophagy, such as atg mutants, struggle with this metabolic shift, which can be alleviated by supplementing iron [245]. Despite extensive research into the role of autophagy in mitochondrial function, there is a notable gap in understanding whether the status of mitochondria physiology influences cellular autophagic activity.

This study aimed to investigate how mitochondrial physiology regulates the progression of autophagy by modulating the Atg8 expression. We illustrated the importance of mitochondrial localized Mxr2 in regulating ATG8 expression by controlling the stability of Ume6 via modulating the activity of deacetylase complexes.

#### 3.2. MATERIALS AND METHODS

#### 3.2.1. Media and Growth conditions

For all experiments, yeast cells are grown at 30°C up to mid-log cells with optical absorbance 600<sub>nm</sub> ranging between 0.8-1.0 in synthetic media with required auxotropic supplements as described earlier [245,246], followed by treatment with nitrogen starvation media, as indicated in [246] if needed. Plasmid transformations within yeast cells have been carried out via standard method using single-stranded carrier DNA and lithium acetate as described [225]. For autophagy assay, cells are at first grown in synthetic minimal media with glucose upto mid-log phase followed by washing with sterile water via centrifugation and finally incubation with nitrogen starvation conditions for 6 hours to induce autophagic stress. On the other hand, for mitophagy assay, cells of mid-log phase were at first incubated in synthetic media with lactate for mitochondrial enrichment followed by washing and incubation with nitrogen starvation

conditions for 10 hours to induce mitophagic stress. To impel oxidative stress, cells from midlog phase cells were incubated with media having 2 mM H<sub>2</sub>O<sub>2</sub> for 2 hours. To check the phosphorylation status of Atg13 or Ume6 and to check the gene transcript level at stress condition, mid-log phase cells were treated with nitrogen starvation media for 2 hours. To check the vacuolar dysfunction, mid-log phase cells were serially diluted and spotted in YPD agar plates (1 % yeast extract (Himedia, RM668), 2% peptone (Himedia, RM001), 2% with dextrose (Himedia, GRM077), 2% agar powder (Himedia, GRM666)) etc. pH 5, pH 7 or 100 mM CaCl<sub>2</sub> (SRL, 70650).

#### 3.2.2. Yeast strains and plasmids

In this study, parent strain BY4741 and its derivatives are used. Genomic tagging of MXR2, ATG13 and UME6 genes was achieved by changing the stop codon of the gene with an amplified cassette containing 3' end of the respective gene without stop codon, myc tag, and HIS cassette, via by PCR-based homologous recombination as indicated [219]. The gene coding sequence were amplified from either yeast genomic DNA or mentioned DNA constructs to create different plasmid constructs. For pNB1042, coding sequence of Mxr2 without the mitochondrial targeting sequence was cloned in pRS425 using NB1398/NB1048 primers. For pNB1043, the coding sequence along with 5'UTR sequence of Ume6 along with 3X FLAG tag was cloned in pRS315 vector using NB1845/NB1950 primers. For pNB1044, 3' portion of the Ume6 gene was amplified form a Ume6 acetylation null mutant construct using NB1845/NB1952 primers. The 5' portion of the Ume6 gene along with 5' UTR was amplified using NB1951/NB1950 primer pair. Both the fragment was then cloned to generate NB1044. For pNB1045, pNB1048, pNB1049, pNB1050, pNB1051, pNB1052 and pNB1053, coding sequence of the DEP1, SSQ1, ISA1, ISA2, YFH1, ISU1 nad GRX5 gene was amplified respectively using respective primer pairs and ligated to BamHI/SalI digested fragment of pNB904. For pNB1046 and pNB1047, the mitochondrial targeting sequence (MTS) and COX4 nuclear localization sequence (NLS) of NUP60 along with DEP1 gene were cloned into BamHI/SalI digested fragment of pNB904 using NB1978/NB1845 and NB1979/NB1845 primer pairs respectively, where MTS and NLS sequences were embedded into 5' end of the forward primers. The strains used in this study are mentioned in this study are listed in Table 4, whereas the plasmids and the primers are listed in Table 5 and table 6 respectively.

**Table 4. Strains** 

Strain	Genotype	Reference
YNB105	BY4741; MATa his $3\Delta$ 1; leu $2\Delta$ 0; met $15\Delta$ 0; ura $3\Delta$	Euroscarf
YNB117	BY4741; <i>mxr</i> 2Δ:: <i>KanMX</i>	Euroscarf
YNB114	BY4741; $mxr1\Delta::KanMX$	Euroscarf
YNB489	BY4741; <i>νma2</i> Δ:: <i>KanMX</i>	Euroscarf
YNB 339	PJ469-A	[220]
YNB513	BY4741; <i>MXR2-13XMYC</i> :: <i>HIS3</i>	This study
YNB518	BY4741; <i>ATG13-13XMYC</i> :: <i>HIS3</i>	This study
YNB519	BY4741; <i>mxr</i> 2Δ:: <i>KanMX ATG13-13XMYC</i> :: <i>HIS3</i>	This study
YNB516	BY4741; <i>UME6-13XMYC</i> :: <i>HIS3</i>	This study
YNB517	BY4741; <i>mxr</i> 2Δ:: <i>KanMX UME6-13XMYC</i> :: <i>HIS3</i>	This study
YNB522	BY4741; <i>ume6</i> Δ:: <i>KanMX</i>	Euroscarf
YNB529	BY4741; $dep1\Delta$ :: $KanMX$	Euroscarf
YNB488	BY4741; <i>ssq1</i> Δ:: <i>KanMX</i>	Euroscarf
YNB411	BY4741; mge1Δ::KanMX pRS425- WT MGE1::LEU2	[247]
YNB431	BY4741; mge1Δ::KanMX pRS425- DM MGE1::LEU2	This study

Table 5. plasmids

Plasmid No.	Plasmid Name	Source/Reference
pNB415	pGBD-C1	[220]
pNB422	pGAD-C1	[220]
pNB901	pGBD-C1 Mxr2-FLAG	[246]
pNB 1041	pGAD-C1 ATG8	This study
pNB362	pRS423 GFP-Atg8	Ravi Manjithaya,
_		JNCASR Bangalore
pNB449	pRS316 Su9-DHFR-GFP	[248]
pNB356	p425 TEF	[222]
pNB904	p425TEF Mxr2-FLAG WT	[246]
pNB500	pFA6a 13 Myc-HisMX6	[219]
pNB 1042	p425TEF Mxr2-FLAG (△29)	This study
pNB494	Ura- MXR2 GFP – WT	[71]
pNB495	Ura- MXR2 GFP - M1L	[71]
pNB496	Ura- MXR2 GFP - M34L	[71]
pNB357	p426 TEF	[222]
pNB399	pRS315	[223]
pNB 1043	pRS315- UME6 WT	This study
pNB 1044	pRS315- UME6 (K736R,K737R,K745R,	This study
_	K812R,K183R,K814R)	-
pNB 1045	p425TEF DEP1-FLAG WT	This study
pNB 1046	p425TEF DEP1-FLAG MTS	This study
pNB 1047	p425TEF DEP1-FLAG NLS	This study
pNB 1048	p425TEF SSQ1-FLAG	This study
pNB 1049	p425TEF ISA1-FLAG	This study
pNB 1050	p425TEF ISA2-FLAG	This study
pNB 1051	p425TEF YFH1-FLAG	This study

pNB 1052	p425TEF ISU1-FLAG	This study
pNB 1053	p425TEF GRX5-FLAG	This study
pNB 457	p425TEF MGE1 WT	[247]
pNB 459	p425TEF MGE1 DM (M115L, H167L)	This study
pNB 1054	pGBD-C1 MGE1 WT	This study
pNB 1055	pGBD-C1 MGE1 DM (M115L, H167L)	This study
pNB 1056	pGAD-C1 DEP1	This study
pNB357	p426 TEF	[222]
pNB 1057	p426TEF MGE1 WT	[247]
pNB 1058	p426TEF MGE1 DM (M115L, H167L)	This study

# **Table 6. Primers**

Primer name	Sequence (5'-3')	
NB1736 ATG8 F.P.	CTG GGATCC ATGAAGTCTACATTTAAGTCTG	BamHI
NB1683 ATG8 R.P.	ATG GAATTC CTACCTGCCAAATGTATTTTCTCC	EcoRI
NB1398 Mxr2 <i>∆29</i> F.P.	CTA GGATCC ATGAAGAGCAAGAAAATGAGTGACG	BamHI
NB1048 MXR2	GTTTAAACCTCGAGTTACTTGTCATCGTCATCCTTGTAATCGA	
FLAG rev	TGTCATGATCTTTATAATCACCGTCATGGTCTTTGTAGTCGGG	
1	CCCGTCGACATCCTTCTTGAGGTTTAAAGACGC	
NB 1894 DEP1 F.P	CTA GGATCC ATGAGTCAGCAAACACCAC	BamHI
NB 1895 DEP1 R.P	ATG GTCGAC CTGGGCCCACTGGTG	SalI
NB1978 Dep1 F.P.	CTA GGATCC	BamHI
with MTS.	ATGCTTTCACTACGTCAATCTATAAGATTTTTCAAGCCAGCC	
ND1070 D 1 E D	ATGAGTCAGCAAACACCAC	D III
NB1979 Dep1 F.P.	CTA GGATCC	BamHI
with NLS-	ATGCATCGTAAATCATTGAGGAGGGCTAGCGCTACTGTGCCTT	
	CCGCTCCCTATCGAAAGCAGATTATTAGC GATATC ATGAGTCAGCAAACACCAC	
NB 1845 UME6 5'	CTA GGGCCC GGCACCGAACGGTCTTG	ApaI
UTR FP- NB 1950 Ume6 3X	ATG GTCGAC	
FLAG R.P	TTACTTGTCATCGTCATCCTTGTAATCGATGTCATGATCTTAT AATCACCGTCATGGTCTTTGTAGTCAAGCTTTTTTTTTT	
NB1951 UME6	GCAAAATCAAAGGCGAAACAGTCATCA	
lysine mutation F.P		
NB1952 UME6	TGATGACTGTTTCGCCTTTGATTTTGC	
lysine mutation R.P		
NB 1869 SSQ1 F.P	CTA GGATCC ATGCTTAAATCTGGTAGACTCAAC	BamHI
NB 1870 SSQ1	ATG GTCGAC TTTACCTTGATTCTGCTGGTTTTTTG	SalI
R.P		
NB 1875 ISA1 F.P	CTA GGATCC ATGATAAACACAGGAAGAAGCAG	BamHI
NB 1876 ISA1 R.P	ATG GTCGAC AACCATGAAACTCTCGCC	SalI
NB 1877 ISA2 F.P	CTA GGATCC ATGCAGGCTAAATTATTGTTTACCAG 62.1 BamHI	BamHI

NB 1878 ISA2 R.P	ATG GTCGAC TTAATTTTCAATATCAAAACTACTTCCACAACC	SalI
NB 1849 YFH1 F.P	CTA GGATCC ATGATTAAGCGGTCTCTCG	BamHI
ND 1047 111111.1.	enrodnice moni innocodicicico	Dannin
NB 1850 YFH1	ATG GTCGAC TTGGCTTTTAGAAATGGCCTTC	SalI
R.P		
NB1110 Isu1 F.P.	CTAGGATCCATGCTTCCTGTTATAACGAG	BamHI
NB1111 Isu1 R.P.	ATGGTCGACTTACGATAACATGGTTGG	SalI
NB 1879 GRX5	CTA GGATCC ATGTTTCTCCCAAAATTCAATCCC	BamHI
F.P		
NB 1880 GRX5	ATG GTCGAC ACGATCTTTGGTTTCTTCTTCTTC	SalI
R.P		
NB341 MGE1p	CTAAGAAAGCTCGGTATTGAA	
SDM H167L F.P.		
1704/4 1707/		
NB342 MGE1p	TTCAATACCGAGCTTTCTTAG	
SDM H167L R.P.		
ND966 MCE1a	GGGGTTAGACTGACAAGAGAT	
NB866 MGE1p SDM M155L F.P.	GUUUTTAUACTUACAAUAUAT	
SDM M133L F.P.		
ND967 MCE1n	ATCTCTTGTCAGTCTAACCCC	
NB867 MGE1p SDM M155L R.P.	AICICITGICAGICIAACCCC	
SDM MISSE K.P.		
NB 1946 MGE1 FP	CTAGAATTCATGAGAGCTTTTTCAGCAGCC	BamHI
NB 1940 MGELFP	CIAGATICATGAGAGCITTICAGCAGCC	Вашні
NB820 MGE1 R.P.	CATAGGATCCTTAGTTCTCTTCGCCCTTAACAATTCC	EcoRI
NB 1980 MGE1	ATG GTCGAC GTTCTCTTCGCCCTTAAC	SalI
Y2H R.P.	hid dreame differenceeer hime	Saii
NB1644 MXR2	GACACCAGACACTGTGTGAACAGTGCGTCTTTAAACCTCAAG	
Myc tagging F.P	AAGGATCGGATCCCCGGGTTAATTAA	
NB1165 MXR2	GTACGTATGCATACACACATATATATATATATATATATAT	
Myc tagging R.P	GAATTCGAGCTCGTTTAAAC	
NB1714 ATG13	ATGATGATCTAGTATTTTTCATGAGTGATATGAACCTTTCTAAA	
Myc tagging F.P	GAAGGTCGGATCCCCGGGTTAATTA	
NB1715 ATG13	TTTGATTATTTTCTTTAGTTGTGCCCTTTAAAATAAAACTTTA	
Myc tagging R.P	CCATTGAATTCGAGCTCGTTTAAAC	
NB1710 UME6	AAATCAAGAAAAAAAAAAGAGGCCAAAAGAAGAAGAAT	
Myc tagging F.P	GAAAAAAAACGGATCCCCGGGTTAATTAA	
NB1711 UME6	AATAATAATAATAATAGTAACAATATCTCTTTTTTTTTT	
Myc tagging R.P	AGCTTGAATTCGAGCTCGTTTAAAC	
NB1542 ATG8 RT	CTAGTTCCTGCTGACCTTAC	
FP-		
NB1543 ATG8 RT	GCAGTAGGTGGCAAAGTA	
RP-		
NB1544 ATG14 RT	AGGCACAGGATAGAACAG	
FP-		
NB1545 ATG14 RT	GTACCAGTACCCACCTTA	
RP-		
NB1758 Actin RT	GAAATCACCGCTTTGGCTCC	
F.P		
NB1758 Actin RT	GTGGTGAACGATAGATGGACCA	
R.P		
NB1777 GCN5 F.P.	GGAGGATCTGAAGTGGTT	
		Ì
RT -		
NB1778 GCN5 R.P.	GACACTGGGTCTCTCTTT	

NB1779 SIN3	GCAGATGCTAACGATGAC
F. P. RT -	
NB1780 SIN3	GACCTGTTCGAGGTAAGA
R. P. RT-	
NB1781 RPD3 F. P.	CTTCTGCTGTCGTGTTAC
RT -	
NB1782 RPD3 R. P.	GGGATCCCAAAGGATTTC
RT -	
NB1629 UME6 RT	GAAGGTCAGTTGGAAACG
F.P	
NB1630 UME6 RT	AAGATGGAGACGATGGAG
R.P	
NB1783 CAR1 F. P.	CGGTGAAGGTCCCATTAT
RT -	
NB1784 CAR1 R. P.	GCCAATCTTTCCACCAAG
RT-	

### 3.2.3. Whole cell extract preparation and Western blot Analysis

Cell lysates from harvested yeast cells were prepared as described earlier [246]. SDS-PAGE and western blotting were carried out using standard protocols. Immunoblotting was done following standard procedures using anti-FLAG antibody (Sigma-Aldrich, F3165, 1:2000), anti-Myc antibody (Proteintech, 16286-1-AP, 1:5000), anti-GFP antibody (Abcam, ab183734, 1:5000), anti-pan acetylation antibody (Proteintech, 66289-1-IG, 1:5000), anti-Pgk1, Por1 serum (kind gift from Prof. Debkumar Pain, New Jersey Medical School, Rutgers University), anti-Mge1 antibody (In house raised)[247], Horseradish peroxidase-conjugated anti-rabbit polyclonal antibody (Jackson Laboratories, 111-035-144, 1:25,000), anti-mouse polyclonal antibody (Jackson Laboratories, 115-035-146, 1:25,000). After immunoblotting, the immunoblotting signal was detected, the immunoblotting images were quantified, and the statistical analysis was done as described earlier [246].

#### 3.2.4. Cycloheximide Chase Assay

For the cycloheximide chase assay, cells were grown up to a mid-log phase, in synthetic minimal media as required and then subjected to cycloheximide [SigmaAldrich, C7698] treatment (50 µg/ml) for different time durations (0, 10, 25, 40, 75 and 120 min) to stop the ribosomal translation. After harvesting at indicated time points, cell lysates were prepared from harvested cells and analyzed via western blotting with anti-GFP antibody to understand the protein degradation profile of Atg8 protein.

#### 3.2.5. Mitochondrial Fractionation

For mitochondria isolation, yeast cells are grown up to the late log phase in synthetic minimal media with optical absorbance<sub>600nm</sub> ranging between 1.2-1.8. After that, cells are either harvested or starved using nitrogen starvation media for indicated time points, before harvesting. Harvested cells were subjected to mitochondria isolation as described earlier [249-251], where crude mitochondrial fraction was isolated as described previously [226]. Along with mitochondria, cytosolic fractions were also collected to determine the protein abundance in the cytosolic fractions.

#### 3.2.6. RNA extraction and quantitative real-time PCR (qRT PCR)

RNA extraction was done from the harvested cells using the hot phenol protocol as described (86 of JBC). After RNA extraction, DNase digestion to remove DNA contamination and cDNA synthesis were done using the procedure described earlier [246]. Relative RNA abundance was determined by qRT-PCR using the PowerUp SYBR Green PCR Master mix (Applied Biosystems, A25742) via a Quanstudio 3 Real-Time PCR System. The results were normalized against ACTI and transcript levels were calculated using  $2^{-\Delta\Delta C}_{T}$  method [252].

#### 3.2.7. Coimmunoprecipitation Assay

Cell extract for coimmunoprecipitation was prepared following procedures described earlier [246]. After protein estimation, 1 mg of cell lysate was at first incubated with protein A/G PLUS-Agarose beads (Santacruz Biotechnology, SC- 2003) at 4°C for 2 hours. Precleared cell extract was then incubated overnight at the same condition with either anti-pan acetylation antibody or anti-FLAG antibody. Next, the cell extract-antibody suspension was incubated again with protein A/G PLUS-Agarose beads for 4 hours with the same condition for binding of antibodies with the beads. After incubation, beads were collected, washed 3 times and then analyzed via western blotting using anti-Myc, anti-FLAG and anti-Mge1 antibodies.

#### 3.2.8. Statistical Analysis

Statistical analysis was done using either unpaired Student's t-test or one-way ANOVA or two-way ANOVA test (mentioned in the figure legends). The significance of differences was marked based on the p value of the respective statistical tests, which is as follows \*\*\*\*p < 0.001, \*\*\*p < 0.001, \*\*\*p < 0.01 and \*p < 0.05. ns, nonsignificant. The values represented in the data quantification are the mean of three independent experiments and the error bars showed in the graph indicate the standard deviation among the experiments.

#### 3.3. RESULTS

#### 3.3.1. The *mxr2* strain exhibits a markedly reduced autophagy flux

Our previous study [246] demonstrated that Mxr2 regulates the Cvt pathway, a specific autophagy pathway, by protecting Ape1 and Atg19, two major components of the Cvt pathway. Therefore, we were intrigued to investigate whether Mxr2 plays a role in the bulk autophagy pathway in yeast. To examine this, we conducted an autophagy flux assay comparing wild-type (WT) and  $mxr2\Delta$  cells, expressing Atg8-GFP ectopically from the pRS423 vector, and induced the autophagy by nitrogen starvation for 6 hrs as mentioned in the materials and methods section. The cell lysates were separated on SDS-PAGE, western transferred and probed with GFP to assess the autophagy flux. We find that the  $mxr2\Delta$  strain exhibited a significant autophagic defect compared to the WT strain (Fig.8A). To validate further the involvement of Mxr2 in bulk autophagy, we overexpressed the Mxr2 protein tagged with 3x FLAG in the  $mxr2\Delta$  strain using the pRS425 vector under the control of the TEF1 promoter, alongside empty vector controls. We find that the overexpression of Mxr2 could completely rescue the autophagic defect observed in the  $mxr2\Delta$  strain, thereby confirming its role in bulk autophagy (Fig.8B).

To confirm Mxr2's specific role in bulk autophagy, we also examined the  $mxr1\Delta$  strain, which lacks the S type of methionine sulfoxide reductase, in the autophagy flux assay. Unlike the  $mxr2\Delta$  strain, the  $mxr1\Delta$  strain demonstrated autophagic flux similar to the WT strain, thereby confirming the specificity of Mxr2's involvement (Fig.8C). Since the  $mxr2\Delta$  strain has more ROS, we intend to determine whether the autophagic defect in the  $mxr2\Delta$  strain is due to this additional ROS. The WT cells were subjected to oxidative stress by treating with 2 mM H<sub>2</sub>O<sub>2</sub> for 2 hrs and compared with the untreated WT and  $mxr2\Delta$  cells. Western blot data shows that with or without oxidative stress could not reduce the Atg8-protein abundance in WT compared to the  $mxr2\Delta$  strain. These results suggest that additional ROS in  $mxr2\Delta$  strain is not the reason for its autophagic defect (Fig. 8D).

To determine the observed autophagic defect in the  $mxr2\Delta$  strain resulted from vacuolar dysfunction, we conducted a survivability assay under vacuolar stress conditions (e.g., high pH and elevated calcium concentration) using WT,  $mxr2\Delta$ , and  $vma2\Delta$  strains. The  $vma2\Delta$  strain, lacking a major subunit of vacuolar H+-ATPase, exhibited significantly reduced growth under high pH conditions and no growth on plates containing 100 mM CaCl<sub>2</sub>, indicative of severe vacuolar dysfunction. In contrast, similar to the WT strain, the  $mxr2\Delta$  strain displayed a

comparable survivability profile, indicating its intact vacuolar health (Fig.8E). Overall, these findings strongly suggest that Mxr2 is involved in the regulation of bulk autophagy.

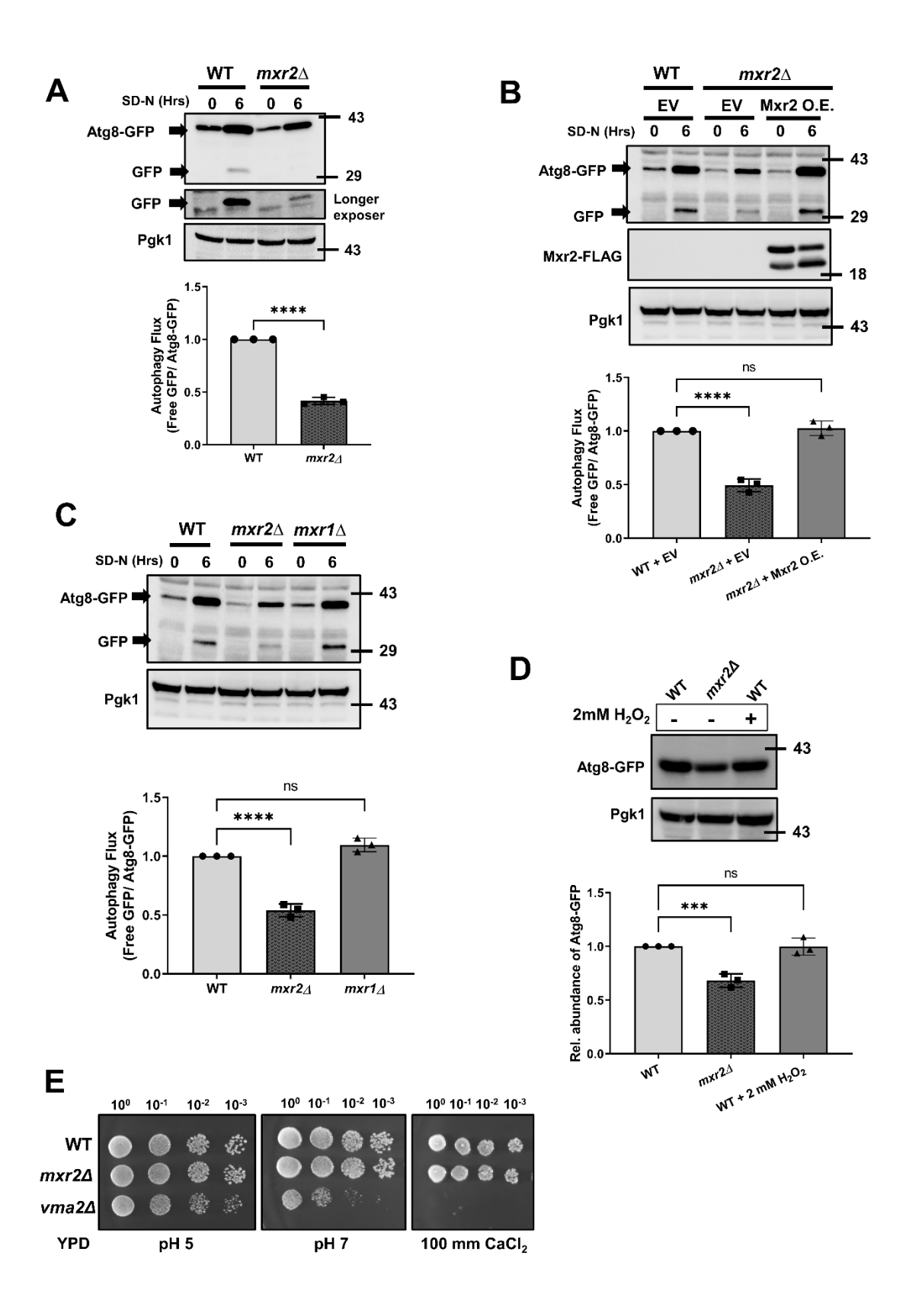


Figure 8. mxr2Δ strain exhibits significantly less autophagy flux. (A) WT and mxr2Δ cells expressing Atg8-GFP protein were grown in minimal media up to mid-log phase and then kept untreated (0 hr time point) or starved in nitrogen starvation media for 6 hrs (6 hr time point). Immunoblotting with an anti-GFP antibody was done to check Atg8-GFP processing to assess autophagy flux. Pgk1 was used as a loading control. Quantification of the autophagic flux is represented in the lower panel. (B) WT cells transformed with empty vector along with Atg8-GFP construct and mxr2Δ cells expressing Atg8-GFP and transformed with either empty vector or Mxr2-FLAG overexpressing construct were used to determine the cellular autophagy flux using Atg8-GFP processing assay. Quantification of the autophagic flux is represented in the lower panel. (C) Autophagy flux assay was carried out with WT,  $mxr2\Delta$ , and  $mxr1\Delta$  cells expressing Atg8-GFP using Atg8-GFP processing assay. Quantification of the autophagic flux is represented in the lower panel. (D) After growing up to the mid-log phase, WT were kept untreated or treated with 2 mM  $H_2O_2$ , whereas  $mxr2\Delta$  cells were left untreated. Harvested cells were analyzed via immunoblotting with anti-GFP antibody to check the Atg8-GFP protein levels. Quantification of the Atg8-GFP protein abundance in different strains is represented in the lower panel. (E) A growth survivability assay was performed with WT, mxr2Δ, and vma2Δ cells in minimal media with pH 5 or 7 or 100 mM CaCl<sub>2</sub>. Cells were first grown in minimal media, and spotting assay was done in agar plates containing indicated media. After serial diluted cell spotting, agar plates were incubated at 30°C for 2 days. The data shown are the mean ± SD of three biologically independent experiments. Statistical analysis was carried out using an unpaired Student's t-test for (A, B, C, D), \*\*\*\*p < 0.0001, \*\*\*p < 0.001, \*\*p < 0.01 and \*p < 0.05. ns, nonsignificant.

#### 3.3.2. ATG8 gene is transcriptionally downregulated in the mxr2∆ strain

We noticed that in our autophagy flux assay, decreased autophagy flux in the  $mxr2\Delta$  strain was also associated with a lower abundance of total Atg8 protein (Fig. 8). This finding, combined with our previous study where we demonstrated that Mxr2's interactions with components of the Cvt autophagy pathway, Ape1 and Atg19, prompted us to investigate whether Mxr2 similarly interacts with Atg8. Initially, we assessed their interaction using a yeast two-hybrid assay. Additionally, we examined Atg8 protein stability in the  $mxr2\Delta$  strain compared to wild type (WT) using a cycloheximide chase assay. The yeast two-hybrid results indicated that Mxr2 does not interact with Atg8 (Fig. 9A), while the cycloheximide chase assay showed that Atg8 protein levels are low, however, the stability is comparable between WT and  $mxr2\Delta$  strains (Fig. 9B).

These findings suggested a potential transcriptional downregulation of the ATG8 gene in the  $mxr2\Delta$  strain. During autophagy induction, the upregulation of the ATG8 and ATG14 genes is notably higher than other ATG genes [124,152]. Therefore, we investigated the transcriptional expression of ATG8 and ATG14 in WT and  $mxr2\Delta$  cells under normal and starved conditions

(using SD-N for 2 hours). Quantitative reverse transcription PCR (qRT-PCR) results confirmed significant downregulation of both ATG8 and ATG14 genes in *mxr2*Δ cells under both conditions (Fig. 9C).

Atg8, a crucial ubiquitin-like protein, plays a vital role in membrane fusion and phagophore expansion during autophagosome formation in yeast, directly influencing autophagosome size [253-255]. Thus, the reduced expression of ATG8 in  $mxr2\Delta$  cells would likely lead to diminished flux in specific autophagy pathways. To validate this hypothesis, we conducted a mitophagy flux assay in WT and  $mxr2\Delta$  cells, as described previously. Consistently, the mitophagy flux profile showed a significant decrease in flux in the  $mxr2\Delta$  strain compared to WT, a deficit that was fully rescued by Mxr2 overexpression (Fig. 9D & E). In summary, these results confirm that the decreased abundance of Atg8 protein in the  $mxr2\Delta$  strain is not due to reduced stability but rather stems from transcriptional downregulation. This deficiency ultimately results in diminished autophagic and mitophagic flux.

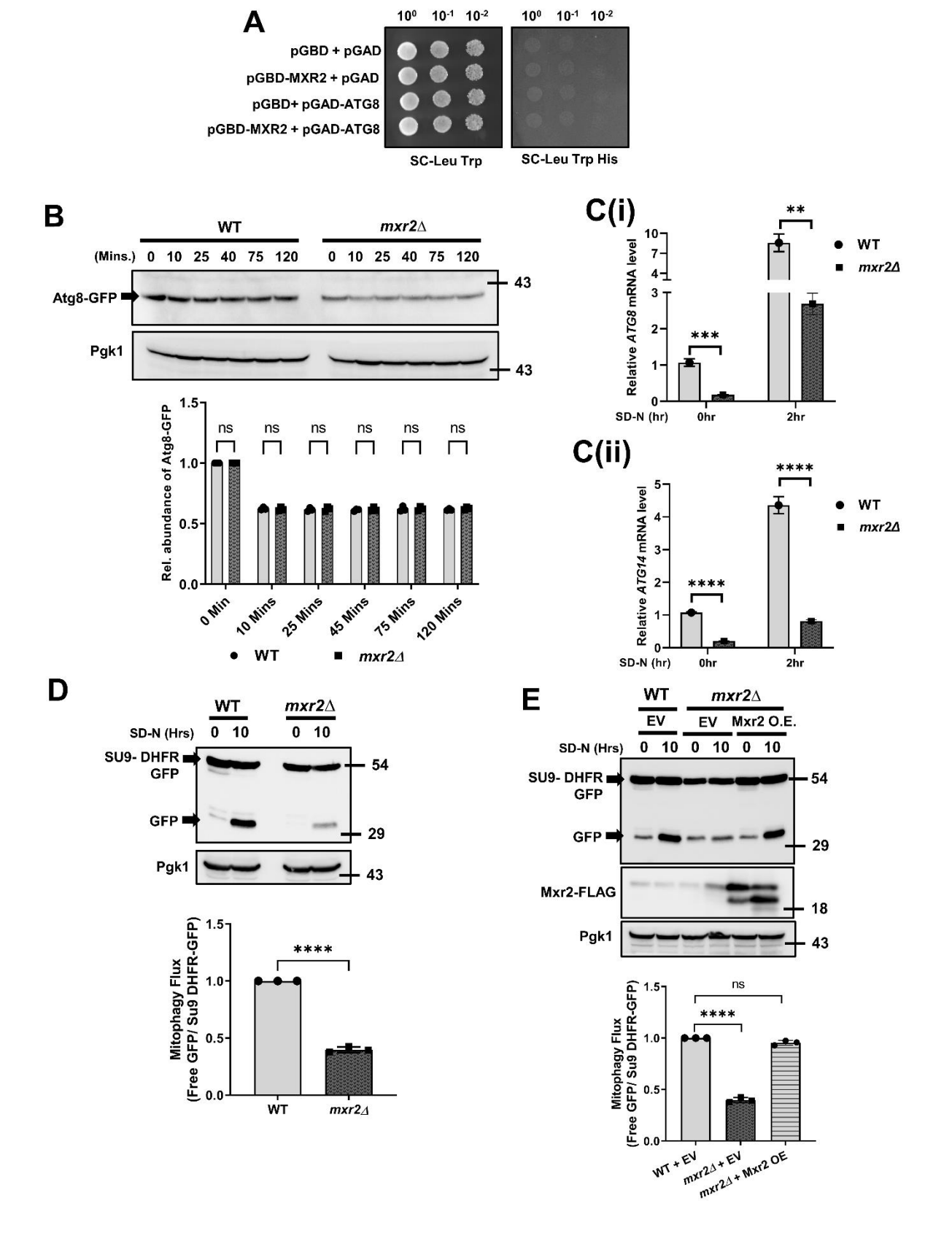


Figure 9. Transcriptional downregulation of ATG8 in the mxr2Δ strain. (A) yeast two-hybrid assay between Mxr2 and Atg8. The PJ69-4A strain, transformed with pGBD-C1- MXR2 and pGAD-C1- ATG8 construct, were spotted along with control strains on agar plates of indicated minimal media. The growth profile was checked after incubation at 30°C for 2 days. (B) cycloheximide chase assay. WT and *mxr*2Δ strains expressing Atg8-GFP protein were grown up to mid-log phase and treated with 50 µg/ml of cycloheximide for different time points up to 2 h. The Atg8 protein turnover profile was measured via Western blotting with an anti-GFP antibody. Quantification of the Atg8-GFP protein abundance in the cyclohexide chase assay is represented in the lower panel. (C) The transcript levels of ATG8(i) and ATG14(ii) were checked in WT and mxr2\Delta cells under either vegetative or 2 hrs of nitrogen starvation condition via qRT- PCR analysis. (D) Mitophagy assay was carried out with WT and mxr2Δ strains. WT and mxr2Δ cells carrying Su9- DHFR- GFP constructs were initially grown up to mid-log phase in minimal media with glucose, resuspended in minimal media with 2% lactate, and incubated for 24 hrs. Harvested cells were left untreated or starved in SD-N media for 10 hrs. Harvested cells were then analyzed via immunoblotting with an anti-GFP antibody to measure mitophagy flux. Quantification of the mitophagic flux is represented in the lower panel. (E) WT and mxr2Δ cells expressing Su9- DHFR- GFP were transformed with either empty vector or Mxr2-FLAG overexpressing construct. Transformants were then used to perform a mitophagy flux assay. Quantification of the mitophagic flux is represented in the lower panel. The data shown are the mean ± SD of three biologically independent experiments. Statistical analysis was done using an unpaired Student's t-test for (C and D), whereas one-way ANOVA tests were done test for (B and E). \*\*\*\*p < 0.0001, \*\*\*p < 0.001, \*\*p < 0.01 and \*p < 0.05. ns, nonsignificant.

# 3.3.3. Stress-induced repositioning of Mxr2 into mitochondria is essential for the progression of autophagy

As we have seen Mxr2 is involved in regulation of autophagy and it is necessary for autophagy progression both in vegetative condition (basal autophagy) and in stress condition like nitrogen starvation condition (stress induced autophagy), we intended to investigate whether stress conditions such as nitrogen starvation influence Mxr2 protein levels and localization and whether its localization influences the autophagy flux. It is known that nitrogen starvation increases the reactive oxygen species levels, leading to greater methionine oxidation than protein carbonylation [256].

Initially, we genomically tagged the MXR2 gene with a Myc Tag using the Pfa6-HISMX6-MYC vector and confirmed by western blotting (Fig. 10A). Cells expressing the myc-Mxr2 protein were subjected to different stress conditions including stationary phase (low nutrient availability), nitrogen starvation, non-fermentable carbon source (glycerol), and oxidative stress (2mM H<sub>2</sub>O<sub>2</sub> treatment for 2 hours), and subsequently harvested. Cell lysates from these harvested cells were separated on SDS-PAGE, western transferred, and probed with myc and Pgk1 antibodies (Fig.3B). The western blotting results showed that a significant increase in Mxr2 protein abundance under all stress conditions (Fig. 10B).

Nicklow et al. [71] previously demonstrated that Mxr1 and Mxr2 regulate the activity of Fes1, the nucleotide exchange factor of cytosolic Hsp70. They also identified two translation-starting methionines, M1 and M34, in Mxr2. Ribosome footprinting assays indicated that translation of Mxr2 primarily initiates from M34, resulting in the absence of a mitochondrial localization signal in the Mxr2 peptide and its subsequent localization in the cytoplasm, contrasting earlier reports of mitochondrial localization of Mxr2 [70].

First, we intended to sort out the localization of Mxr2 using subcellular fractionation in the Mxr2-myc strain, as described in the methods. Whole cell extracts, mitochondria, and cytosolic fractions were separated on SDS-PAGE, western transferred, and probed with Porin (mitochondria), Pgk1 (cytosol), and Myc antibodies. The fractionation assay confirmed that most Mxr2 protein localizes in the cytosol (Fig. 10C).

We next explored whether stress conditions influence the localization of the Mxr2 protein. Alongside vegetative growth conditions, we examined two stress conditions: growth in nonfermentable glycerol media and nitrogen starvation media for 4 hours. Mitochondrial fractionation was performed on harvested cells and analyzed via western blotting. The data demonstrated that under vegetative conditions, the majority of Mxr2 protein localized to the cytosol, with a smaller portion in mitochondria. Interestingly, a significant portion of the Mxr2 protein pool under both stress conditions localized to mitochondria, while only a minor fraction remained in the cytosol (Fig. 10D). These findings indicate that Mxr2 protein levels increase under stress conditions and preferentially relocate to mitochondria, whereas it predominantly resides in the cytoplasm under vegetative conditions.

Observing that treatment of cells with SD-N media causes Mxr2 to relocate to mitochondria led us to investigate whether the mitochondrial localization of Mxr2 affects autophagy progression. Mxr2 contains a 29-amino acid N-terminal mitochondrial targeting signal (MTS). To retain Mxr2 in the cytoplasm, we constructed another overexpression variant where the MTS, excluding M1 ( $\Delta 29 \, Mxr2$ ), was deleted and expressed under the *TEF1* promoter with a FLAG tag. Autophagy flux assays using wild-type (WT) Mxr2 and the  $\Delta 29 \, Mxr2$  showed that while the WT construct fully restored defective autophagy flux in the  $mxr2\Delta$  strain, the  $\Delta 29 \, Mxr2$  construct did not (Fig. 10E). Given that the  $mxr2\Delta$  strain exhibits reduced autophagic flux due to ATG8 downregulation, we examined the transcriptional expression of ATG8 under overexpression conditions with these two Mxr2 constructs. RT-PCR data indicated that while

WT Mxr2 overexpression could restore the ATG8 expression, overexpression of  $\Delta$ 29 Mxr2 resulted in ATG8 expression similar to that observed in the  $mxr2\Delta$  strain (Fig. 10F).

To further validate the importance of Mxr2's mitochondrial localization in autophagy progression, we employed three GFP-tagged Mxr2 constructs [71] to assess their ability to rescue the downregulated transcriptional expression of ATG8. These constructs included WT Mxr2, a mutant with point mutations at either the M1 or M34 positions to leucine. Previous studies [71] indicated that the mutant carrying the M1 mutation initiates Mxr2 peptide synthesis from M34 without the MTS, leading to cytoplasmic localization. In contrast, the M34L mutant produces only the full-length peptide, localizing exclusively in mitochondria. These constructs were introduced into  $mxr2\Delta$  cells, and ATG8 expression was quantified using RT-PCR. The data showed that the WT construct completely rescued the defect, whereas the M1L mutant did not. Interestingly, the M34L mutant exhibited unusually high ATG8 transcript levels (Fig. 10G). These findings underscore that the presence and mitochondrial relocalization of Mxr2 under stress conditions are critical for ATG8 expression and the progression of autophagy.

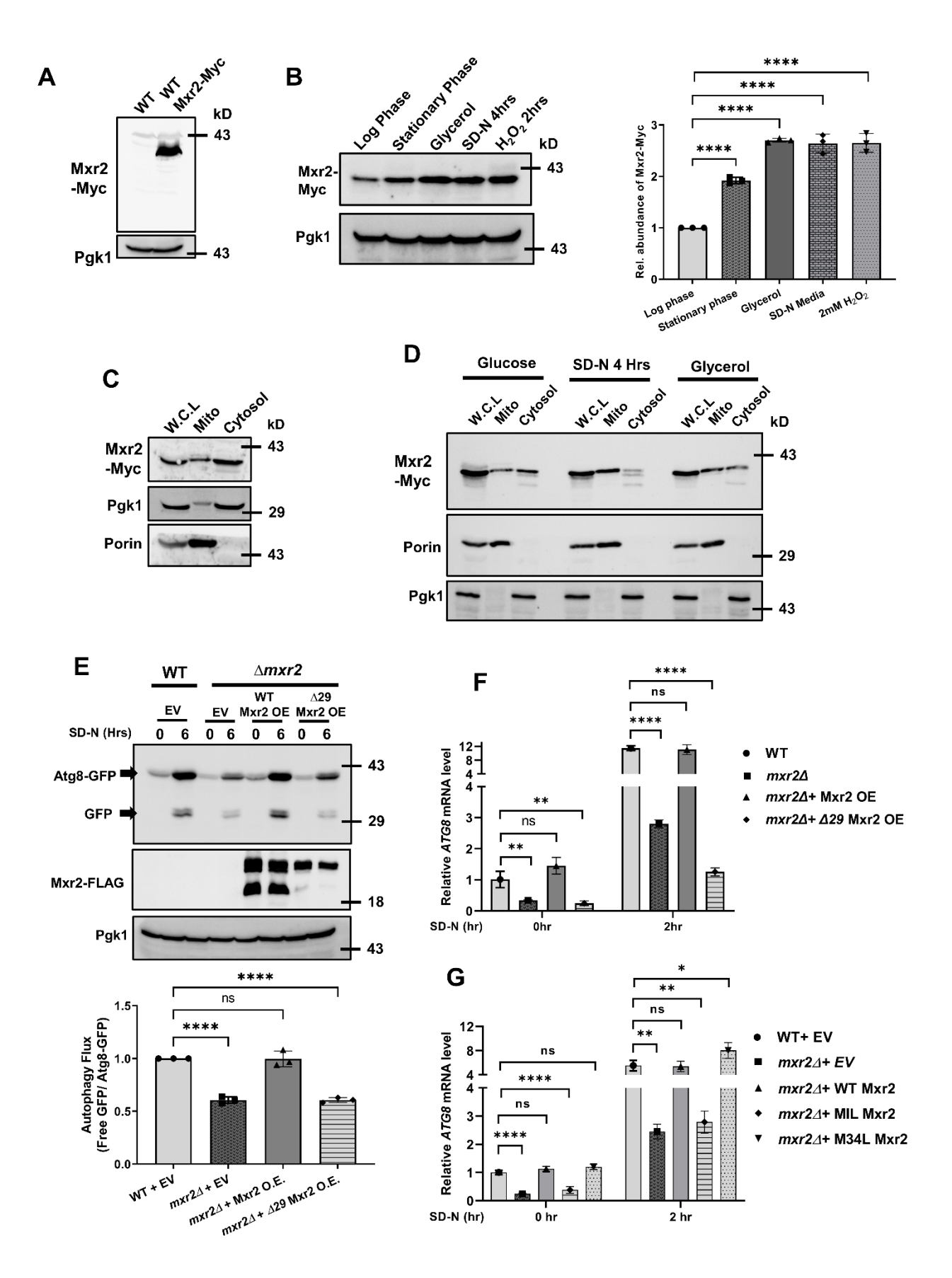


Figure 10. Stress induced mitochondrial localized Mxr2 is necessary for autophagy progression. (A) Western blotting with anti-myc antibody to show genomic myc tagging of Mxr2 protein in WT cells. Pgk1 was used as a loading control. (B) WT cells expressing Mxr2myc protein were grown under vegetative conditions or indicated stress conditions and harvested. Harvested cells were then analyzed via western blotting with an anti-myc antibody to check the Mxr2 protein abundance at different stress conditions. Pgk1 was used as a loading control. Quantification of the Mxr2-myc protein abundance under different stress conditions is represented in the right side panel. (C) WT cells expressing Mxr2-Myc were grown to log phase under vegetative conditions and harvested, and the organellar fraction was carried out as described in the methods. Western blots were probed with Myc, Porin and Pgk1 antibodies. Porin and Pgk1 were used as a loading controls for mitochondria and cytosol, respectively. (D) WT cells expressing Mxr2-myc protein were grown either in vegetative condition, in glycerol minimal media, or at first in glucose media and then starved in SD-N media for 4 hrs. Cells harvested in different conditions were subjected to organellar fractionation and probed with Myc, porin, and Pgk1 to show the Mxr2 protein abundance in cytosol and mitochondria. (E) WT cells were transformed with Atg8-GFP construct or empty vector, and *mxr2*∆ cells carrying Atg8-GFP construct were transformed with either empty vector or WT Mxr2-FLAG or Δ29 Mxr2-FLAG expressing construct. Transformants were grown in minimal media followed by treatment with nitrogen starved media for 0 or 6 hrs, and whole cell extracts were probed with GFP, Flag and Pgk1 antibodies. GFP antibody was used to analyze the autophagy flux assay while Pgk1 was used as a loading control, and Flag was used to show the over expression of Mxr2. Quantification of the autophagic flux is represented in the lower panel. (F) WT cells and  $mxr2\Delta$  cells expressing either full length or  $\Delta 29$  Mxr2-FLAG protein were grown to mid log phase and subjected to 0 or 2 hours of nitrogen starvation, and ATG8 transcript level was measured via qRT-PCR analysis. (G) WT cells carrying empty vector and mxr2Δ cells carrying either empty vector or WT or M1L or M34L Mxr2-GFP construct were treated with SD-N media for 2 hrs or kept untreated. Harvested cells were used to check the ATG8 transcript level via gRT-PCR analysis. The data shown are the mean ± SD of three biologically independent experiments. Statistical analysis was done using a one-way ANOVA test for (B, E, Fand G). \*\*\*\*p < 0.0001, \*\*\*p < 0.001, \*\*p < 0.01 and \*p < 0.05. ns, nonsignificant.

### 3.3.4. The $mxr2\Delta$ strain stabilizes the Ume6 and deacetylase complex proteins

The transcriptional downregulation of ATG8 in the  $mxr2\Delta$  strain prompted us to investigate whether defects in the initiation of autophagy activation are defective in the  $mxr2\Delta$  strain. During the activation of autophagy, Tor and PKA kinases are deactivated, leading to the dephosphorylation of hyperphosphorylated Atg13 proteins, which then associate with Atg1 to activate the Atg1 kinase complex to initiate Atg protein activation [257-260]. We intended to compare the Atg13 phosphorylation profiles between WT and  $mxr2\Delta$  strains. To examine the Atg13 phosphorylation profile, we utilized WT and  $mxr2\Delta$  strains with genomically myctagged ATG13. Cells were grown to mid-log phase and treated with SD-N for 2 hours. Cell lysates were separated on SDS-PAGE, western transferred, and probed with myc and Pgk1

antibodies. The fast-migrating Atg13 band is indicative of dephosphorylated protein. Figure 11A shows a similar shift in the mobility of Atg13-myc protein in both autophagy induced cell extracts of WT and  $mxr2\Delta$  strain compared to uninduced cells. These results suggest no difference in the dephosphorylation status of Atg13 protein between the two strains, ruling out the possibility of defects in autophagy activation.

The transcriptional regulation of ATG genes is pivotal during autophagy progression and is tightly regulated to prevent autophagic dysregulation [240,261]. Under nutrients are abundant nutrients, Tor kinases phosphorylate Sch9 kinase [262], which phosphorylates Rim15 kinase, leading to its cytoplasmic localization [159,160,263]. In such circumstances, Ume6 binds to the ATG8 promoter and represses its expression with histone deacetylase Rpd3 and corepressor Sin3 [154,194,264,265]. However, under nitrogen starvation conditions, Tor and Sch9 kinases become inactive and unable to phosphorylate Rim15. Additionally, Tps2 dephosphorylates Rim15's phosphorylated residue [162]. Dephosphorylated Rim15 then translocates to the nucleus and undergoes autophosphorylation [159]. Hyperphosphorylated Rim15 subsequently phosphorylates Ume6, disrupting its association with Sin3 and Rpd3 [266], thereby allowing for the reinstatement of ATG8 gene expression. Therefore, our initial interest was to determine if there were any differences in the phosphorylation status of Ume6 protein between the WT and mxr2∆ strains. We used genomically myc-tagged Ume6 gene was used to determine its phosphorylation status in WT and mxr2∆ strains. The Ume6-myc tagged WT and mxr2∆ cells were grown to log phase and starved with SD-N media for 2 hours. Western blotting data revealed that no change in phosphorylation status between the two strains (Fig 11B). Despite the lack of changes in the phosphorylation profile, we observed a consistent and moderate increase in Ume6 protein abundance in the mxr2\Delta strain compared to WT in vegetative and starved conditions (Fig 11B). To ascertain if the higher transcriptional expression of Ume6 protein is responsible for its increased abundance in the mxr $2\Delta$  strain, we quantified UME6 transcript levels in both strains using RT-PCR. The results show no significant difference in *UME6* transcript amounts between the two strains (Fig 11C).

In addition to phosphorylation, Ume6 undergoes acetylation at two distinct lysine clusters at its C-terminal end [196,197]. Acetylation at the first lysine cluster in Ume6 determines its faster turnover rate, tightly controlled by the Gcn5 acetylase and Rpd3-Sin3 deacetylase complex [196]. Consequently, we were interested in determining whether acetylation plays a role in slower turnover and higher stability of Ume6 in the  $mxr2\Delta$  strain compared to WT cells. Ume6 undergoes increased acetylation under stress conditions. Genomically myc tagged Ume6 WT

and  $mxr2\Delta$  cells were grown to log phase and starved with SD-N medium for 2 hours. Cells were harvested and immunoprecipitated with acetylated antibodies and probed with myc antibody. Immunoprecipitation assays using pan-acetylation antibodies reveal that a significant amount of Ume6 protein was immunoprecipitated in WT cells compared to  $mxr2\Delta$  cells, despite the total amount of Ume6 protein being higher in the  $mxr2\Delta$  strain (Fig.11D). The acetylation status of Ume6 governs the expression of meiosis regulatory genes and other genes involved in metabolic reprogramming. Therefore, we examined the transcriptional expression of CAR1, which encodes arginase required during nitrogen starvation, in WT and  $mxr2\Delta$  strains, as its expression is influenced by Ume6 acetylation status. RT-PCR data demonstrated significantly lower expression of the CAR1 gene in the  $mxr2\Delta$  strain compared to the WT strain (Fig.11E). These findings confirm that Ume6 protein undergoes less acetylation in the  $mxr2\Delta$  strain compared to the WT strain.

In yeast and mammalian cells, the acetylation status of various Atg proteins regulates autophagy progression [267]. However, the impact of Ume6 acetylation status on autophagy remains unclear. To determine the role of Ume6 acetylation in autophagy, we cloned both the WT and a mutant form of Flag-Ume6 into a pRS315 vector, where all lysine residues in the first and third lysine clusters (K736, K737, K745, K812, K813, and K814) were mutated to arginine. We introduced these constructs into the  $ume6\Delta$  strain alongside an empty vector transformed into WT,  $mxr2\Delta$ , and  $ume6\Delta$  strains. Transformed cells were subjected to autophagy flux assays for 6 hours as described in the methods. The results showed that the  $ume6\Delta$  strain exhibited high autophagy flux with excess Atg8 expression, as it failed to control the ATG8 gene expression (Fig. 11F, compare lanes 2, 4 to 6). Expression of WT Ume6 in the  $ume6\Delta$  strain nearly fully restored normal autophagy flux by repressing ATG8 expression (Fig.11F, lane 8). Interestingly, expression of the mutant Ume6 protein, which could not be acetylated, repressed ATG8 expression similarly to the  $mxr2\Delta$  strain and exhibited reduced autophagy flux comparable to the  $mxr2\Delta$  strain (Fig.11F, lane 10).

Given the presence of less acetylated Ume6 protein in the  $mxr2\Delta$  strain, we were interested in determining whether this was due to reduced acetylation or increased deacetylation. We examined the transcriptional expression of GCN5, RPD3, and SIN3 in these two strains using RT-PCR. The data showed that while the expression of GCN5 was comparable between the two strains, transcript levels of both RPD3 and SIN3 were significantly higher in the  $mxr2\Delta$  strain compared to WT (Fig.11G). These results suggest that the increased abundance of Rpd3 and Sin3 in the  $mxr2\Delta$  strain leads to reduced deacetylation of Ume6, thereby prolonging its

stability and increasing Ume6 protein levels, ultimately resulting in enhanced repression of the ATG8 gene.

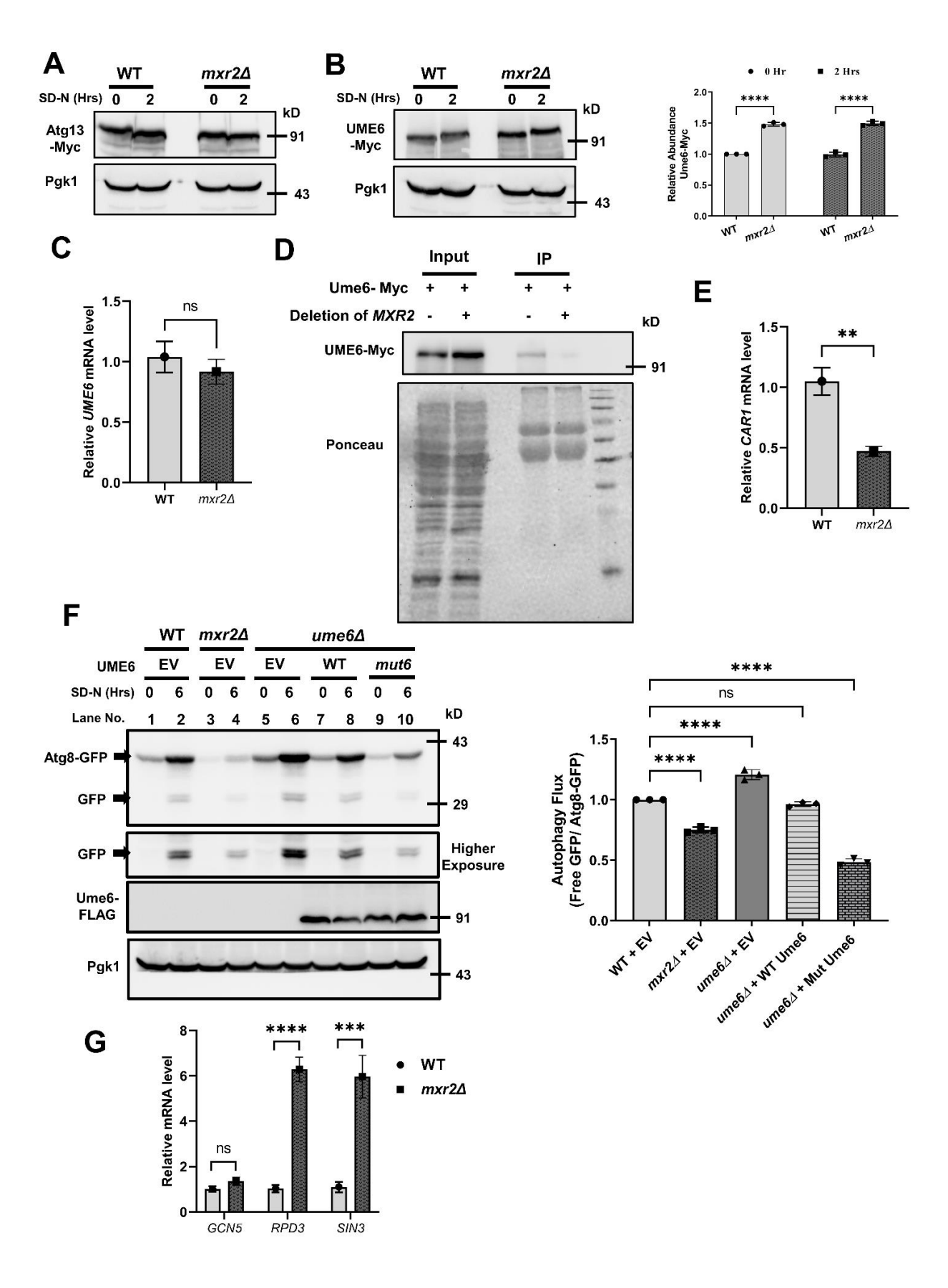


Figure 11. Ume6 protein abundance and expression of deacetylase complexes elevate in  $mxr2\Delta$  cells. (A, B). WT and  $mxr2\Delta$  cells expressing genomically tagged Atg13-myc (A) or Ume6-myc (B) were grown up to the mid-log phase and left untreated or treated with SD-N media for 2 hours. Harvested cells were analyzed to check the phosphorylation status of Atg13(A) or Ume6 (B) via mobility shift on immune blotting with an anti-myc antibody. Pgk1 was used as a loading control. Quantification of the Ume6-myc protein abundance in vegetative and nitrogen starved condition is represented in the right side panel. (C) WT and mxr2Δ cells were grown up to the mid-log phase and harvested. Harvested cells were then subjected to whole RNA isolation, which is further used to check the UME6 transcript level via qRT-PCR method. (D) Immunoprecipitation of Ume6 via anti-pan acetylation antibody. WT and mxr2Δ cells expressing genomically tagged Ume6-myc protein were grown up to the mid-log phase and then treated with SD-N media for 2 hours. Harvested cells were subjected to the preparation of soluble cell lysates. Cell lysates were then used to immunoprecipitate Ume6protein via anti-pan acetylation antibody to check the acetylation status of Ume6 in WT and mxr2Δ cells. Ponceau-stained blot was used as a loading control. (E) CAR1 transcript level was checked in WT and mxr2Δ cells via qRT-PCR method. (F) WT and mxr2Δ cells were transformed with Atg8-GFP construct and empty vector, whereas ume6∆ cells carrying Atg8-GFP construct were transformed with either empty vector or WT Ume6-FLAG expressing construct or mut Ume6-FLAG expressing construct. Autophagy flux assay was performed in these strains by analyzing Atg8-GFP processing. Quantification of the autophagic flux is represented in the right side panel. (G) GCN5, RPD3 and SIN3 transcript levels were checked in WT and mxr2Δ cells via qRT-PCR method. The data shown are the mean ± SD of three biologically independent experiments. Statistical analysis was done using an unpaired Student's t test for (C, E and G), a one-way ANOVA test for (F), whereas for (B). \*\*\*\*p < 0.0001, \*\*\*p < 0.001, \*\*p < 0.01 and \*p < 0.05. ns, nonsignificant.

### 3.3.5. Dep1 relays the signal from mitochondria to the Rpd3-Sin3 complex

As we delved into understanding how Mxr2 influences the regulation of the Rpd3-Sin3 complex, we encountered a recent study [268] revealing Dep1, a component of the Rpd3-Sin3 complex, as a novel regulator of mitophagy. This study highlighted that a portion of Dep1 resides within mitochondria, and deletion of DEP1 results in reduced autophagy flux. We found that loss of DEP1 results in reduced autophagy flux and also Atg8-GFP protein abundance and reduced expression of ATG8 similar to  $mxr2\Delta$  strain (Fig.12A and 12B). Given the similarity in autophagic defects between the  $mxr2\Delta$  and  $dep1\Delta$  strains, we investigated whether the  $mxr2\Delta$  strain exhibits a reduced abundance of Dep1 protein. RT-PCR analysis using cDNA from WT and  $mxr2\Delta$  strains demonstrated significantly lower levels of DEP1 transcripts in the  $mxr2\Delta$  strain compared to WT, both under normal growth conditions and during starvation, aligning with our hypothesis (Fig. 12C). To validate this finding, we conducted an autophagy flux assay

with WT and  $mxr2\Delta$  strains overexpressing FLAG-tagged Dep1, which fully restored the autophagic defect observed in the  $mxr2\Delta$  strain (Fig. 12D). Furthermore, RT-PCR data confirmed that Dep1 overexpression restored downregulated ATG8 expression and mitigated the elevated expression of RPD3 and SIN3 (Fig. 12E).

Given the upregulated expression of RPD3 and SIN3 in the  $mxr2\Delta$  strain, resulting in ATG8 repression, we sought to determine if the  $dep1\Delta$  strain exhibits similar upregulation of deacetylase complex proteins and reduced ATG8 expression. The RT-PCR analysis revealed that, as anticipated, RPD3 and SIN3 transcripts were significantly elevated in the  $dep1\Delta$  strain compared to WT, indicating that the autophagic defects in  $mxr2\Delta$  and  $dep1\Delta$  strains stem from disruptions in the same cellular machinery (Fig. 12F).

As an earlier report [268] have showed the presence of Dep1 in mitochondria, we were interested in investigating the impact of Dep1 localization on autophagic progression, we constructed Dep1 overexpression vectors containing either the mitochondrial targeting signal from the COX4 gene (MTS construct) or the nuclear localization signal from NUP60 (NLS construct). Autophagy flux assays in *dep1*\$\Delta\$ strains with these constructs demonstrated that the WT and MTS constructs successfully rescued the autophagic defect, whereas the NLS construct did not (Fig. 12G). Interestingly, analysis of the expression levels of different Dep1 constructs revealed that the protein abundance of the NLS construct was significantly higher than that of the others, despite comparable DEP1 transcriptional expression across all constructs (Fig. 12H). These findings underscore the critical role of the precise stoichiometry ratio of Dep1 in the deacetylated complex and its mitochondrial localization in autophagy progression.

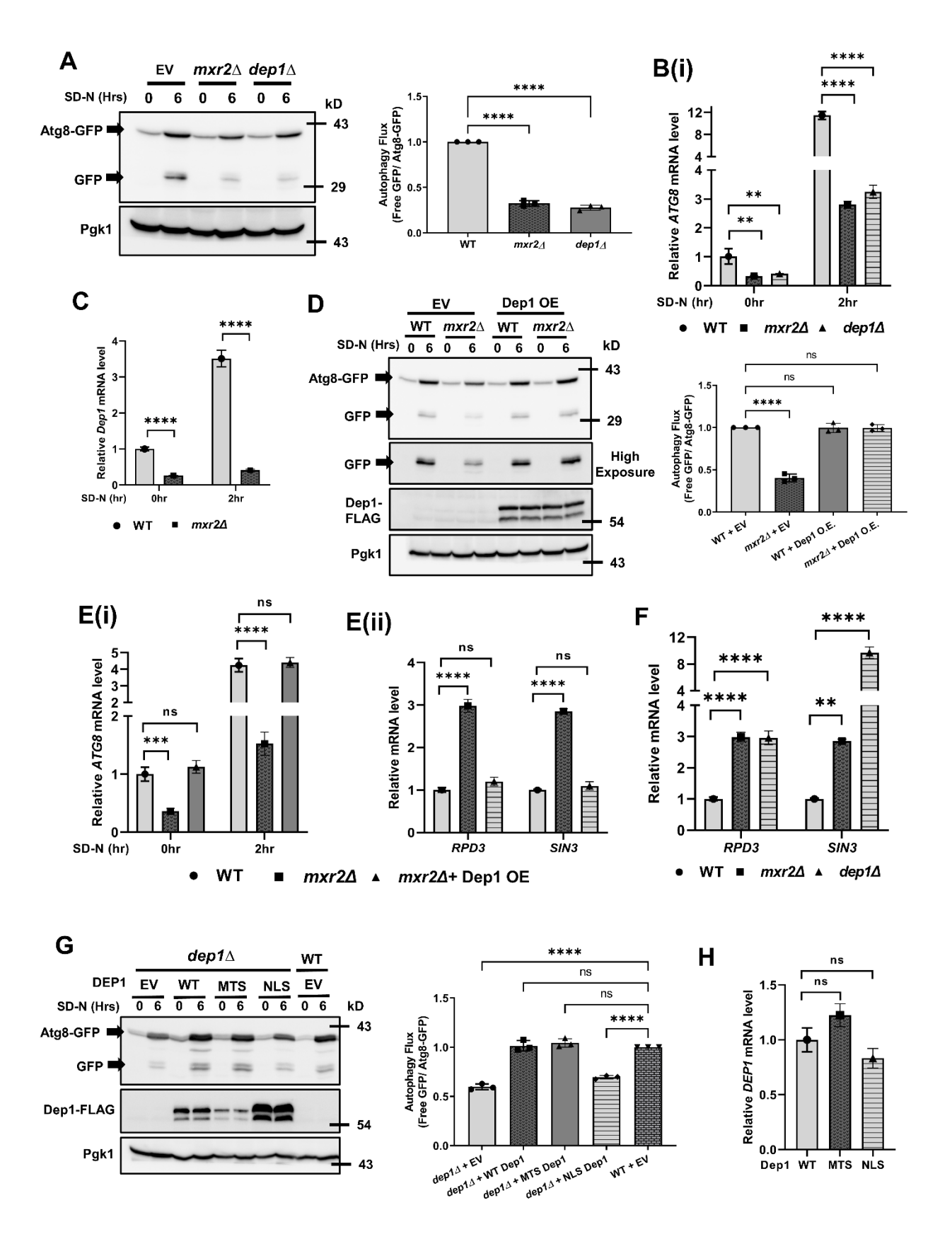


Figure 12. The signal from the mitochondria is relayed to the deacetylase complex via **Dep1.** (A) Autophagy flux assay was carried out with WT,  $mxr2\Delta$  and  $dep1\Delta$  cells expressing Atg8-GFP using Atg8-GFP processing assay. Quantification of the autophagic flux is represented in the right side panel. (B) WT,  $mxr2\Delta$  and  $dep1\Delta$  cells were grown to mid log phase in minimal media and subjected to 0 or 2 hours of nitrogen starvation, and ATG8 transcript level was measured via qRT-PCR analysis. (C) The transcript levels of DEP1 were checked in WT and mxr2\Delta cells under either vegetative or 2 hrs of nitrogen starvation condition via qRT- PCR analysis. (D) WT and mxr2Δ cells carrying Atg8-GFP construct were transformed with either empty vector or WT Dep1-FLAG overexpressing construct. Autophagy flux assay was performed in these strains by checking Atg8-GFP processing. Flag and Pgk1 immunoblots to show the expression of Dep1 and equal loading levels, respectively. Quantification of the autophagic flux is represented in the right side panel. (E) WT cells with empty vector and mxr2Δ cells carrying either empty vector or WT Dep1-FLAG overexpressing construct were at first grown in grown minimal condition followed by no treatment or further treated with nitrogen starvation condition for 2 hr. Harvested cells were further subjected for RNA isolation for qRT-PCR analysis. cDNA samples from both samples were used for checking ATG8 (i) transcript level whereas cDNA samples from cells that were not starved were used for checking RPD3 and SIN3 (ii) transcript levels. (F) WT, mxr2Δ and dep1Δ cells were grown to mid-log phase in minimal media and subjected RNA isolation to measure the transcript level of RPD3 and SIN3 via gRT-PCR analysis. (G) WT cells were transformed with Atg8-GFP construct and empty vector whereas dep1∆ cells carrying Atg8-GFP construct were transformed with either empty vector or overexpression construct of either WT Dep1-FLAG or MTS tagged Dep1-FLAG or NLS tagged Dep1-FLAG. Autophagy flux assay was performed using these transformants by checking Atg8-GFP processing. Quantification of the autophagic flux is represented in the right side panel. (H) dep1\Delta cells with overexpression construct of either WT Dep1-FLAG or MTS tagged Dep1-FLAG or NLS tagged Dep1-FLAG were grown in minimal media and DEP1 transcript level was measured via qRT-PCR analysis. The data shown are the mean ± SD of three biologically independent experiments. Statistical analysis was done using an unpaired Student's t test for (C and Ei), whereas one-way ANOVA tests were done test for (A, B, D, Eii, F, G and H). \*\*\*\*p < 0.0001, \*\*\*p < 0.001, \*\*p < 0.01 and \*p < 0.05. ns, nonsignificant.

# 3.3.6. Improved iron sulfur cluster biogenesis rescues the autophagic defect in the $mxr2\Delta$ strain

A previous study demonstrated that methionine sulfoxide reductases (MSR) play a protective role for iron-sulfur clusters, and deletion of MSR genes accelerates the turnover of these clusters, resulting in reduced activity of iron-sulfur cluster-containing enzymes [239]. This prompted us to investigate whether the decreased abundance of iron-sulfur clusters and reduced autophagic flux in the  $mxr2\Delta$  strain are interconnected. To explore this, we initially examined the  $ssq1\Delta$  strain, known for severe defects in iron-sulfur cluster biogenesis, to assess its autophagy flux. The autophagy flux assay revealed that the  $ssq1\Delta$  strain also exhibits significantly reduced autophagy flux (Fig. 13A). Furthermore, RT-PCR analysis of ATG8,

*DEP1*, *RPD3*, and *SIN3* genes showed that the  $ssq1\Delta$  strain has lower transcripts of *ATG8* and *DEP1*, and elevated expression of *RPD3* and *SIN3* genes, similar to the  $mxr2\Delta$  strain (Fig. 13Bi, ii).

Considering reports that the  $mxr2\Delta$  strain experiences enhanced turnover of iron-sulfur clusters leading to their reduced abundance, we investigated whether overproduction of iron-sulfur clusters by overexpressing key biosynthetic genes could rescue the autophagic defect in the  $mxr2\Delta$  strain. To test this, we overexpressed several genes involved in iron-sulfur cluster biosynthesis (SSQ1, ISA1, ISA2, YFH1, ISU1, and GRX5) in the  $mxr2\Delta$  strain and monitored autophagy flux (Fig. 13Ci). The assay results indicated that overexpression of four genes (SSQ1, ISA1, ISA2, and YFH1) completely restored autophagic flux in the  $mxr2\Delta$  strain, whereas overexpression of ISU1 and GRX5 did not (Fig. 13Cii). Moreover, RT-PCR data confirmed that overexpression of these genes successfully rescued the repression of the ATG8 gene and elevated transcriptional expression of RPD3 and SIN3, highlighting their role in mitigating the autophagic defect observed in the  $mxr2\Delta$  strain (Fig.13 Di, ii).

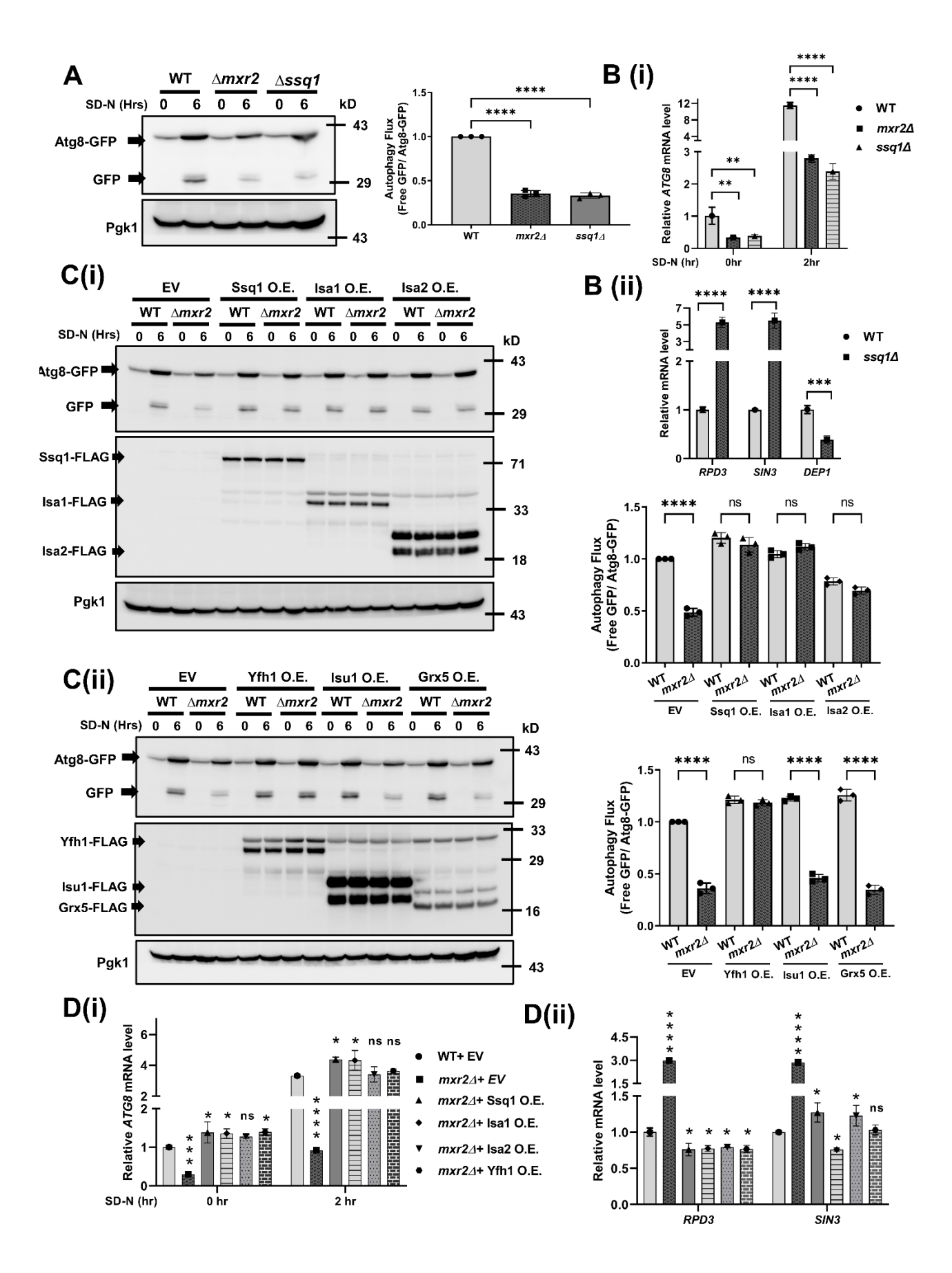


Figure 13. Autophagic defect in the mxr2Δ strain is rescued by modulating iron-sulfur cluster biogenesis. The indicated strains were grown to the mid-log phase in minimal media and subjected to 0 or 2 hrs (for qRT-PCR analysis) 6 hrs (for western blotting analysis) of nitrogen starvation, and cells were harvested. Cell lysates were either used to isolate total RNA for gRTPCR or separated on SDS-PAGE, western transferred and probed with GFP antibody to analyze the autophagy flux. Pgk1 was used as a loading control. FLAG antibody probe to show the expression of tagged proteins. (A) Autophagy flux assay was performed in WT, mxr2Δ, and ssq1Δ strains expressing Atg8-GFP using Atg8-GFP processing assay. Quantification of the autophagic flux is represented in the right panel. (B) ATG8(i) transcript level was checked in WT,  $mxr2\Delta$ , and  $ssg1\Delta$  cells, whereas RPD3, SIN3 and DEP1(ii) transcript levels were checked in WT and  $ssq1\Delta$  cells via qRT-PCR. (C) WT and  $mxr2\Delta$  cells carrying Atg8-GFP construct were transformed with either empty vector or construct overexpressing either one of the following proteins- Ssq1, Isa1, Isa2, (i) Yfh1, Isu1 or Grx5 (ii). Autophagy flux assay was performed using these transformants by checking Atg8-GFP processing. Quantification of the autophagic flux (both i and ii) is represented in the right side panel. (D) mxr2Δ cells carrying either empty vector or overexpressing one of the following proteins Ssq1, Isa1, Isa2, Yfh1, and WT cells transformed with empty vector were either treated with SD-N media for 2 hrs or kept untreated. Harvested cells were used to check ATG8 (i) transcript level via qRT-PCR analysis. The levels of RPD3 and SIN3 (ii) transcripts were checked in untreated cells. The data shown are the mean ± SD of three biologically independent experiments. Statistical analysis was done using an unpaired Student's t test for (Bii), whereas one-way ANOVA tests were done test for (A, Bi, C and D). \*\*\*\*p < 0.0001, \*\*\*p < 0.001, \*\*p < 0.01 and \*p < 0.05. ns, nonsignificant.

# 3.3.7. Mge1 connects iron-sulfur cluster machinery with Rpd3-Sin3 deacetylase complex required for autophagy progression via Dep1

Our previous studies have demonstrated that Mxr2 interacts with Mge1, protecting it from oxidative damage and thereby maintaining its functional dimeric form [70]. Furthermore, Mge1 plays a role in iron-sulfur cluster biogenesis by acting as a nucleotide exchange factor for Ssq1 [247]. Consequently, we aimed to investigate whether ectopic overexpression of Mge1 could rescue the autophagic defect observed in the  $mxr2\Delta$  strain. Autophagy flux assays conducted with  $mxr2\Delta$  cells overexpressing Mge1 showed autophagy flux levels comparable to WT cells (Fig. 14A). Moreover, the transcriptional expression of the ATG8 gene was restored in these cells, and the elevated expression of RPD3 and SIN3 genes in  $mxr2\Delta$  cells returned to WT levels following Mge1 overexpression (Fig. 14Bi, ii).

To further validate the role of Mge1 in autophagy, we examined whether defective Mge1 itself could induce an autophagic defect. Previous studies indicated that mutations (M115L and H167L) in Mge1 confer resistance to oxidative and heat stresses respectively [247,269]. However, combining both mutations into a double mutant (DM) renders cells more sensitive

to abiotic stress and causes structural changes in the Mge1 protein (data not shown). Autophagy flux assays performed with cells expressing WT Mge1, single mutants, and DM Mge1 proteins revealed that cells expressing DM Mge1 exhibited reduced autophagy flux, whereas cells expressing single mutants showed autophagy flux similar to those expressing WT Mge1 (Fig. 14C). Mitophagy flux measurements with the same strains yielded comparable results to the autophagy flux measurements (Fig. 14D). To explore whether the reduction in autophagy flux in DM Mge1-expressing strains is due to defects in the deacetylase complex, we measured the transcriptional expression of RPD3 and SIN3 genes. RT-PCR results indicated that RPD3 and SIN3 genes were upregulated in the DM Mge1 strain, along with downregulated ATG8 gene compared to the WT Mge1 strain (Fig. 14E i, ii). Along with ATG8 gene and deacetylase complex, we tried to check transcriptional expression of two other genes, CAR1 and DEP1, whose expression were significantly altered in mxr2∆ strain. RT-PCR result revealed significant downregulation of both genes in DM Mge1 expressing strain that the WT Mge1 strain, similar to  $mxr2\Delta$  strain (Fig. 14Eii). These findings suggest that functional Mge1 is essential for the transcriptional upregulation of Atg8 during autophagy induction, and the autophagic defect observed in the  $mxr2\Delta$  strain is dependent on Mge1.

Earlier experiments suggested that ectopic expression of both Dep1 and Mge1 can rescue the autophagic defect in the *mxr2*Δ strain, and an earlier report [268] identified localization of Dep1 in mitochondria, where Mge1 is also present. Therefore, we investigated whether Mge1 physically interacts with Dep1 using the yeast two-hybrid method. The results of the yeast two-hybrid assay revealed that Dep1 interacts with Mge1 (Fig. 14F). Given that DM Mge1-expressing cells exhibited an autophagic defect, we were curious to determine if DM Mge1 could still interact with Dep1. Surprisingly, yeast two-hybrid assays with the DM Mge1 construct showed that while WT Mge1 interacted effectively with Dep1, DM Mge1 failed to interact with Dep1 (Fig. 14G). These observations were further confirmed by immunoprecipitation assays. Co-overexpression of FLAG-tagged Dep1 with either WT or DM Mge1 followed by immunoprecipitation with FLAG antibody and subsequent Western blotting with Mge1 antibody showed that WT Mge1 co-precipitated with Dep1, whereas DM Mge1 did not (Fig. 14H). These results indicate that the interaction between Dep1 and Mge1 is crucial for the transcriptional regulation of ATG8 and progression of autophagy.

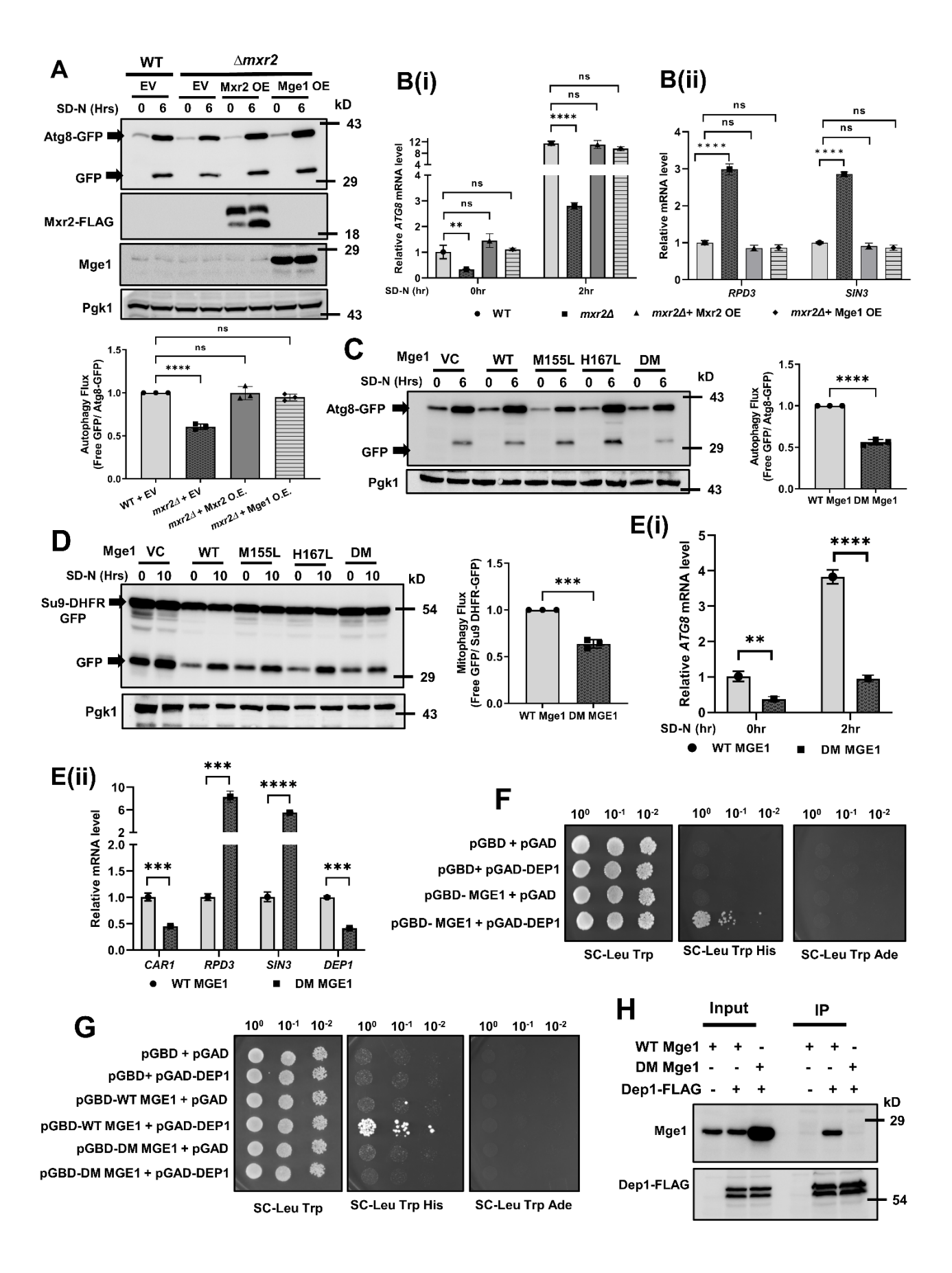


Figure 14. Mge1 links iron-sulfur cluster machinery and Rpd3-Sin3 deacetylase complex via Dep1. (A) WT cells were transformed with Atg8-GFP construct and empty vector whereas mxr2Δ cells carrying Atg8-GFP construct were transformed with either empty vector or constructs overexpressing Mxr2-FLAG or WT Mge1 protein. Autophagy flux assay was performed using these transformants by checking Atg8-GFP processing. Quantification of the autophagic flux is represented in the lower panel. (B) The same strains used in 7A were grown in minimal media and then either harvested or further treated with nitrogen starvation media for 2 hr. The RNA samples were isolated from the harvested cells and subjected to gRT-PCR analysis to measure the level of ATG8 (i) transcripts. cDNA samples from untreated cells were used to measure the level of RPD3 and SIN3 transcripts. (C) and (D) Autophagy and mitophagy flux assay was carried out in strains overexpressing WT and different Mge1 mutants (M155L, H167L and DM) using these transformants by checking Atg8-GFP processing. Quantification of the autophagic and mitophagic flux is represented in the right side panel. (E) Cells expressing either WT or DM Mge1 were grown in minimal media and then either harvested or further treated with nitrogen starvation media for 2 hr. The RNA samples were isolated from the harvested cells and subjected to qRT-PCR analysis to measure the level of ATG8 (i) transcripts. cDNA samples from untreated cells were used to measure the level of CAR1, RPD3, SIN3 and DEP1 transcripts. (F) Yeast two-hybrid assay was performed to check the interaction between WT Mge1 and Dep1. The PJ69-4A strain, transformed with pGBD-C1- WT MGE1 and pGAD-C1- DEP1 construct, were spotted along with control strains on agar plates of indicated minimal media. The growth profile was checked after incubation at 30°C for 2 days. (G) Yeast two hybrid assay was performed to check the interaction between DM Mge1 and Dep1. The PJ69-4A strain, transformed with pGBD-C1- DM MGE1 and pGAD-C1- DEP1 construct, were spotted along with control strains on agar plates of indicated minimal media. The growth profile was checked after incubation at 30°C for 2 days. (H) Immunoprecipitation assay to check the interaction between Dep1 with WT or DM Mge1. Strains expressing either WT or DM mge1 protein were transformed with Dep1-FLAG overexpressing construct. Transformants were grown up to the mid-log phase and the harvested cells were subjected to the preparation of soluble cell lysates. Cell lysates were then used to immunoprecipitate Dep1-FLAG protein via anti-FLAG antibody to check the copurification of Mge1 proteins. The data shown are the mean ± SD of three biologically independent experiments. Statistical analysis was done using either an unpaired Student's t test for (C, D, Ei and Eii) a one-way ANOVA test for (A,Bi and Bii). \*\*\*\*p < 0.0001, \*\*\*p < 0.001, \*\*p < 0.01 and \*p < 0.05. ns, nonsignificant.

## 2.4. CONCLUSION

In this chapter, we showed that different physiological stress condition upregulates Mxr2's expression and concentrate it within mitochondria. We also demonstrated that loss of MXR2 leads to dysregulation of the deacetylase complex and altered acetylation status of Ume6, which is crucial for ATG8 expression and autophagy progression. Further, altered Fe-S cluster metabolism due to loss of Mxr2 also correlated with impaired autophagy, which can be rescued by overexpressing genes involved in iron-sulfur cluster biosynthesis or Mge1, a nucleotide

exchange factor of Hsp70 and Mxr2's physiological substrate. Investigating the signaling pathway from mitochondrial machinery to the deacetylase complex, we discovered that Dep1, a component of the deacetylase complex, is localized in the mitochondria and physically interacts with Mge1. This interaction was critical for *ATG8* expression and the progression of autophagy. Overall, our study shows how mitochondrial physiology regulates autophagy by linking the mitochondrial redox regulation system, iron-sulfur cluster machinery, and the deacetylation apparatus to the transcriptional control of autophagy.

# **CHAPTER 4**

# **Discussion**

## 4.1. DISCUSSION FOR CHAPTER 2

ROS has been implicated in numerous signaling pathways that modulate developmental stages in different organisms. ROS has been noted to be involved in regulating various physiological processes and signaling circuits [270]. However, excess ROS generates oxidative stress that has deleterious consequences on proteins, DNA, lipids, and other biomolecules and ultimately leads to pathophysiological conditions [271]. Of all the amino acids, sulfur-containing amino acids methionine and cysteine are the most vulnerable to oxidation. Oxidative stress induces a disulfide link between two cysteines to form a cystine. In contrast, methionine is converted to methionine sulfoxide, which can be further oxidized to irreversible sulfone residues via the sequential addition of oxygen atoms. Being a hydrophobic amino acid, methionine residues establish hydrophobic bonds with the aromatic amino acids in the protein core, thus providing structural stability to proteins [272]. Oxidation of methionine causes the loss of hydrophobic bonds, exposing buried hydrophobic amino acids to the cellular milieu, thereby compromising the integrity of the three-dimensional protein structure. As a result, oxidized proteins present an increased propensity to degradation [273]. Consistent with this knowledge, we observe increased turnover of Atg19 and Ape1 proteins of the Cvt pathway during oxidative stress (Fig. 2E).

By reducing methionine sulfoxides to native methionines, Msrs neutralize oxidative damage. Prior reports in yeast show that deletion of MXR1 leads to mitochondrial dysfunction [67]. However, our earlier studies demonstrated that yeast cells devoid of MXR2 are more susceptible to oxidative stress than that of MXR1 and identified Mxr2 primarily as a mitochondrial matrix resident protein [70]. We first identified mitochondrially localized yeast Mge1 as the first in vivo substrate of Mxr2 [105]. Besides acting as a nucleotide exchange factor for Hsp70, Mge1 is an oxidative stress sensor [247]. Later, another study showed that the nucleotide exchange factor of cytosolic Hsp70, Fes1, is regulated by Mxr1 and Mxr2 via reversible methionine oxidation and Mxr2 is additionally present in the cytosol besides mitochondria [71]. These earlier studies opened up the possibility of identification of other cytosolic substrates of Mxr2.

This study employs yeast two-hybrid and immunoprecipitation methods to identify novel cytosolic substrates for Mxr2. For the first time, we show that Mxr2 regulates two Cvt pathway proteins, Atg19 and Ape1 (Fig. 1). Deletion of MXR2 decreases the abundance of Ape1 and Atg19 without affecting their transcript levels (Fig. 2, A and B). The absence of Mxr2 has a

more profound effect on the Apel protein level than Atg19 despite showing higher binding to Atg19 by two-hybrid analysis (Figs. 2Ai versus 2Aii versus 1A). Atg19 may be facilitating the interaction between Mxr2 and Ape1. Results from the cycloheximide chase assay depict the unstable nature of Ape1 in the absence of Mxr2 and its propensity to degradation. This result can be reconciled with our earlier finding that  $mxr2\Delta$  cells are more susceptible to oxidative stress as they carry more ROS than wt cells grown in the presence or absence of nonfermentable carbon sources. This reasoning is confirmed when we observe the degradation of Ape1 and Atg19 in wt cells exposed to oxidative stress (Fig. 2). This study shows that the absence of Mxr2 or oxidative stress destabilizes the Cvt pathway proteins, Ape1 and Atg19 (Fig. 7). However, further studies are required to unravel the oxidative stress-induced structural alterations these proteins undergo.

Mxr2 interacts only with prApe1 and not processed Ape1 (Fig. 3). This result is substantiated by the finding that the interaction between Mxr2 and Ape1 is contingent on M17 alone, although Ape1 harbors more methionine (Fig. 3). It is possible that prApe1 adopts a conformation where M17 is the only methionine susceptible to oxidation, making it mandatory to interact with Mxr2 for its reduction. Additionally, it shows that Mxr2 intervenes at a very early stage of the Cvt pathway when the proteins are more exposed to oxidative stress.

Msrs interact with oxidized methionine sulfoxides to reduce them to methionines. Our earlier study identified Met155 within Mge1, which interacts with Mxr2. Substitution of this methionine with leucine disrupted the interaction between Mxr2 and Mge1 and made the protein more stable, conferring oxidative stress resistance to cells [247,274]. Mutation of methionine 17 to leucine in Ape1 renders it resistant to degradation (Figs. 4C and 7) and does not interact with Mxr2 (Fig. 3C); however, it does not affect its maturation. Met17 lies in the propeptide region of the Ape1 protein and plays a vital role in Ape1 assembly and interaction with Atg19. Structural analysis of the first 1 to 22 amino acids of Ape1 shows that this region comprises an α-helical structure, which interacts with two other alpha helices to form an Ape1 trimer. It has been shown that, Leu11Ser mutation impairs Ape1 oligomerization and downstream processing [89]. By characterizing another residue in the propeptide, Met17, in Ape1 stability and response to oxidative stress, we underscore the importance of Ape1 propeptide in the Cvt pathway. The identity of the methionine residues in Atg19 that interact with Mxr2 remains to be identified.

Vacuoles in yeast and lysosomes in higher eukaryotes are involved in storing nutrients, maintaining metal ion homeostasis and also act as hubs for protein degradation [275]. This ranges from 40% (in vegetative conditions) to 85% during (in nutrient starvation) [276]. Compromised vacuolar or lysosomal-mediated protein degradation can cause physiological abnormalities, leading to many diseases. The Cvt pathway transports three vacuolar hydrolases: Ape1, Ams1, and Ape4, where Ape1 is a leucine aminopeptidase. We observe a significant reduction in LAP activity in the  $mxr2\Delta$  strain compared to the wt strain (Fig. 5B). Curiously, the LAP activity of the  $mxr2\Delta$  strain is comparable to that of the  $ape1\Delta$  strain, suggesting that the residual Ape1 protein in  $mxr2\Delta$  strain is not enzymatically efficient (Fig. 5).

The Apel complex communicates with the autophagy machinery via Atg19. As the Apel maturation is abolished in the absence of Atg19 (Fig. 2Ai), we tried to rescue the instability phenotype of Apel in the  $mxr2\Delta$  strain via overexpression of Atg19. Surprisingly, overexpression of Atg19 further destabilizes Apel in the  $mxr2\Delta$  strain. Interestingly, overexpression of Atg19 in the wt strain has a dominant negative effect, possibly by overwhelming the antioxidant machinery and competing with Apel for binding to Mxr2 (Fig. 6). An imbalance in the stoichiometry of Mxr2 to Apel may occur in the wt strain when Atg19 is overexpressed, resulting in an accelerated turnover of Apel (Fig. 6). This assumption is vindicated when overexpression of Mxr2 nullifies the dominant negative effect of Atg19 overexpression in both wt and  $mxr2\Delta$  strain robustly during nitrogen starvation and partially during normal physiological conditions. Based on these results, we conclude that the dependence of Apel and Atg19 proteins of the Cvt pathway on Mxr2 is critical for the operation of the Cvt pathway during oxidative stress.

#### 4.2. DISCUSSION FOR CHAPTER 3

Loss or reduction in methionine sulfoxide reductase (MSR) activity is linked to various cellular abnormalities in yeast and various clinical conditions in humans [67,212-216]. This study demonstrated that the Mxr2-Mge1-Dep1 triad functions as a positive regulator of the non-selective autophagy pathway. Atg8 protein incorporation into the phagophore membrane is crucial for membrane expansion and autophagosome formation, thereby governing cellular autophagic activity [253,254,277]. Controlling the cellular level of the Atg8 protein is a key strategy to inhibit autophagy activation under favorable growth conditions [145,240]. We find that the  $mxr2\Delta$  strain exhibited significantly reduced autophagy flux and a lower amount of

Atg8 protein (Fig. 8). As a methionine sulfoxide reductase, Mxr2 restores oxidized methionine residues in proteins to their native form, thereby protecting them from degradation and restoring their function [68,278]. However, we found that Mxr2 neither interacts nor affects Atg8 protein stability (Fig. 9). Further investigation revealed that the ATG8 gene is transcriptionally downregulated in the  $mxr2\Delta$  strain, contributing to the autophagic defect (Fig 9).

Cells depend on antioxidant proteins and enzymes whose transcriptional expression undergoes significant changes upon exposure to oxidative stress. Key transcription factors such as Msn2/Msn4, Yap1, Skn7, and Hsf1 are known to play pivotal roles in orchestrating this stress response [229,279-282]. Previous studies have indicated that nitrogen starvation increases the oxidation of methionine residues within cells [256]. Similarly, we observed that Mxr2 protein levels rise under various stress conditions and predominantly localizes to mitochondria (Fig 10), potentially protecting these organelles from oxidative damage. However, the mechanisms regulating this relocalization under stress conditions need to be investigated. Furthermore, our study demonstrated that enriching Mxr2 protein in mitochondria is crucial for autophagy progression and the upregulation of ATG8 (Fig 10). Our findings highlight the intricate regulation of Mxr2 in response to different environmental stress, its localization dynamics within cells, and autophagy regulation by modulating the transcriptional expression of a critical mediator, Atg8.

Autophagy induction in yeast is initiated by the Atg1 kinase and its adapter protein Atg13, and Atg17-Atg31-Atg20 complex [283]. Atg13 phosphorylation under nutrient rich conditions either by TORC1 or PKA inhibits the interaction between Atg13 and Atg1 and thereby reduces the Atg1 activity and downstream autophagy initiation. We found that autophagy induction was not compromised in  $mxr2\Delta$  strain as there was no change in the phosphorylation status of the Atg13 protein (Fig 11A). Numerous studies have elucidated the role of phosphorylation in regulating the Ume6 repressor, which is controlled by various kinases such as Tor, Sch9, and Rim15, affecting ATG8 transcriptional expression [154,159,284]. Interestingly, the  $mxr2\Delta$  strain exhibited no impairment in Ume6 phosphorylation but showed a significantly elevated protein abundance compared to the wild-type strain (Fig 11B), despite no transcriptional upregulation (Fig 11C).

Lysine acetylation is a critical post-translational modification, which modifies different proteins like transcription factors, components of the transcription machinery, chaperones,

tubulin, and numerous mitochondrial proteins and thus regulates diverse cellular signaling pathways [165,285]. Lysine acetylation is pivotal in regulating autophagy, influencing proteins involved in initiation, cargo assembly, autophagosome formation, and fusion with lysosomes [286-291]. In yeast, acetylation of Atg3 at K19/K48 enhances its activity in Atg8 lipidation [292]. However, there have been no reports on the transcriptional regulation of ATG8 through Ume6 acetylation. Previous studies [196,197] have extensively investigated how Ume6 acetylation status regulates meiotic gene expression. Ume6 possesses five lysine clusters in its C-terminal end, with acetylation at clusters 1 and 3 crucial for its role in gene regulation. Acetylation at cluster 1 targets Ume6 for faster turnover, limiting its abundance and repressive capacity [196]. Conversely, acetylation at cluster 3 prevents Ume6 from binding to gene promoters, thereby relieving repression [197]. Moreover, Ume6 can undergo simultaneous acetylation and phosphorylation [197]. We confirmed that reduced acetylation of Ume6 at both lysine clusters 1 and 3 significantly reduced the autophagic flux, comparable to the  $mxr2\Delta$ strain (Fig. 11). Collectively, these findings suggest that reduced acetylation of Ume6 in the mxr2\Delta strain increases its protein abundance, allowing it to recruit itself and the deacetylase complex to the ATG8 promoter for enhanced repression. The reduced acetylation of Ume6 in the  $mxr2\Delta$  strain was found to be associated with the upregulation of the deacetylase complex proteins Rpd3 and Sin3, despite comparable transcriptional expression of the Ume6 acetylase Gcn5 to that in the wild-type strain (Fig. 11).

The Rpd3 deacetylase complexes represent crucial groups of lysine deacetylases conserved from unicellular yeast to humans [186]. Typically, Rpd3 associates with three distinct protein complexes: Rpd3L, Rpd3S, and Rpd3 $\mu$ . Rpd3L is involved in ribosome biogenesis and responds to various abiotic stresses such as heat [187,188]. Conversely, Rpd3S maintains chromatin integrity [189], while the Rpd3 $\mu$  complex aids in cellular responses to oxidative stress [190]. The RPD3L complex comprises approximately 10 protein subunits, with Dep1 being one of its constituents. A recent study identified Dep1 as a regulator of mitophagy, noting that the  $dep1\Delta$  strain exhibits downregulation of ATG32, resulting in reduced mitophagy flux [268]. Despite reports stating no change in autophagy flux in the  $dep1\Delta$  strain, a clear decrease in Atg8 expression was observed in that study [268]. Similarly, our findings demonstrated a significant decrease in autophagy flux and Atg8 expression in the  $dep1\Delta$  strain compared to the wild-type strain (Fig. 12). Interestingly, the  $dep1\Delta$  strain also exhibited upregulation of deacetylase complex proteins, akin to the  $mxr2\Delta$  strain. This led us to hypothesize that the  $mxr2\Delta$  strain might have reduced Dep1 abundance, contributing to unregulated expression of

deacetylase complex proteins and consequent autophagy repression. This hypothesis was substantiated when we confirmed downregulation of DEP1 in the  $mxr2\Delta$  strain (Fig 12). However, the cellular signaling network underlying DEP1 downregulation remains to be elucidated. Intriguingly, we find that mitochondrial localization of Dep1 is crucial for autophagy progression while Dep1 with a nuclear-localizing signal exhibited autophagy repression similar to the  $mxr2\Delta$  strain (Fig. 12).

Iron-sulfur clusters serve as vital protein cofactors located in mitochondria, cytoplasm, endoplasmic reticulum, and the nucleus [293]. Autophagy plays a key role in the iron recycling mechanism during nutrient starvation, crucial for mitochondrial respiration and the diauxic shift [245]. This relationship is underscored by the fact that the proper functioning of mitochondria requires adequate iron availability, essential for iron-sulfur cluster biogenesis. In yeast, methionine sulfoxide reductases (MSRs) are involved in maintaining iron-sulfur clusters, as deletion strains of MSRs exhibit increased turnover of these clusters [239]. Remarkably, overexpression of certain genes rescued the autophagic defect in the  $mxr2\Delta$  strain (Fig. 13). Subsequently, the  $ssq1\Delta$  strain, which has a defect in iron-sulfur cluster biosynthesis, exhibited a similar autophagic defect characterized by upregulation of deacetylase complex components, downregulation of ATG8, and reduced autophagy flux (Fig 13). These findings underscore that cellular iron-sulfur cluster status regulates autophagy progression and that dysfunction in the iron-sulfur cluster machinery significantly impacts the autophagy process. Thus, our data confirm that the autophagic defect observed in the  $mxr2\Delta$  strain results from accelerated turnover of iron-sulfur clusters.

Mge1 functions as the nucleotide exchange factor for the mitochondrial Hsp70 chaperone Ssc1, and Ssq1facilitating mitochondrial protein import and iron-sulfur cluster biogenesis. Our previous research identified Mge1 as a cellular oxidative stress sensor, highlighting its sensitivity to oxidative stress at residue M155 [247]. Furthermore, prolonged oxidative stress leads to Mge1 protein unfolding and dissociation from the Hsp70 molecule, a process rescued by Mxr2 [70,274]. Another study identified residue H167 in Mge1 as sensitive to heat stress, and mutating this residue renders cells resistant to heat stress [269]. Given Mge1's involvement in iron-sulfur cluster biogenesis and its status as a physiological substrate for Mxr2, we investigated whether Mge1 plays a role in regulating autophagy. Interestingly, overexpressing Mge1 rescued the autophagic defect in the  $mxr2\Delta$  strain (Fig 14). Moreover, yeast strains with defective Mge1 expression (DM Mge1 expressing strain), exhibited autophagic defects akin to those seen in  $mxr2\Delta$ ,  $ssq1\Delta$ , or  $dep1\Delta$  strains (Fig 14). These experiments support our

hypothesis that the *mxr2*Δ strain's accelerated iron-sulfur cluster machinery is sensed by the associated Mge1 protein. This signal is relayed to the deacetylase complex, resulting in dysregulated expression of its protein components and ultimately repressing autophagy. Our study also revealed that mitochondria-localized Dep1 is crucial for autophagy progression as nuclear localized Dep1 could not revoke Ume6-mediated ATG8 gene downregulation (Fig 12). We demonstrated that Mge1 and Dep1 physically interact and DM Mge1, with minor structural changes in its conformation (data not shown), fails to interact with Dep1 and exhibits similar autophagic defects (Fig.14). Our study manifests that Dep1-Mge1-Mxr2 axis regulates the Rpd3-Sin3 complex mediated Ume6 stability and subsequent ATG8 transcription. In summary, our study links mitochondrial iron-sulfur cluster machinery and the lysine deacetylase complex to the transcriptional regulation of autophagy, an area previously unexplored.

### 4.3. IMPORTANCE OF THE STUDY

Selective autophagy is involved in diverse vital physiological pathways, for example, secretory pathways, vesicular trafficking, and other intracellular transport processes [294]. Impairment of selective autophagy has been well characterized in different clinical conditions like Alzheimer's and Parkinson's disease [295], chronic obstructive pulmonary disease [296], tuberculosis [297], HIV [298], and acute lung injury in hyperoxia [299]. Cvt pathway has been depicted only in *S. cerevisiae* and *Pichia pastoris* and is not conserved through evolution [300]. Nevertheless, it is one of the most characterized specific autophagy pathways. It serves as a model system to understand how particular cargos are selected, interact with the autophagy machinery, and get packed within the vesicle and delivered to the vacuole due to fewer molecular players and less cargo. Hence, investigating and elucidating the Cvt pathway and understanding its regulation will provide insights into other more complex autophagy pathways in higher eukaryotes. By identifying Atg19 and Ape1 as cytosolic substrates of Mxr2, we spotlight a hitherto unmapped link between two unrelated physiological machineries: the MSR system and the Cvt autophagy pathway.

Bulk autophagy or nonselective autophagy is one of the most fundamental physiological phenomena that help cells withstand different stress conditions. Defects in autophagy machinery led to several disorders and even cancer. In yeast, more than 40 ATG genes are involved in the autophagy process, and optimum autophagic activity depends upon the Atg proteins' accurate stoichiometry. Hence, transcriptional expression of Atg genes should be

tightly regulated. This understanding of regulation has been of great interest in the scientific field for more than a decade. However, the regulation of autophagic process is still not well understood. Autophagy is also involved in the maintenance of mitochondrial physiology, and defects in autophagy lead to mitochondrial abnormality, which has been broadly studied. But if mitochondrial function is impaired, what will be the effect on autophagy machinery and is there any mitochondrial signal necessary for autophagy progression? There are no studies to depict the role of mitochondria to address the above questions. So, our study identified that the Mxr2- Mge1 duo in mitochondria regulate transcriptional expression of Atg8 via controlling the deacetylase activity of the Rpd3-Sin3 complex. Though protein acetylation has been shown to modulate the activity of Atg proteins, for the first time, we are showing protein acetylation to be involved in the transcriptional regulation of autophagy genes. This study also showed impaired mitochondrial iron-sulfur cluster biogenesis leads to defects in autophagy progression. Our study will help to understand the transcriptional regulation of autophagy more precisely and enable others to identify other molecular players involved in this network. A better understanding of autophagy regulation will enable us to discover new ways to battle against many critical pathological conditions that develop due to dysfunctional autophagic activity.

# References

- [1] Bedwell S, Dean RT, Jessup W. The action of defined oxygen-centred free radicals on human low-density lipoprotein. Biochem J. 1989 Sep 15;262(3):707-12.
- [2] Halliwell B. Oxidants and human disease: some new concepts. Faseb j. 1987 Nov;1(5):358-64.
- [3] Kuppusamy P, Zweier JL. Characterization of free radical generation by xanthine oxidase. Evidence for hydroxyl radical generation. J Biol Chem. 1989 Jun 15;264(17):9880-4.
- [4] Kontos HA, Wei EP, Ellis EF, et al. Appearance of superoxide anion radical in cerebral extracellular space during increased prostaglandin synthesis in cats. Circ Res. 1985 Jul;57(1):142-51.
- [5] De Grey AD. HO2\*: the forgotten radical. DNA Cell Biol. 2002 Apr;21(4):251-7.
- [6] Halliwell B, Clement MV, Long LH. Hydrogen peroxide in the human body. FEBS Lett. 2000 Dec 1;486(1):10-3.
- [7] Hojo Y, Okado A, Kawazoe S, et al. In vivo singlet-oxygen generation in blood of chromium(VI)-treated mice: an electron spin resonance spin-trapping study. Biol Trace Elem Res. 2000 Jul;76(1):85-93.
- [8] Hampton MB, Kettle AJ, Winterbourn CC. Inside the neutrophil phagosome: oxidants, myeloperoxidase, and bacterial killing. Blood. 1998 Nov 1;92(9):3007-17.
- [9] Kanofsky JR. Singlet oxygen production by biological systems. Chem Biol Interact. 1989;70(1-2):1-28.
- [10] Chan HW. Singlet oxygen analogs in biological systems. Peroxidase-catalyzed oxygenation of 1,3-dienes. J Am Chem Soc. 1971 Sep 8;93(18):4632-3.
- [11] Hayaishi O, Nozaki M. Nature and mechanisms of oxygenases. Science. 1969 Apr 25;164(3878):389-96.
- [12] Kanofsky JR. Singlet oxygen production by lactoperoxidase. J Biol Chem. 1983 May 25;258(10):5991-3.
- [13] Sies H, Menck CF. Singlet oxygen induced DNA damage. Mutat Res. 1992 Sep;275(3-6):367-75.
- [14] Finkel T, Holbrook NJ. Oxidants, oxidative stress and the biology of ageing. Nature. 2000 Nov 9;408(6809):239-47.
- [15] De Duve C, Baudhuin P. Peroxisomes (microbodies and related particles). Physiol Rev. 1966 Apr;46(2):323-57.
- [16] Cheeseman KH, Slater TF. An introduction to free radical biochemistry. Br Med Bull. 1993 Jul;49(3):481-93.

- [17] Gross E, Sevier CS, Heldman N, et al. Generating disulfides enzymatically: reaction products and electron acceptors of the endoplasmic reticulum thiol oxidase Ero1p. Proc Natl Acad Sci U S A. 2006 Jan 10;103(2):299-304.
- [18] Valko M, Leibfritz D, Moncol J, et al. Free radicals and antioxidants in normal physiological functions and human disease. Int J Biochem Cell Biol. 2007;39(1):44-84.
- [19] Nordberg J, Arnér ES. Reactive oxygen species, antioxidants, and the mammalian thioredoxin system. Free Radic Biol Med. 2001 Dec 1;31(11):1287-312.
- [20] Ylä-Herttuala S. Oxidized LDL and atherogenesis. Ann N Y Acad Sci. 1999 Jun 30;874:134-7.
- [21] Stadtman ER, Levine RL. Protein oxidation. Ann N Y Acad Sci. 2000;899:191-208.
- [22] Marnett LJ. Oxyradicals and DNA damage. Carcinogenesis. 2000 Mar;21(3):361-70.
- [23] Dizdaroglu M, Jaruga P, Birincioglu M, et al. Free radical-induced damage to DNA: mechanisms and measurement. Free Radic Biol Med. 2002 Jun 1;32(11):1102-15.
- [24] Hofer T, Badouard C, Bajak E, et al. Hydrogen peroxide causes greater oxidation in cellular RNA than in DNA. Biol Chem. 2005 Apr;386(4):333-7.
- [25] Abe T, Tohgi H, Isobe C, et al. Remarkable increase in the concentration of 8-hydroxyguanosine in cerebrospinal fluid from patients with Alzheimer's disease. J Neurosci Res. 2002 Nov 1;70(3):447-50.
- [26] Martinet W, de Meyer GR, Herman AG, et al. Reactive oxygen species induce RNA damage in human atherosclerosis. Eur J Clin Invest. 2004 May;34(5):323-7.
- [27] Kikuchi A, Takeda A, Onodera H, et al. Systemic increase of oxidative nucleic acid damage in Parkinson's disease and multiple system atrophy. Neurobiol Dis. 2002 Mar;9(2):244-8.
- [28] Siems WG, Grune T, Esterbauer H. 4-Hydroxynonenal formation during ischemia and reperfusion of rat small intestine. Life Sci. 1995;57(8):785-9.
- [29] Marnett LJ. Lipid peroxidation-DNA damage by malondialdehyde. Mutat Res. 1999 Mar 8;424(1-2):83-95.
- [30] Dean RT, Fu S, Stocker R, et al. Biochemistry and pathology of radical-mediated protein oxidation. Biochem J. 1997 May 15;324 (Pt 1)(Pt 1):1-18.
- [31] Butterfield DA, Koppal T, Howard B, et al. Structural and functional changes in proteins induced by free radical-mediated oxidative stress and protective action of the antioxidants N-tert-butyl-alpha-phenylnitrone and vitamin E. Ann N Y Acad Sci. 1998 Nov 20;854:448-62.

- [32] Dubois-Deruy E, Peugnet V, Turkieh A, et al. Oxidative Stress in Cardiovascular Diseases. Antioxidants (Basel). 2020 Sep 14;9(9).
- [33] Uttara B, Singh AV, Zamboni P, et al. Oxidative stress and neurodegenerative diseases: a review of upstream and downstream antioxidant therapeutic options. Curr Neuropharmacol. 2009 Mar;7(1):65-74.
- [34] Bhattacharyya A, Chattopadhyay R, Mitra S, et al. Oxidative stress: an essential factor in the pathogenesis of gastrointestinal mucosal diseases. Physiol Rev. 2014 Apr;94(2):329-54.
- [35] Hayes JD, Dinkova-Kostova AT, Tew KD. Oxidative Stress in Cancer. Cancer Cell. 2020 Aug 10;38(2):167-197.
- [36] Romano AD, Serviddio G, de Matthaeis A, et al. Oxidative stress and aging. J Nephrol. 2010 Sep-Oct;23 Suppl 15:S29-36.
- [37] Jung K, Reszka R. Mitochondria as subcellular targets for clinically useful anthracyclines. Adv Drug Deliv Rev. 2001 Jul 2;49(1-2):87-105.
- [38] Culotta VC, Yang M, O'Halloran TV. Activation of superoxide dismutases: putting the metal to the pedal. Biochim Biophys Acta. 2006 Jul;1763(7):747-58.
- [39] Sturtz LA, Diekert K, Jensen LT, et al. A fraction of yeast Cu,Zn-superoxide dismutase and its metallochaperone, CCS, localize to the intermembrane space of mitochondria. A physiological role for SOD1 in guarding against mitochondrial oxidative damage. J Biol Chem. 2001 Oct 12;276(41):38084-9.
- [40] van Loon AP, Pesold-Hurt B, Schatz G. A yeast mutant lacking mitochondrial manganese-superoxide dismutase is hypersensitive to oxygen. Proc Natl Acad Sci U S A. 1986 Jun;83(11):3820-4.
- [41] Guidot DM, McCord JM, Wright RM, et al. Absence of electron transport (Rho 0 state) restores growth of a manganese-superoxide dismutase-deficient Saccharomyces cerevisiae in hyperoxia. Evidence for electron transport as a major source of superoxide generation in vivo. J Biol Chem. 1993 Dec 15;268(35):26699-703.
- [42] Costa V, Amorim MA, Reis E, et al. Mitochondrial superoxide dismutase is essential for ethanol tolerance of Saccharomyces cerevisiae in the post-diauxic phase. Microbiology (Reading). 1997 May;143 ( Pt 5):1649-1656.
- [43] Gralla EB, Valentine JS. Null mutants of Saccharomyces cerevisiae Cu,Zn superoxide dismutase: characterization and spontaneous mutation rates. J Bacteriol. 1991 Sep;173(18):5918-20.

- [44] Liu XF, Elashvili I, Gralla EB, et al. Yeast lacking superoxide dismutase. Isolation of genetic suppressors. J Biol Chem. 1992 Sep 15;267(26):18298-302.
- [45] Longo VD, Gralla EB, Valentine JS. Superoxide dismutase activity is essential for stationary phase survival in Saccharomyces cerevisiae. Mitochondrial production of toxic oxygen species in vivo. J Biol Chem. 1996 May 24;271(21):12275-80.
- [46] Hiltunen JK, Mursula AM, Rottensteiner H, et al. The biochemistry of peroxisomal beta-oxidation in the yeast Saccharomyces cerevisiae. FEMS Microbiol Rev. 2003 Apr;27(1):35-64.
- [47] Izawa S, Inoue Y, Kimura A. Importance of catalase in the adaptive response to hydrogen peroxide: analysis of acatalasaemic Saccharomyces cerevisiae. Biochem J. 1996 Nov 15;320 (Pt 1)(Pt 1):61-7.
- [48] Inoue Y, Matsuda T, Sugiyama K, et al. Genetic analysis of glutathione peroxidase in oxidative stress response of Saccharomyces cerevisiae. J Biol Chem. 1999 Sep 17;274(38):27002-9.
- [49] Avery AM, Avery SV. Saccharomyces cerevisiae expresses three phospholipid hydroperoxide glutathione peroxidases. J Biol Chem. 2001 Sep 7;276(36):33730-5.
- [50] Avery AM, Willetts SA, Avery SV. Genetic dissection of the phospholipid hydroperoxidase activity of yeast gpx3 reveals its functional importance. J Biol Chem. 2004 Nov 5;279(45):46652-8.
- [51] Basu U, Southron JL, Stephens JL, et al. Reverse genetic analysis of the glutathione metabolic pathway suggests a novel role of PHGPX and URE2 genes in aluminum resistance in Saccharomyces cerevisiae. Mol Genet Genomics. 2004 Jun;271(5):627-37.
- [52] Wood ZA, Schröder E, Robin Harris J, et al. Structure, mechanism and regulation of peroxiredoxins. Trends Biochem Sci. 2003 Jan;28(1):32-40.
- [53] Rhee SG, Chae HZ, Kim K. Peroxiredoxins: a historical overview and speculative preview of novel mechanisms and emerging concepts in cell signaling. Free Radic Biol Med. 2005 Jun 15;38(12):1543-52.
- [54] Holmgren A. Thioredoxin and glutaredoxin systems. J Biol Chem. 1989 Aug 25;264(24):13963-6.
- [55] Fernandes AP, Holmgren A. Glutaredoxins: glutathione-dependent redox enzymes with functions far beyond a simple thioredoxin backup system. Antioxid Redox Signal. 2004 Feb;6(1):63-74.

- [56] Toledano MB, Kumar C, Le Moan N, et al. The system biology of thiol redox system in Escherichia coli and yeast: differential functions in oxidative stress, iron metabolism and DNA synthesis. FEBS Lett. 2007 Jul 31;581(19):3598-607.
- [57] Luikenhuis S, Perrone G, Dawes IW, et al. The yeast Saccharomyces cerevisiae contains two glutaredoxin genes that are required for protection against reactive oxygen species. Mol Biol Cell. 1998 May;9(5):1081-91.
- [58] Porras P, Padilla CA, Krayl M, et al. One single in-frame AUG codon is responsible for a diversity of subcellular localizations of glutaredoxin 2 in Saccharomyces cerevisiae. J Biol Chem. 2006 Jun 16;281(24):16551-62.
- [59] Garrido EO, Grant CM. Role of thioredoxins in the response of Saccharomyces cerevisiae to oxidative stress induced by hydroperoxides. Mol Microbiol. 2002 Feb;43(4):993-1003.
- [60] Levine RL, Moskovitz J, Stadtman ER. Oxidation of methionine in proteins: roles in antioxidant defense and cellular regulation. IUBMB Life. 2000 Oct-Nov;50(4-5):301-7.
- [61] Brot N, Weissbach H. Biochemistry of methionine sulfoxide residues in proteins. Biofactors. 1991 Jun;3(2):91-6.
- [62] Stadtman ER, Moskovitz J, Berlett BS, et al. Cyclic oxidation and reduction of protein methionine residues is an important antioxidant mechanism. Mol Cell Biochem. 2002 May-Jun;234-235(1-2):3-9.
- [63] Kim HY, Gladyshev VN. Role of structural and functional elements of mouse methionine-S-sulfoxide reductase in its subcellular distribution. Biochemistry. 2005 Jun 7;44(22):8059-67.
- [64] Zhang XH, Weissbach H. Origin and evolution of the protein-repairing enzymes methionine sulphoxide reductases. Biol Rev Camb Philos Soc. 2008 Aug;83(3):249-57.
- [65] Lowther WT, Brot N, Weissbach H, et al. Thiol-disulfide exchange is involved in the catalytic mechanism of peptide methionine sulfoxide reductase. Proc Natl Acad Sci U S A. 2000 Jun 6;97(12):6463-8.
- [66] Neiers F, Kriznik A, Boschi-Muller S, et al. Evidence for a new sub-class of methionine sulfoxide reductases B with an alternative thioredoxin recognition signature. J Biol Chem. 2004 Oct 8;279(41):42462-8.
- [67] Kaya A, Koc A, Lee BC, et al. Compartmentalization and regulation of mitochondrial function by methionine sulfoxide reductases in yeast. Biochemistry. 2010 Oct 5;49(39):8618-25.

- [68] Boschi-Muller S, Gand A, Branlant G. The methionine sulfoxide reductases: Catalysis and substrate specificities. Arch Biochem Biophys. 2008 Jun 15;474(2):266-73.
- [69] Le DT, Lee BC, Marino SM, et al. Functional analysis of free methionine-R-sulfoxide reductase from Saccharomyces cerevisiae. J Biol Chem. 2009 Feb 13;284(7):4354-64.
- [70] Allu PK, Marada A, Boggula Y, et al. Methionine sulfoxide reductase 2 reversibly regulates Mge1, a cochaperone of mitochondrial Hsp70, during oxidative stress. Mol Biol Cell. 2015 Feb 1;26(3):406-19.
- [71] Nicklow EE, Sevier CS. Activity of the yeast cytoplasmic Hsp70 nucleotide-exchange factor Fes1 is regulated by reversible methionine oxidation. J Biol Chem. 2020 Jan 10;295(2):552-569.
- [72] Lowther WT, Weissbach H, Etienne F, et al. The mirrored methionine sulfoxide reductases of Neisseria gonorrhoeae pilB. Nat Struct Biol. 2002 May;9(5):348-52.
- [73] Lowther WT, Brot N, Weissbach H, et al. Structure and mechanism of peptide methionine sulfoxide reductase, an "anti-oxidation" enzyme. Biochemistry. 2000 Nov 7;39(44):13307-12.
- [74] Moskovitz J, Poston JM, Berlett BS, et al. Identification and characterization of a putative active site for peptide methionine sulfoxide reductase (MsrA) and its substrate stereospecificity. J Biol Chem. 2000 May 12;275(19):14167-72.
- [75] Boschi-Muller S, Azza S, Sanglier-Cianferani S, et al. A sulfenic acid enzyme intermediate is involved in the catalytic mechanism of peptide methionine sulfoxide reductase from Escherichia coli. J Biol Chem. 2000 Nov 17;275(46):35908-13.
- [76] Tête-Favier F, Cobessi D, Boschi-Muller S, et al. Crystal structure of the Escherichia coli peptide methionine sulphoxide reductase at 1.9 A resolution. Structure. 2000 Nov 15;8(11):1167-78.
- [77] Reggiori F, Klionsky DJ. Autophagic processes in yeast: mechanism, machinery and regulation. Genetics. 2013 Jun;194(2):341-61.
- [78] Suzuki K. Selective autophagy in budding yeast. Cell Death Differ. 2013 Jan;20(1):43-8.
- [79] Yorimitsu T, Klionsky DJ. Atg11 links cargo to the vesicle-forming machinery in the cytoplasm to vacuole targeting pathway. Mol Biol Cell. 2005 Apr;16(4):1593-605.
- [80] Kanki T, Wang K, Cao Y, et al. Atg32 is a mitochondrial protein that confers selectivity during mitophagy. Dev Cell. 2009 Jul;17(1):98-109.
- [81] Baba M, Osumi M, Scott SV, et al. Two distinct pathways for targeting proteins from the cytoplasm to the vacuole/lysosome. J Cell Biol. 1997 Dec 29;139(7):1687-95.

- [82] Scott SV, Baba M, Ohsumi Y, et al. Aminopeptidase I is targeted to the vacuole by a nonclassical vesicular mechanism. J Cell Biol. 1997 Jul 14;138(1):37-44.
- [83] Umekawa M, Klionsky DJ. The Cytoplasm-to-Vacuole Targeting Pathway: A Historical Perspective. Int J Cell Biol. 2012;2012:142634.
- [84] Kim J, Scott SV, Oda MN, et al. Transport of a large oligomeric protein by the cytoplasm to vacuole protein targeting pathway. J Cell Biol. 1997 May 5;137(3):609-18.
- [85] Shintani T, Klionsky DJ. Cargo proteins facilitate the formation of transport vesicles in the cytoplasm to vacuole targeting pathway. J Biol Chem. 2004 Jul 16;279(29):29889-94.
- [86] Oda MN, Scott SV, Hefner-Gravink A, et al. Identification of a cytoplasm to vacuole targeting determinant in aminopeptidase I. J Cell Biol. 1996 Mar;132(6):999-1010.
- [87] Scott SV, Guan J, Hutchins MU, et al. Cvt19 is a receptor for the cytoplasm-to-vacuole targeting pathway. Mol Cell. 2001 Jun;7(6):1131-41.
- [88] Shintani T, Huang WP, Stromhaug PE, et al. Mechanism of cargo selection in the cytoplasm to vacuole targeting pathway. Dev Cell. 2002 Dec;3(6):825-37.
- [89] Yamasaki A, Watanabe Y, Adachi W, et al. Structural Basis for Receptor-Mediated Selective Autophagy of Aminopeptidase I Aggregates. Cell Rep. 2016 Jun 28;16(1):19-27.
- [90] Morales Quinones M, Winston JT, Stromhaug PE. Propeptide of aminopeptidase 1 protein mediates aggregation and vesicle formation in cytoplasm-to-vacuole targeting pathway. J Biol Chem. 2012 Mar 23;287(13):10121-10133.
- [91] Sawa-Makarska J, Abert C, Romanov J, et al. Cargo binding to Atg19 unmasks additional Atg8 binding sites to mediate membrane-cargo apposition during selective autophagy. Nat Cell Biol. 2014 May;16(5):425-433.
- [92] Hutchins MU, Klionsky DJ. Vacuolar localization of oligomeric alpha-mannosidase requires the cytoplasm to vacuole targeting and autophagy pathway components in Saccharomyces cerevisiae. J Biol Chem. 2001 Jun 8;276(23):20491-8.
- [93] Suzuki K, Kondo C, Morimoto M, et al. Selective transport of alpha-mannosidase by autophagic pathways: identification of a novel receptor, Atg34p. J Biol Chem. 2010 Sep 24;285(39):30019-25.
- [94] Watanabe Y, Noda NN, Kumeta H, et al. Selective transport of alpha-mannosidase by autophagic pathways: structural basis for cargo recognition by Atg19 and Atg34. J Biol Chem. 2010 Sep 24;285(39):30026-33.

- [95] Yuga M, Gomi K, Klionsky DJ, et al. Aspartyl aminopeptidase is imported from the cytoplasm to the vacuole by selective autophagy in Saccharomyces cerevisiae. J Biol Chem. 2011 Apr 15;286(15):13704-13.
- [96] Reggiori F, Monastyrska I, Shintani T, et al. The actin cytoskeleton is required for selective types of autophagy, but not nonspecific autophagy, in the yeast Saccharomyces cerevisiae. Mol Biol Cell. 2005 Dec;16(12):5843-56.
- [97] Monastyrska I, Reggiori F, Klionsky DJ. Harpooning the Cvt complex to the phagophore assembly site. Autophagy. 2008 Oct;4(7):914-6.
- [98] Geng J, Klionsky DJ. Quantitative regulation of vesicle formation in yeast nonspecific autophagy. Autophagy. 2008 Oct;4(7):955-7.
- [99] Noda NN, Kumeta H, Nakatogawa H, et al. Structural basis of target recognition by Atg8/LC3 during selective autophagy. Genes Cells. 2008 Dec;13(12):1211-8.
- [100] Reggiori F, Klionsky DJ. Atg9 sorting from mitochondria is impaired in early secretion and VFT-complex mutants in Saccharomyces cerevisiae. J Cell Sci. 2006 Jul 15;119(Pt 14):2903-11.
- [101] Reggiori F, Wang CW, Stromhaug PE, et al. Vps51 is part of the yeast Vps fifty-three tethering complex essential for retrograde traffic from the early endosome and Cvt vesicle completion. J Biol Chem. 2003 Feb 14;278(7):5009-20.
- [102] Kirisako T, Ichimura Y, Okada H, et al. The reversible modification regulates the membrane-binding state of Apg8/Aut7 essential for autophagy and the cytoplasm to vacuole targeting pathway. J Cell Biol. 2000 Oct 16;151(2):263-76.
- [103] Epple UD, Suriapranata I, Eskelinen EL, et al. Aut5/Cvt17p, a putative lipase essential for disintegration of autophagic bodies inside the vacuole. J Bacteriol. 2001 Oct;183(20):5942-55.
- [104] Teter SA, Eggerton KP, Scott SV, et al. Degradation of lipid vesicles in the yeast vacuole requires function of Cvt17, a putative lipase. J Biol Chem. 2001 Jan 19;276(3):2083-7.
- [105] Klionsky DJ, Cueva R, Yaver DS. Aminopeptidase I of Saccharomyces cerevisiae is localized to the vacuole independent of the secretory pathway. J Cell Biol. 1992 Oct;119(2):287-99.
- [106] Klionsky DJ. Autophagy revisited: a conversation with Christian de Duve. Autophagy. 2008 Aug;4(6):740-3.
- [107] Levine B, Klionsky DJ. Development by self-digestion: molecular mechanisms and biological functions of autophagy. Dev Cell. 2004 Apr;6(4):463-77.

- [108] Mizushima N, Komatsu M. Autophagy: renovation of cells and tissues. Cell. 2011 Nov 11;147(4):728-41.
- [109] Kobayashi S. Choose Delicately and Reuse Adequately: The Newly Revealed Process of Autophagy. Biol Pharm Bull. 2015;38(8):1098-103.
- [110] Kamada Y, Funakoshi T, Shintani T, et al. Tor-mediated induction of autophagy via an Apg1 protein kinase complex. J Cell Biol. 2000 Sep 18;150(6):1507-13.
- [111] Suzuki K, Kubota Y, Sekito T, et al. Hierarchy of Atg proteins in pre-autophagosomal structure organization. Genes Cells. 2007 Feb;12(2):209-18.
- [112] Papinski D, Schuschnig M, Reiter W, et al. Early steps in autophagy depend on direct phosphorylation of Atg9 by the Atg1 kinase. Mol Cell. 2014 Feb 6;53(3):471-83.
- [113] Kihara A, Noda T, Ishihara N, et al. Two distinct Vps34 phosphatidylinositol 3-kinase complexes function in autophagy and carboxypeptidase Y sorting in Saccharomyces cerevisiae. J Cell Biol. 2001 Feb 5;152(3):519-30.
- [114] Schu PV, Takegawa K, Fry MJ, et al. Phosphatidylinositol 3-kinase encoded by yeast VPS34 gene essential for protein sorting. Science. 1993 Apr 2;260(5104):88-91.
- [115] Stack JH, DeWald DB, Takegawa K, et al. Vesicle-mediated protein transport: regulatory interactions between the Vps15 protein kinase and the Vps34 PtdIns 3-kinase essential for protein sorting to the vacuole in yeast. J Cell Biol. 1995 Apr;129(2):321-34.
- [116] Burman C, Ktistakis NT. Regulation of autophagy by phosphatidylinositol 3-phosphate. FEBS Lett. 2010 Apr 2;584(7):1302-12.
- [117] Nice DC, Sato TK, Stromhaug PE, et al. Cooperative binding of the cytoplasm to vacuole targeting pathway proteins, Cvt13 and Cvt20, to phosphatidylinositol 3-phosphate at the pre-autophagosomal structure is required for selective autophagy. J Biol Chem. 2002 Aug 16;277(33):30198-207.
- [118] Guan J, Stromhaug PE, George MD, et al. Cvt18/Gsa12 is required for cytoplasm-to-vacuole transport, pexophagy, and autophagy in Saccharomyces cerevisiae and Pichia pastoris. Mol Biol Cell. 2001 Dec;12(12):3821-38.
- [119] Strømhaug PE, Reggiori F, Guan J, et al. Atg21 is a phosphoinositide binding protein required for efficient lipidation and localization of Atg8 during uptake of aminopeptidase I by selective autophagy. Mol Biol Cell. 2004 Aug;15(8):3553-66.
- [120] Obara K, Sekito T, Niimi K, et al. The Atg18-Atg2 complex is recruited to autophagic membranes via phosphatidylinositol 3-phosphate and exerts an essential function. J Biol Chem. 2008 Aug 29;283(35):23972-80.

- [121] Ohsumi Y. Molecular dissection of autophagy: two ubiquitin-like systems. Nat Rev Mol Cell Biol. 2001 Mar;2(3):211-6.
- [122] Hanada T, Noda NN, Satomi Y, et al. The Atg12-Atg5 conjugate has a novel E3-like activity for protein lipidation in autophagy. J Biol Chem. 2007 Dec 28;282(52):37298-302.
- [123] Huang WP, Scott SV, Kim J, et al. The itinerary of a vesicle component, Aut7p/Cvt5p, terminates in the yeast vacuole via the autophagy/Cvt pathways. J Biol Chem. 2000 Feb 25;275(8):5845-51.
- [124] Kirisako T, Baba M, Ishihara N, et al. Formation process of autophagosome is traced with Apg8/Aut7p in yeast. J Cell Biol. 1999 Oct 18;147(2):435-46.
- [125] Kabeya Y, Mizushima N, Ueno T, et al. LC3, a mammalian homologue of yeast Apg8p, is localized in autophagosome membranes after processing. Embo j. 2000 Nov 1;19(21):5720-8.
- [126] Mizushima N, Noda T, Yoshimori T, et al. A protein conjugation system essential for autophagy. Nature. 1998 Sep 24;395(6700):395-8.
- [127] Tanida I, Mizushima N, Kiyooka M, et al. Apg7p/Cvt2p: A novel protein-activating enzyme essential for autophagy. Mol Biol Cell. 1999 May;10(5):1367-79.
- [128] Shintani T, Mizushima N, Ogawa Y, et al. Apg10p, a novel protein-conjugating enzyme essential for autophagy in yeast. Embo j. 1999 Oct 1;18(19):5234-41.
- [129] Kuma A, Mizushima N, Ishihara N, et al. Formation of the approximately 350-kDa Apg12-Apg5.Apg16 multimeric complex, mediated by Apg16 oligomerization, is essential for autophagy in yeast. J Biol Chem. 2002 May 24;277(21):18619-25.
- [130] Ichimura Y, Kirisako T, Takao T, et al. A ubiquitin-like system mediates protein lipidation. Nature. 2000 Nov 23;408(6811):488-92.
- [131] Ichimura Y, Imamura Y, Emoto K, et al. In vivo and in vitro reconstitution of Atg8 conjugation essential for autophagy. J Biol Chem. 2004 Sep 24;279(39):40584-92.
- [132] He C, Song H, Yorimitsu T, et al. Recruitment of Atg9 to the preautophagosomal structure by Atg11 is essential for selective autophagy in budding yeast. J Cell Biol. 2006 Dec 18;175(6):925-35.
- [133] Noda T, Kim J, Huang WP, et al. Apg9p/Cvt7p is an integral membrane protein required for transport vesicle formation in the Cvt and autophagy pathways. J Cell Biol. 2000 Feb 7;148(3):465-80.
- [134] Reggiori F, Shintani T, Nair U, et al. Atg9 cycles between mitochondria and the preautophagosomal structure in yeasts. Autophagy. 2005 Jul;1(2):101-9.

- [135] Legakis JE, Yen WL, Klionsky DJ. A cycling protein complex required for selective autophagy. Autophagy. 2007 Sep-Oct;3(5):422-32.
- [136] Yen WL, Legakis JE, Nair U, et al. Atg27 is required for autophagy-dependent cycling of Atg9. Mol Biol Cell. 2007 Feb;18(2):581-93.
- [137] Monastyrska I, He C, Geng J, et al. Arp2 links autophagic machinery with the actin cytoskeleton. Mol Biol Cell. 2008 May;19(5):1962-75.
- [138] Monastyrska I, Shintani T, Klionsky DJ, et al. Atg11 directs autophagosome cargoes to the PAS along actin cables. Autophagy. 2006 Apr-Jun;2(2):119-21.
- [139] Klionsky DJ. The molecular machinery of autophagy: unanswered questions. J Cell Sci. 2005 Jan 1;118(Pt 1):7-18.
- [140] Epple UD, Eskelinen EL, Thumm M. Intravacuolar membrane lysis in Saccharomyces cerevisiae. Does vacuolar targeting of Cvt17/Aut5p affect its function? J Biol Chem. 2003 Mar 7;278(10):7810-21.
- [141] Yang Z, Huang J, Geng J, et al. Atg22 recycles amino acids to link the degradative and recycling functions of autophagy. Mol Biol Cell. 2006 Dec;17(12):5094-104.
- [142] Russnak R, Konczal D, McIntire SL. A family of yeast proteins mediating bidirectional vacuolar amino acid transport. J Biol Chem. 2001 Jun 29;276(26):23849-57.
- [143] Murphy MP. How mitochondria produce reactive oxygen species. Biochem J. 2009 Jan 1;417(1):1-13.
- [144] Zheng L, Shu WJ, Li YM, et al. The Pafl complex transcriptionally regulates the mitochondrial-anchored protein Atg32 leading to activation of mitophagy. Autophagy. 2020 Aug;16(8):1366-1379.
- [145] Shu WJ, Zhao MJ, Klionsky DJ, et al. Old factors, new players: transcriptional regulation of autophagy. Autophagy. 2020 May;16(5):956-958.
- [146] Aihara M, Jin X, Kurihara Y, et al. Tor and the Sin3-Rpd3 complex regulate expression of the mitophagy receptor protein Atg32 in yeast. J Cell Sci. 2014 Jul 15;127(Pt 14):3184-96.
- [147] Aoki Y, Kanki T, Hirota Y, et al. Phosphorylation of Serine 114 on Atg32 mediates mitophagy. Mol Biol Cell. 2011 Sep;22(17):3206-17.
- [148] Wang K, Jin M, Liu X, et al. Proteolytic processing of Atg32 by the mitochondrial i-AAA protease Yme1 regulates mitophagy. Autophagy. 2013 Nov 1;9(11):1828-36.
- [149] Abeliovich H, Dunn WA, Jr., Kim J, et al. Dissection of autophagosome biogenesis into distinct nucleation and expansion steps. J Cell Biol. 2000 Nov 27;151(5):1025-34.

- [150] Lang T, Schaeffeler E, Bernreuther D, et al. Aut2p and Aut7p, two novel microtubule-associated proteins are essential for delivery of autophagic vesicles to the vacuole. Embo j. 1998 Jul 1;17(13):3597-607.
- [151] Nakatogawa H, Ichimura Y, Ohsumi Y. Atg8, a ubiquitin-like protein required for autophagosome formation, mediates membrane tethering and hemifusion. Cell. 2007 Jul 13;130(1):165-78.
- [152] Chan TF, Bertram PG, Ai W, et al. Regulation of APG14 expression by the GATA-type transcription factor Gln3p. J Biol Chem. 2001 Mar 2;276(9):6463-7.
- [153] Hardwick JS, Kuruvilla FG, Tong JK, et al. Rapamycin-modulated transcription defines the subset of nutrient-sensitive signaling pathways directly controlled by the Tor proteins. Proc Natl Acad Sci U S A. 1999 Dec 21;96(26):14866-70.
- [154] Bartholomew CR, Suzuki T, Du Z, et al. Ume6 transcription factor is part of a signaling cascade that regulates autophagy. Proc Natl Acad Sci U S A. 2012 Jul 10;109(28):11206-10.
- [155] Backues SK, Lynch-Day MA, Klionsky DJ. The Ume6-Sin3-Rpd3 complex regulates ATG8 transcription to control autophagosome size. Autophagy. 2012 Dec;8(12):1835-6.
- [156] Jin M, He D, Backues SK, et al. Transcriptional regulation by Pho23 modulates the frequency of autophagosome formation. Curr Biol. 2014 Jun 16;24(12):1314-1322.
- [157] Bernard A, Klionsky DJ. Rph1 mediates the nutrient-limitation signaling pathway leading to transcriptional activation of autophagy. Autophagy. 2015 Apr 3;11(4):718-9.
- [158] Vlahakis A, Lopez Muniozguren N, Powers T. Stress-response transcription factors Msn2 and Msn4 couple TORC2-Ypk1 signaling and mitochondrial respiration to ATG8 gene expression and autophagy. Autophagy. 2017;13(11):1804-1812.
- [159] Pedruzzi I, Dubouloz F, Cameroni E, et al. TOR and PKA signaling pathways converge on the protein kinase Rim15 to control entry into G0. Mol Cell. 2003 Dec;12(6):1607-13.
- [160] Wanke V, Pedruzzi I, Cameroni E, et al. Regulation of G0 entry by the Pho80-Pho85 cyclin-CDK complex. Embo j. 2005 Dec 21;24(24):4271-8.
- [161] Swinnen E, Wanke V, Roosen J, et al. Rim15 and the crossroads of nutrient signalling pathways in Saccharomyces cerevisiae. Cell Div. 2006 Apr 3;1:3.
- [162] Kim B, Lee Y, Choi H, et al. The trehalose-6-phosphate phosphatase Tps2 regulates ATG8 transcription and autophagy in Saccharomyces cerevisiae. Autophagy. 2021 Apr;17(4):1013-1027.

- [163] Kouzarides T. Chromatin modifications and their function. Cell. 2007 Feb 23;128(4):693-705.
- [164] Shahbazian MD, Grunstein M. Functions of site-specific histone acetylation and deacetylation. Annu Rev Biochem. 2007;76:75-100.
- [165] Kim SC, Sprung R, Chen Y, et al. Substrate and functional diversity of lysine acetylation revealed by a proteomics survey. Mol Cell. 2006 Aug;23(4):607-18.
- [166] Choudhary C, Kumar C, Gnad F, et al. Lysine acetylation targets protein complexes and co-regulates major cellular functions. Science. 2009 Aug 14;325(5942):834-40.
- [167] Lin YY, Lu JY, Zhang J, et al. Protein acetylation microarray reveals that NuA4 controls key metabolic target regulating gluconeogenesis. Cell. 2009 Mar 20;136(6):1073-84.
- [168] Kaluarachchi Duffy S, Friesen H, Baryshnikova A, et al. Exploring the yeast acetylome using functional genomics. Cell. 2012 May 11;149(4):936-48.
- [169] Albaugh BN, Arnold KM, Lee S, et al. Autoacetylation of the histone acetyltransferase Rtt109. J Biol Chem. 2011 Jul 15;286(28):24694-701.
- [170] Tanner KG, Langer MR, Kim Y, et al. Kinetic mechanism of the histone acetyltransferase GCN5 from yeast. J Biol Chem. 2000 Jul 21;275(29):22048-55.
- [171] Berndsen CE, Albaugh BN, Tan S, et al. Catalytic mechanism of a MYST family histone acetyltransferase. Biochemistry. 2007 Jan 23;46(3):623-9.
- [172] Roth SY, Denu JM, Allis CD. Histone acetyltransferases. Annu Rev Biochem. 2001;70:81-120.
- [173] Sobel RE, Cook RG, Perry CA, et al. Conservation of deposition-related acetylation sites in newly synthesized histones H3 and H4. Proc Natl Acad Sci U S A. 1995 Feb 14;92(4):1237-41.
- [174] Sterner DE, Berger SL. Acetylation of histones and transcription-related factors. Microbiol Mol Biol Rev. 2000 Jun;64(2):435-59.
- [175] Ekwall K. Genome-wide analysis of HDAC function. Trends Genet. 2005 Nov;21(11):608-15.
- [176] Blander G, Guarente L. The Sir2 family of protein deacetylases. Annu Rev Biochem. 2004;73:417-35.
- [177] Millar CB, Grunstein M. Genome-wide patterns of histone modifications in yeast. Nat Rev Mol Cell Biol. 2006 Sep;7(9):657-66.
- [178] Zhao S, Xu W, Jiang W, et al. Regulation of cellular metabolism by protein lysine acetylation. Science. 2010 Feb 19;327(5968):1000-4.

- [179] Lu JY, Lin YY, Sheu JC, et al. Acetylation of yeast AMPK controls intrinsic aging independently of caloric restriction. Cell. 2011 Sep 16;146(6):969-79.
- [180] VanDemark AP, Kasten MM, Ferris E, et al. Autoregulation of the rsc4 tandem bromodomain by gcn5 acetylation. Mol Cell. 2007 Sep 7;27(5):817-28.
- [181] Kim JH, Saraf A, Florens L, et al. Gcn5 regulates the dissociation of SWI/SNF from chromatin by acetylation of Swi2/Snf2. Genes Dev. 2010 Dec 15;24(24):2766-71.
- [182] Yuan H, Rossetto D, Mellert H, et al. MYST protein acetyltransferase activity requires active site lysine autoacetylation. Embo j. 2012 Jan 4;31(1):58-70.
- [183] Lin YY, Qi Y, Lu JY, et al. A comprehensive synthetic genetic interaction network governing yeast histone acetylation and deacetylation. Genes Dev. 2008 Aug 1;22(15):2062-74.
- [184] Cai L, Sutter BM, Li B, et al. Acetyl-CoA induces cell growth and proliferation by promoting the acetylation of histones at growth genes. Mol Cell. 2011 May 20;42(4):426-37.
- [185] Weinert BT, Iesmantavicius V, Moustafa T, et al. Acetylation dynamics and stoichiometry in Saccharomyces cerevisiae. Mol Syst Biol. 2014;10(1):716.
- [186] Yang XJ, Seto E. The Rpd3/Hda1 family of lysine deacetylases: from bacteria and yeast to mice and men. Nat Rev Mol Cell Biol. 2008 Mar;9(3):206-18.
- [187] Huber A, French SL, Tekotte H, et al. Sch9 regulates ribosome biogenesis via Stb3, Dot6 and Tod6 and the histone deacetylase complex RPD3L. Embo j. 2011 Jul 5;30(15):3052-64.
- [188] Ruiz-Roig C, Viéitez C, Posas F, et al. The Rpd3L HDAC complex is essential for the heat stress response in yeast. Mol Microbiol. 2010 May;76(4):1049-62.
- [189] Wagner EJ, Carpenter PB. Understanding the language of Lys36 methylation at histone H3. Nat Rev Mol Cell Biol. 2012 Jan 23;13(2):115-26.
- [190] McDaniel SL, Strahl BD. Stress-free with Rpd3: a unique chromatin complex mediates the response to oxidative stress. Mol Cell Biol. 2013 Oct;33(19):3726-7.
- [191] Vershon AK, Pierce M. Transcriptional regulation of meiosis in yeast. Curr Opin Cell Biol. 2000 Jun;12(3):334-9.
- [192] Strich R, Surosky RT, Steber C, et al. UME6 is a key regulator of nitrogen repression and meiotic development. Genes Dev. 1994 Apr 1;8(7):796-810.
- [193] Mallory MJ, Cooper KF, Strich R. Meiosis-specific destruction of the Ume6p repressor by the Cdc20-directed APC/C. Mol Cell. 2007 Sep 21;27(6):951-61.

- [194] Kadosh D, Struhl K. Repression by Ume6 involves recruitment of a complex containing Sin3 corepressor and Rpd3 histone deacetylase to target promoters. Cell. 1997 May 2;89(3):365-71.
- [195] Rundlett SE, Carmen AA, Suka N, et al. Transcriptional repression by UME6 involves deacetylation of lysine 5 of histone H4 by RPD3. Nature. 1998 Apr 23;392(6678):831-5.
- [196] Mallory MJ, Law MJ, Sterner DE, et al. Gcn5p-dependent acetylation induces degradation of the meiotic transcriptional repressor Ume6p. Mol Biol Cell. 2012 May;23(9):1609-17.
- [197] Law MJ, Mallory MJ, Dunbrack RL, Jr., et al. Acetylation of the transcriptional repressor Ume6p allows efficient promoter release and timely induction of the meiotic transient transcription program in yeast. Mol Cell Biol. 2014 Feb;34(4):631-42.
- [198] Rubin-Bejerano I, Mandel S, Robzyk K, et al. Induction of meiosis in Saccharomyces cerevisiae depends on conversion of the transcriptional repressor Ume6 to a positive regulator by its regulated association with the transcriptional activator Ime1. Mol Cell Biol. 1996 May;16(5):2518-26.
- [199] Xiao Y, Mitchell AP. Shared roles of yeast glycogen synthase kinase 3 family members in nitrogen-responsive phosphorylation of meiotic regulator Ume6p. Mol Cell Biol. 2000 Aug;20(15):5447-53.
- [200] Malathi K, Xiao Y, Mitchell AP. Interaction of yeast repressor-activator protein Ume6p with glycogen synthase kinase 3 homolog Rim11p. Mol Cell Biol. 1997 Dec;17(12):7230-6.
- [201] Lill R, Dutkiewicz R, Freibert SA, et al. The role of mitochondria and the CIA machinery in the maturation of cytosolic and nuclear iron-sulfur proteins. Eur J Cell Biol. 2015 Jul-Sep;94(7-9):280-91.
- [202] Lill R, Hoffmann B, Molik S, et al. The role of mitochondria in cellular iron-sulfur protein biogenesis and iron metabolism. Biochim Biophys Acta. 2012 Sep;1823(9):1491-508.
- [203] Braymer JJ, Lill R. Iron-sulfur cluster biogenesis and trafficking in mitochondria. J Biol Chem. 2017 Aug 4;292(31):12754-12763.
- [204] Torelli NQ, Ferreira-Júnior JR, Kowaltowski AJ, et al. RTG1- and RTG2-dependent retrograde signaling controls mitochondrial activity and stress resistance in Saccharomyces cerevisiae. Free Radic Biol Med. 2015 Apr;81:30-7.

- [205] Jia Y, Rothermel B, Thornton J, et al. A basic helix-loop-helix-leucine zipper transcription complex in yeast functions in a signaling pathway from mitochondria to the nucleus. Mol Cell Biol. 1997 Mar;17(3):1110-7.
- [206] Liao X, Butow RA. RTG1 and RTG2: two yeast genes required for a novel path of communication from mitochondria to the nucleus. Cell. 1993 Jan 15;72(1):61-71.
- [207] Sekito T, Thornton J, Butow RA. Mitochondria-to-nuclear signaling is regulated by the subcellular localization of the transcription factors Rtg1p and Rtg3p. Mol Biol Cell. 2000 Jun;11(6):2103-15.
- [208] Liu Z, Sekito T, Spírek M, et al. Retrograde signaling is regulated by the dynamic interaction between Rtg2p and Mks1p. Mol Cell. 2003 Aug;12(2):401-11.
- [209] Liu Z, Spírek M, Thornton J, et al. A novel degron-mediated degradation of the RTG pathway regulator, Mks1p, by SCFGrr1. Mol Biol Cell. 2005 Oct;16(10):4893-904.
- [210] Yu H, Braun P, Yildirim MA, et al. High-quality binary protein interaction map of the yeast interactome network. Science. 2008 Oct 3;322(5898):104-10.
- [211] Taggart C, Cervantes-Laurean D, Kim G, et al. Oxidation of either methionine 351 or methionine 358 in alpha 1-antitrypsin causes loss of anti-neutrophil elastase activity. J Biol Chem. 2000 Sep 1;275(35):27258-65.
- [212] Panzenböck U, Stocker R. Formation of methionine sulfoxide-containing specific forms of oxidized high-density lipoproteins. Biochim Biophys Acta. 2005 Jan 17;1703(2):171-81.
- [213] Brennan LA, Lee W, Cowell T, et al. Deletion of mouse MsrA results in HBO-induced cataract: MsrA repairs mitochondrial cytochrome c. Mol Vis. 2009 May 15;15:985-99.
- [214] Gabbita SP, Aksenov MY, Lovell MA, et al. Decrease in peptide methionine sulfoxide reductase in Alzheimer's disease brain. J Neurochem. 1999 Oct;73(4):1660-6.
- [215] Glaser CB, Yamin G, Uversky VN, et al. Methionine oxidation, alpha-synuclein and Parkinson's disease. Biochim Biophys Acta. 2005 Jan 17;1703(2):157-69.
- [216] Bleackley MR, Young BP, Loewen CJ, et al. High density array screening to identify the genetic requirements for transition metal tolerance in Saccharomyces cerevisiae. Metallomics. 2011 Feb;3(2):195-205.
- [217] Lynch-Day MA, Klionsky DJ. The Cvt pathway as a model for selective autophagy. FEBS Lett. 2010 Apr 2;584(7):1359-66.
- [218] Allu PK, Boggula Y, Karri S, et al. A conserved R type Methionine Sulfoxide Reductase reverses oxidized GrpEL1/Mge1 to regulate Hsp70 chaperone cycle. Sci Rep. 2018 Feb 9;8(1):2716.

- [219] Longtine MS, McKenzie A, 3rd, Demarini DJ, et al. Additional modules for versatile and economical PCR-based gene deletion and modification in Saccharomyces cerevisiae. Yeast. 1998 Jul;14(10):953-61.
- [220] Büttner S, Eisenberg T, Carmona-Gutierrez D, et al. Endonuclease G regulates budding yeast life and death. Mol Cell. 2007 Jan 26;25(2):233-46.
- [221] Moreira KE, Schuck S, Schrul B, et al. Seg1 controls eisosome assembly and shape. J Cell Biol. 2012 Aug 6;198(3):405-20.
- [222] Mumberg D, Müller R, Funk M. Yeast vectors for the controlled expression of heterologous proteins in different genetic backgrounds. Gene. 1995 Apr 14;156(1):119-22.
- [223] Sikorski RS, Hieter P. A system of shuttle vectors and yeast host strains designed for efficient manipulation of DNA in Saccharomyces cerevisiae. Genetics. 1989 May;122(1):19-27.
- [224] Sherman F. Getting started with yeast. Methods Enzymol. 1991;194:3-21.
- [225] Gietz RD, Woods RA. Transformation of yeast by lithium acetate/single-stranded carrier DNA/polyethylene glycol method. Methods Enzymol. 2002;350:87-96.
- [226] Pal A, Paripati AK, Deolal P, et al. Eisosome protein Pil1 regulates mitochondrial morphology, mitophagy, and cell death in Saccharomyces cerevisiae. J Biol Chem. 2022 Nov;298(11):102533.
- [227] Collart MA, Oliviero S. Preparation of yeast RNA. Curr Protoc Mol Biol. 2001 May; Chapter 13:Unit13.12.
- [228] Müller M, Schmidt O, Angelova M, et al. The coordinated action of the MVB pathway and autophagy ensures cell survival during starvation. Elife. 2015 Apr 22;4:e07736.
- [229] Seguí-Real B, Martinez M, Sandoval IV. Yeast aminopeptidase I is post-translationally sorted from the cytosol to the vacuole by a mechanism mediated by its bipartite N-terminal extension. Embo j. 1995 Nov 15;14(22):5476-84.
- [230] Brot N, Weissbach L, Werth J, et al. Enzymatic reduction of protein-bound methionine sulfoxide. Proc Natl Acad Sci U S A. 1981 Apr;78(4):2155-8.
- [231] Frey J, Röhm KH. Subcellular localization and levels of aminopeptidases and dipeptidase in Saccharomyces cerevisiae. Biochim Biophys Acta. 1978 Nov 10;527(1):31-41.
- [232] Metz G, Röhm KH. Yeast aminopeptidase I. Chemical composition and catalytic properties. Biochim Biophys Acta. 1976 May 13;429(3):933-49.

- [233] Trumbly RJ, Bradley G. Isolation and characterization of aminopeptidase mutants of Saccharomyces cerevisiae. J Bacteriol. 1983 Oct;156(1):36-48.
- [234] Schu P. Aminopeptidase I enzymatic activity. Methods Enzymol. 2008;451:67-78.
- [235] Anjum NA, Sofo A, Scopa A, et al. Lipids and proteins--major targets of oxidative modifications in abiotic stressed plants. Environ Sci Pollut Res Int. 2015 Mar;22(6):4099-121.
- [236] Imlay JA. Pathways of oxidative damage. Annu Rev Microbiol. 2003;57:395-418.
- [237] Stadtman ER, Berlett BS. Reactive oxygen-mediated protein oxidation in aging and disease. Drug Metab Rev. 1998 May;30(2):225-43.
- [238] Weissbach H, Etienne F, Hoshi T, et al. Peptide methionine sulfoxide reductase: structure, mechanism of action, and biological function. Arch Biochem Biophys. 2002 Jan 15;397(2):172-8.
- [239] Sideri TC, Willetts SA, Avery SV. Methionine sulphoxide reductases protect iron-sulphur clusters from oxidative inactivation in yeast. Microbiology (Reading). 2009 Feb;155(Pt 2):612-623.
- [240] Delorme-Axford E, Klionsky DJ. Transcriptional and post-transcriptional regulation of autophagy in the yeast Saccharomyces cerevisiae. J Biol Chem. 2018 Apr 13;293(15):5396-5403.
- [241] Geng J, Klionsky DJ. The Atg8 and Atg12 ubiquitin-like conjugation systems in macroautophagy. 'Protein modifications: beyond the usual suspects' review series. EMBO Rep. 2008 Sep;9(9):859-64.
- [242] Nakatogawa H, Ohbayashi S, Sakoh-Nakatogawa M, et al. The autophagy-related protein kinase Atg1 interacts with the ubiquitin-like protein Atg8 via the Atg8 family interacting motif to facilitate autophagosome formation. J Biol Chem. 2012 Aug 17;287(34):28503-7.
- [243] Raithatha SA, Vaza S, Islam MT, et al. Ume6 Acts as a Stable Platform To Coordinate Repression and Activation of Early Meiosis-Specific Genes in Saccharomyces cerevisiae. Mol Cell Biol. 2021 Jun 23;41(7):e0037820.
- [244] Zhang Y, Qi H, Taylor R, et al. The role of autophagy in mitochondria maintenance: characterization of mitochondrial functions in autophagy-deficient S. cerevisiae strains. Autophagy. 2007 Jul-Aug;3(4):337-46.
- [245] Horie T, Kawamata T, Matsunami M, et al. Recycling of iron via autophagy is critical for the transition from glycolytic to respiratory growth. J Biol Chem. 2017 May 19;292(20):8533-8543.

- [246] Chatterjee A, Sepuri NBV. Methionine sulfoxide reductase 2 regulates Cvt autophagic pathway by altering the stability of Atg19 and Ape1 in Saccharomyces cerevisiae. J Biol Chem. 2024 Mar;300(3):105662.
- [247] Marada A, Allu PK, Murari A, et al. Mge1, a nucleotide exchange factor of Hsp70, acts as an oxidative sensor to regulate mitochondrial Hsp70 function. Mol Biol Cell. 2013 Mar;24(6):692-703.
- [248] Heo JM, Livnat-Levanon N, Taylor EB, et al. A stress-responsive system for mitochondrial protein degradation. Mol Cell. 2010 Nov 12;40(3):465-80.
- [249] Sepuri NB, Yadav S, Anandatheerthavarada HK, et al. Mitochondrial targeting of intact CYP2B1 and CYP2E1 and N-terminal truncated CYP1A1 proteins in Saccharomyces cerevisiae--role of protein kinase A in the mitochondrial targeting of CYP2E1. Febs j. 2007 Sep;274(17):4615-30.
- [250] Sepuri NB, Gorla M, King MP. Mitochondrial lysyl-tRNA synthetase independent import of tRNA lysine into yeast mitochondria. PLoS One. 2012;7(4):e35321.
- [251] Reinders J, Zahedi RP, Pfanner N, et al. Toward the complete yeast mitochondrial proteome: multidimensional separation techniques for mitochondrial proteomics. J Proteome Res. 2006 Jul;5(7):1543-54.
- [252] Livak KJ, Schmittgen TD. Analysis of relative gene expression data using real-time quantitative PCR and the 2(-Delta Delta C(T)) Method. Methods. 2001 Dec;25(4):402-8.
- [253] Xie Z, Nair U, Klionsky DJ. Atg8 controls phagophore expansion during autophagosome formation. Mol Biol Cell. 2008 Aug;19(8):3290-8.
- [254] Shpilka T, Weidberg H, Pietrokovski S, et al. Atg8: an autophagy-related ubiquitin-like protein family. Genome Biol. 2011 Jul 27;12(7):226.
- [255] Jin M, Klionsky DJ. Regulation of autophagy: modulation of the size and number of autophagosomes. FEBS Lett. 2014 Aug 1;588(15):2457-63.
- [256] Stadtman ER, Van Remmen H, Richardson A, et al. Methionine oxidation and aging. Biochim Biophys Acta. 2005 Jan 17;1703(2):135-40.
- [257] Kamada Y, Yoshino K, Kondo C, et al. Tor directly controls the Atg1 kinase complex to regulate autophagy. Mol Cell Biol. 2010 Feb;30(4):1049-58.
- [258] Kraft C, Kijanska M, Kalie E, et al. Binding of the Atg1/ULK1 kinase to the ubiquitin-like protein Atg8 regulates autophagy. Embo j. 2012 Sep 12;31(18):3691-703.

- [259] Yeh YY, Shah KH, Herman PK. An Atg13 protein-mediated self-association of the Atg1 protein kinase is important for the induction of autophagy. J Biol Chem. 2011 Aug 19;286(33):28931-28939.
- [260] Fujioka Y, Suzuki SW, Yamamoto H, et al. Structural basis of starvation-induced assembly of the autophagy initiation complex. Nat Struct Mol Biol. 2014 Jun;21(6):513-21.
- [261] Cebollero E, Reggiori F. Regulation of autophagy in yeast Saccharomyces cerevisiae. Biochim Biophys Acta. 2009 Sep;1793(9):1413-21.
- [262] Urban J, Soulard A, Huber A, et al. Sch9 is a major target of TORC1 in Saccharomyces cerevisiae. Mol Cell. 2007 Jun 8;26(5):663-74.
- [263] Görner W, Durchschlag E, Wolf J, et al. Acute glucose starvation activates the nuclear localization signal of a stress-specific yeast transcription factor. Embo j. 2002 Jan 15;21(1-2):135-44.
- [264] Washburn BK, Esposito RE. Identification of the Sin3-binding site in Ume6 defines a two-step process for conversion of Ume6 from a transcriptional repressor to an activator in yeast. Mol Cell Biol. 2001 Mar;21(6):2057-69.
- [265] Carrozza MJ, Florens L, Swanson SK, et al. Stable incorporation of sequence specific repressors Ash1 and Ume6 into the Rpd3L complex. Biochim Biophys Acta. 2005 Nov 10;1731(2):77-87; discussion 75-6.
- [266] Pnueli L, Edry I, Cohen M, et al. Glucose and nitrogen regulate the switch from histone deacetylation to acetylation for expression of early meiosis-specific genes in budding yeast. Mol Cell Biol. 2004 Jun;24(12):5197-208.
- [267] Sun J, Tai S, Tang L, et al. Acetylation Modification During Autophagy and Vascular Aging. Front Physiol. 2021;12:598267.
- [268] Camougrand N, Vigié P, Dompierre J, et al. The Dep1 protein: A new regulator of mitophagy in yeast. Biochem Biophys Res Commun. 2022 Dec 20;635:218-226.
- [269] Marada A, Karri S, Singh S, et al. A Single Point Mutation in Mitochondrial Hsp70 Cochaperone Mge1 Gains Thermal Stability and Resistance. Biochemistry. 2016 Dec 27;55(51):7065-7072.
- [270] Nathan C. Specificity of a third kind: reactive oxygen and nitrogen intermediates in cell signaling. J Clin Invest. 2003 Mar;111(6):769-78.
- [271] Simonian NA, Coyle JT. Oxidative stress in neurodegenerative diseases. Annu Rev Pharmacol Toxicol. 1996;36:83-106.

- [272] Valley CC, Cembran A, Perlmutter JD, et al. The methionine-aromatic motif plays a unique role in stabilizing protein structure. J Biol Chem. 2012 Oct 12;287(42):34979-34991.
- [273] Chao CC, Ma YS, Stadtman ER. Modification of protein surface hydrophobicity and methionine oxidation by oxidative systems. Proc Natl Acad Sci U S A. 1997 Apr 1;94(7):2969-74.
- [274] Karri S, Singh S, Paripati AK, et al. Adaptation of Mge1 to oxidative stress by local unfolding and altered Interaction with mitochondrial Hsp70 and Mxr2. Mitochondrion. 2019 May;46:140-148.
- [275] Li SC, Kane PM. The yeast lysosome-like vacuole: endpoint and crossroads. Biochim Biophys Acta. 2009 Apr;1793(4):650-63.
- [276] Teichert U, Mechler B, Müller H, et al. Lysosomal (vacuolar) proteinases of yeast are essential catalysts for protein degradation, differentiation, and cell survival. J Biol Chem. 1989 Sep 25;264(27):16037-45.
- [277] Slobodkin MR, Elazar Z. The Atg8 family: multifunctional ubiquitin-like key regulators of autophagy. Essays Biochem. 2013;55:51-64.
- [278] Tarrago L, Kaya A, Weerapana E, et al. Methionine sulfoxide reductases preferentially reduce unfolded oxidized proteins and protect cells from oxidative protein unfolding. J Biol Chem. 2012 Jul 13;287(29):24448-59.
- [279] Yamaguchi M, Namiki Y, Okada H, et al. Structome of Saccharomyces cerevisiae determined by freeze-substitution and serial ultrathin-sectioning electron microscopy. J Electron Microsc (Tokyo). 2011;60(5):321-35.
- [280] Martínez-Pastor MT, Marchler G, Schüller C, et al. The Saccharomyces cerevisiae zinc finger proteins Msn2p and Msn4p are required for transcriptional induction through the stress response element (STRE). Embo j. 1996 May 1;15(9):2227-35.
- [281] Tamai KT, Gralla EB, Ellerby LM, et al. Yeast and mammalian metallothioneins functionally substitute for yeast copper-zinc superoxide dismutase. Proc Natl Acad Sci U S A. 1993 Sep 1;90(17):8013-7.
- [282] Okazaki S, Tachibana T, Naganuma A, et al. Multistep disulfide bond formation in Yap1 is required for sensing and transduction of H2O2 stress signal. Mol Cell. 2007 Aug 17;27(4):675-88.
- [283] Chang YY, Neufeld TP. An Atg1/Atg13 complex with multiple roles in TOR-mediated autophagy regulation. Mol Biol Cell. 2009 Apr;20(7):2004-14.

- [284] Wanke V, Cameroni E, Uotila A, et al. Caffeine extends yeast lifespan by targeting TORC1. Mol Microbiol. 2008 Jul;69(1):277-85.
- [285] Ali I, Conrad RJ, Verdin E, et al. Lysine Acetylation Goes Global: From Epigenetics to Metabolism and Therapeutics. Chem Rev. 2018 Feb 14;118(3):1216-1252.
- [286] Xu Y, Wan W. Acetylation in the regulation of autophagy. Autophagy. 2023 Feb;19(2):379-387.
- [287] Shen Q, Shi Y, Liu J, et al. Acetylation of STX17 (syntaxin 17) controls autophagosome maturation. Autophagy. 2021 May;17(5):1157-1169.
- [288] Su H, Yang F, Wang Q, et al. VPS34 Acetylation Controls Its Lipid Kinase Activity and the Initiation of Canonical and Non-canonical Autophagy. Mol Cell. 2017 Sep 21;67(6):907-921.e7.
- [289] Zhang J, Wang J, Zhou Z, et al. Importance of TFEB acetylation in control of its transcriptional activity and lysosomal function in response to histone deacetylase inhibitors. Autophagy. 2018;14(6):1043-1059.
- [290] Huang R, Xu Y, Wan W, et al. Deacetylation of nuclear LC3 drives autophagy initiation under starvation. Mol Cell. 2015 Feb 5;57(3):456-66.
- [291] Lee IH, Cao L, Mostoslavsky R, et al. A role for the NAD-dependent deacetylase Sirt1 in the regulation of autophagy. Proc Natl Acad Sci U S A. 2008 Mar 4;105(9):3374-9.
- [292] Li YT, Yi C, Chen CC, et al. A semisynthetic Atg3 reveals that acetylation promotes Atg3 membrane binding and Atg8 lipidation. Nat Commun. 2017 Mar 22;8:14846.
- [293] Alfadhel M, Nashabat M, Abu Ali Q, et al. Mitochondrial iron-sulfur cluster biogenesis from molecular understanding to clinical disease. Neurosciences (Riyadh). 2017 Jan;22(1):4-13.
- [294] Stolz A, Ernst A, Dikic I. Cargo recognition and trafficking in selective autophagy. Nat Cell Biol. 2014 Jun;16(6):495-501.
- [295] Youle RJ, Narendra DP. Mechanisms of mitophagy. Nat Rev Mol Cell Biol. 2011 Jan;12(1):9-14.
- [296] Mizumura K, Cloonan SM, Nakahira K, et al. Mitophagy-dependent necroptosis contributes to the pathogenesis of COPD. J Clin Invest. 2014 Sep;124(9):3987-4003.
- [297] Vergne I, Chua J, Singh SB, et al. Cell biology of mycobacterium tuberculosis phagosome. Annu Rev Cell Dev Biol. 2004;20:367-94.
- [298] Campbell GR, Spector SA. Vitamin D inhibits human immunodeficiency virus type 1 and Mycobacterium tuberculosis infection in macrophages through the induction of autophagy. PLoS Pathog. 2012;8(5):e1002689.

- [299] Liang X, Wei SQ, Lee SJ, et al. p62 sequestosome 1/light chain 3b complex confers cytoprotection on lung epithelial cells after hyperoxia. Am J Respir Cell Mol Biol. 2013 Apr;48(4):489-96.
- [300] Meijer WH, van der Klei IJ, Veenhuis M, et al. ATG genes involved in non-selective autophagy are conserved from yeast to man, but the selective Cvt and pexophagy pathways also require organism-specific genes. Autophagy. 2007 Mar-Apr;3(2):106-16.

# **Publications**

## **BC** RESEARCH ARTICLE



# Methionine sulfoxide reductase 2 regulates Cvt autophagic pathway by altering the stability of Atg19 and Ape1 in Saccharomyces cerevisiae

Received for publication, October 3, 2023, and in revised form, December 31, 2023 Published, Papers in Press, January 20, 2024, https://doi.org/10.1016/j.jbc.2024.105662

#### Arpan Chatterjee and Naresh Babu V. Sepuri\*

From the Department of Biochemistry, School of Life Sciences, University of Hyderabad, Hyderabad, Telangana, India

Reviewed by members of the JBC Editorial Board. Edited by Ursula Jakob

The reversible oxidation of methionine plays a crucial role in redox regulation of proteins. Methionine oxidation in proteins causes major structural modifications that can destabilize and abrogate their function. The highly conserved methionine sulfoxide reductases protect proteins from oxidative damage by reducing their oxidized methionines, thus restoring their stability and function. Deletion or mutation in conserved methionine sulfoxide reductases leads to aging and several human neurological disorders and also reduces yeast growth on nonfermentable carbon sources. Despite their importance in human health, limited information about their physiological substrates in humans and yeast is available. For the first time, we show that Mxr2 interacts in vivo with two core proteins of the cytoplasm to vacuole targeting (Cvt) autophagy pathway, Atg19, and Ape1 in Saccharomyces cerevisiae. Deletion of MXR2 induces instability and early turnover of immature Ape1 and Atg19 proteins and reduces the leucine aminopeptidase activity of Ape1 without affecting the maturation process of Ape1. Additionally, Mxr2 interacts with the immature Ape1, dependent on Met17 present within the propeptide of Ape1 as a single substitution mutation of Met17 to Leu abolishes this interaction. Importantly, Apel M17L mutant protein resists oxidative stress-induced degradation in WT and  $mxr2\Delta$  cells. By identifying Atg19 and Ape1 as cytosolic substrates of Mxr2, our study maps the hitherto unexplored connection between Mxr2 and the Cvt autophagy pathway and sheds light on Mxr2dependent oxidative regulation of the Cvt pathway.

Reactive oxygen species (ROS) act as a double-edged sword in the cell. At low concentrations, it manifests as a signaling molecule for growth and differentiation; however, uncontrolled accumulation causes oxidative stress. ROS-triggered oxidative stress impairs biomolecule function, leading to pathological conditions (1-5). Cells have evolved diverse strategies to combat oxidative insults, including enzymatic and nonenzymatic antioxidants (6). Sulfur-containing amino acids such as cysteine and methionine are the prime targets of ROS (7, 8). Methionine oxidation gives rise to reversible methionine

Loss or reduction in Msrs' activity has been implicated in many diseases, including pulmonary, vascular, ocular, aging, and neurological disorders (19-23). The known physiological consequences of dysfunctional Msrs are mitochondrial dysfunction, decreased cytochrome C biosynthesis, and metal resistance in yeast (17, 24). Given the dynamic nature of ROS levels, the importance of redox homeostasis, the alacrity at which the cells reactivate Msrs, the number of diseases associated with dysfunctional Msrs, and the plethora of proteins that harbor methionine, more studies are required to identify the substrates of Msrs rapidly and to unravel the ramifications of Msrs role that impinge on the structural and functional stability of proteins.

Cytoplasm to vacuole targeting (Cvt) pathway is a wellcharacterized selective autophagy pathway in yeast that delivers vacuolar hydrolases from the cytoplasm to the vacuolar lumen (25-27). Cvt vesicles are specialized autophagosomes which specifically enclose Cvt cargos and are much smaller (~150 nm) than starvation-induced autophagosomes (300 nm-900 nm) (25, 28). The vacuolar hydrolases that are transported via the Cvt pathway are leucine aminopeptidase (Ape1), αmannosidase (Ams1), and aspartyl aminopeptidase (Ape4). Among the three hydrolases, Ape1 is the primary cargo and

<sup>\*</sup> For correspondence: Naresh Babu V. Sepuri, nareshuohyd@gmail.com, nbvssl@uohyd.ernet.in.



sulfoxide (Met-SO) or irreversible methionine sulfenic acid (Met-SO2). Methionine sulfoxides obtain R or S enantiomeric forms that can be reduced by the canonical methionine sulfoxide reductases (MSRs), which are evolutionarily conserved from bacteria to humans (9-11). To prevent the accumulation of oxidized methionine, Msrs employ its native active cysteines to reduce methionine sulfoxides in the substrates (12-14). In reducing methionine sulfoxides, Msrs concomitantly get oxidized and are rendered inactive. However, the cell uses the thioredoxin and thioredoxin reductases to reduce and activate the Msrs, underscoring their importance in redox homeostasis (15, 16). Based on the type of enantiomeric form of the methionine sulfoxide that Msrs act on, Msrs are classified into A and B families. While members of the A family act on the Met-(S)-SO, the B family members act on the Met-(R)-SO (9). Yeast has three Msrs, Mxr1, Mxr2, and free methionine-(R)sulfoxide reductase (fRMsr). Mxr1 belongs to the A family, while the latter belongs to the B family (17). Curiously, while Mxr1 and Mxr2 act on oxidized methionine in proteins, fRMsr works on free methionine (14, 18).

## **BC** RESEARCH ARTICLE



# Eisosome protein Pil1 regulates mitochondrial morphology, mitophagy, and cell death in Saccharomyces cerevisiae

Received for publication, March 30, 2022, and in revised form, September 18, 2022 Published, Papers in Press, September 24, 2022, https://doi.org/10.1016/j.jbc.2022.102533

Amita Pal, Arun Kumar Paripati, Pallavi Deolalo, Arpan Chatterjee, Pushpa Rani Prasad, Priyanka Adla, and Naresh Babu V. Sepuri\*

From the Department of Biochemistry, University of Hyderabad, Hyderabad, Telangana, India

Edited by Ursula Jakob

Mitochondrial morphology and dynamics maintain mitochondrial integrity by regulating its size, shape, distribution, and connectivity, thereby modulating various cellular processes. Several studies have established a functional link between mitochondrial dynamics, mitophagy, and cell death, but further investigation is needed to identify specific proteins involved in mitochondrial dynamics. Any alteration in the integrity of mitochondria has severe ramifications that include disorders like cancer and neurodegeneration. In this study, we used budding yeast as a model organism and found that Pil1, the major component of the eisosome complex, also localizes to the periphery of mitochondria. Interestingly, the absence of Pil1 causes the branched tubular morphology of mitochondria to be abnormally fused or aggregated, whereas its overexpression leads to mitochondrial fragmentation. Most importantly,  $pil1\Delta$  cells are defective in mitophagy and bulk autophagy, resulting in elevated levels of reactive oxygen species and protein aggregates. In addition, we show that  $pil1\Delta$ cells are more prone to cell death. Yeast two-hybrid analysis and co-immunoprecipitations show the interaction of Pil1 with two major proteins in mitochondrial fission, Fis1 and Dnm1. Additionally, our data suggest that the role of Pil1 in maintaining mitochondrial shape is dependent on Fis1 and Dnm1, but it functions independently in mitophagy and cell death pathways. Together, our data suggest that Pil1, an eisosome protein, is a novel regulator of mitochondrial morphology, mitophagy, and cell death.

Organelles have evolved a variety of stress response processes to maintain their proteostasis and cellular homeostasis. Mitochondrion, one of the essential organelles that carry out several important cellular processes, ensures its quality control through various pathways at the molecular, organellar, and cellular levels (1). Mitochondrial fission and fusion, generally referred to as mitochondrial dynamics, maintain mitochondrial integrity by regulating its size, shape, distribution, and connectivity. Mitochondrial dynamics regulate mitochondrial quality control, metabolism, apoptosis, mitophagy, and other essential processes. Fusion of mitochondria is required to mitigate the damage and nonfunctionality by mixing

components and protecting them from autophagic degradation during starvation (2, 3). Fission helps produce new mitochondria and ensures quality control by removing damaged or unwanted mitochondria through mitophagy (4). A coordinated balance of fission and fusion is critical for maintaining mitochondrial biology and therefore a plethora of important cellular processes (5, 6). In Saccharomyces cerevisiae, Fzo1, Mgm1, and Ugo1 facilitate mitochondrial fusion. Outer membrane-anchored proteins, Fzo1p and Ugo1p, carry out the outer membrane fusion of adjacent mitochondria and inner membrane-anchored Mgm1 forms transcomplexes to tether the apposing inner membranes together (7-9). Dnm1, a dynamin-related GTPase, is the major protein in mitochondrial fission (10, 11). It is predominantly present in the cytosol and recruited to mitochondria via Fis1 (12). Dnm1 assembles into oligomers which form rings and spirals at the outer membrane of mitochondria. Recruitment of Dnm1 to the mitochondrial surface is mediated through two adaptor proteins, Mdv1 and Caf4 (13, 14). These four proteins together constitute the core proteins of the mitochondrial fission machinery. However, there is a possibility that other unidentified factors still exist that take part in mitochondrial dynamics (15). Several studies have shown that any dysregulation in mitochondrial dynamics leads to neuronal disorders like Alzheimer's, Parkinson's, and Huntington's (16-18). When the damage is beyond repair, mitochondria undergo mitophagy. Mitophagy is a selective autophagy where autophagosomes engulf the entire mitochondria and deliver them to the vacuole for their degradation (19-21). Mitophagy is required to eliminate the bad mitochondria from cells. Any kind of aberration in mitochondrial dynamics or mitophagy is harmful to cells. Mitochondrial dysfunction has also been linked with protein aggregation and reactive oxygen species (ROS) generation in cells which in turn leads to cell death.

Cellular organelles communicate with each other in order to cope with stress. Since the plasma membrane is positioned at the frontline to combat the external stress stimuli, it requires high degree of organization as it carries out a diverse array of functions and forms the protective barrier around the cell. The fungal plasma membrane is organized in lateral domains with specialized functions like cell wall synthesis, environmental sensing, nutrient uptake, secretion, and endocytosis (22-24). High-resolution electron microscopy of freeze-etched

<sup>\*</sup> For correspondence: Naresh Babu V. Sepuri, nareshuohyd@gmail.com, nbvssl@uohyd.ernet.in.





# Mitochondrial Import of Dengue Virus NS3 Protease and Cleavage of GrpEL1, a Cochaperone of Mitochondrial Hsp70

Chaitanya Gandikota, Fareed Mohammed, Lekha Gandhi, Deepti Maisnam, Ushodaya Mattam, Deepika Rathore, Arpan Chatterjee, Katyayani Mallick, Arcy Billoria, V. S. V. Prasad, Naresh Babu Venkata Sepuri, Musturi Venkataramana

ABSTRACT Dengue virus infections, which have been reported in nearly 140 countries, pose a significant threat to human health. The genome of dengue virus encodes three structural and seven nonstructural (NS) proteins along with two untranslated regions, one each on both ends. Among them, dengue protease (NS3) plays a pivotal role in polyprotein processing and virus multiplication. NS3 is also known to regulate several host proteins to induce and maintain pathogenesis. Certain viral proteins are known to interact with mitochondrial membrane proteins and interfere with their functions, but the association of a virus-coded protein with the mitochondrial matrix is not known. In this report, by using in silico analysis, we show that NS3pro alone is capable of mitochondrial import; however, this is dependent on its innate mitochondrial transport signal (MTS). Transient-transfection and protein import studies confirm the import of NS3pro to the mitochondrial matrix. Similarly, NS3pro-helicase (amino acids 1 to 464 of NS3) also targets the mitochondria. Intriguingly, reduced levels of matrix-localized GrpE protein homolog 1 (GrpEL1), a cochaperone of mitochondrial Hsp70 (mtHsp70), were noticed in NS3pro-expressing, NS3pro-helicase-expressing, and virus-infected cells. Upon the use of purified components, GrpEL1 undergoes cleavage, and the cleavage sites have been mapped to KR81A and QR92S. Importantly, GrpEL1 levels are seriously compromised in severe dengue virus-infected clinical samples. Our studies provide novel insights into the import of NS3 into host mitochondria and identify a hitherto unknown factor, GrpEL1, as a cleavage target, thereby providing new avenues for dengue virus research and the design of potential therapeutics.

**IMPORTANCE** Approximately 40% of the world's population is at risk of dengue virus infection. There is currently no specific drug or potential vaccine for these infections. Lack of complete understanding of the pathogenesis of the virus is one of the hurdles that must be overcome in developing antivirals for this virus infection. In the present study, we observed that the dengue virus-coded protease imports to the mitochondrial matrix, and our report is the first ever of a virus-coded protein, either animal or human, importing to the mitochondrial matrix. Our analysis indicates that the observed mitochondrial import is due to an inherited mitochondrial transport signal. We also show that matrix-localized GrpE protein homolog 1 (GrpEL1), a cochaperone of mitochondrial Hsp70 (mtHsp70), is also the substrate of dengue virus protease, as observed *in vitro* and *ex vivo* in virus-infected cells and dengue virus-infected clinical samples. Hence, our studies reveal an essential aspect of the pathogenesis of dengue virus infections, which may aid in developing antidengue therapeutics.

KEYWORDS dengue virus, NS3, GrpEL1, GrpEL2, mtHsp70, mitochondria

Citation Gandikota C, Mohammed F, Gandhi L, Maisnam D, Mattam U, Rathore D, Chatterjee A, Mallick K, Billoria A, Prasad VSV, Sepuri NBV, Venkataramana M. 2020. Mitochondrial import of dengue virus NS3 protease and cleavage of GrpEL1, a cochaperone of mitochondrial Hsp70. J Virol 94:e01178-20. https://doi.org/10.1128/JVI.01178-20.

**Editor** Susana López, Instituto de Biotecnologia/UNAM

**Copyright** © 2020 American Society for Microbiology. All Rights Reserved.

Address correspondence to Naresh Babu Venkata Sepuri, nareshuohyd@gmail.com, or Musturi Venkataramana, mvrsl@uohyd.ernet.in.

Received 12 June 2020 Accepted 13 June 2020

Accepted manuscript posted online 24 June 2020

Published 17 August 2020

<sup>&</sup>lt;sup>a</sup>Department of Biotechnology and Bioinformatics, School of Life Sciences, University of Hyderabad, Hyderabad, Telangana, India

Department of Biochemistry, School of Life Sciences, University of Hyderabad, Hyderabad, Telangana, India

<sup>&</sup>lt;sup>c</sup>Lotus Children's Hospital, Lakdikapul, Hyderabad, Telangana, India

# Unraveling the role of Mxr2 in regulating CVT pathway and nonselective macro-autophagy pathway in Saccharomyces cerevisiae

by Arpan Chatterjee

**Submission date:** 10-Sep-2024 12:16PM (UTC+0530)

**Submission ID:** 2449893062

File name: Arpan Chatterjee.docx (7.7M)

Word count: 23985

Character count: 137899

Unraveling the role of Mxr2 in regulating CVT pathway and nonselective macro-autophagy pathway in Saccharomyces cerevisiae

ORIGINALITY REPORT

35% SIMILARITY INDEX

31%

INTERNET SOURCES

35%

PUBLICATIONS

2%

STUDENT PAPERS

#### **PRIMARY SOURCES**

Arpan Chatterjee, Naresh Babu V. Sepuri.
"Methionine sulfoxide reductase 2 regulates
Cvt autophagic pathway by altering the
stability of Atg19 and Ape1 in Saccharomyces
cerevisiae", Journal of Biological Chemistry,
2024

NARESH B SEPURI, Ph.D

Professor
Dept. of Biochemistry
School of Life Science
University of Hyderabad
Hyderabad-500 046. T.S.

2%

from his pare

Publication

www.ncbi.nlm.nih.gov

Internet Source

Amita Pal, Arun Kumar Paripati, Pallavi Deolal, Arpan Chatterjee, Pushpa Rani Prasad, Priyanka Adla, Naresh Babu V. Sepuri. "Eisosome protein Pil1 regulates mitochondrial morphology, mitophagy, and cell death in Saccharomyces cerevisiae", Journal of Biological Chemistry, 2022

<1%

4

Current Topics in Microbiology and Immunology, 2009.

<1%

Publication

5	salford-repository.worktribe.com  Internet Source	<1%
6	Zulin Wu, Haiqian Xu, Pei Wang, Ling Liu et al. "The entry of unclosed autophagosomes into vacuoles and its physiological relevance", PLOS Genetics, 2022 Publication	<1%
7	hdl.handle.net Internet Source	<1%
8	"Abstracts from 8th International ISSX Meeting", Drug Metabolism Reviews, 2010	<1%
9	Joseph J. Braymer, Roland Lill. "Iron-sulfur cluster biogenesis and trafficking in mitochondria", Journal of Biological Chemistry, 2017 Publication	<1%
10	journals.aai.org Internet Source	<1%
11	Submitted to King Mongkut's University of Technology Thonburi Student Paper	<1%
12	pubmed.ncbi.nlm.nih.gov Internet Source	<1%
13	Submitted to University of Hyderabad, Hyderabad	<1%

14	repositorium.sdum.uminho.pt Internet Source	<1%
15	www.unboundmedicine.com Internet Source	<1%
16	academic.oup.com Internet Source	<1%
17	etd.fcla.edu Internet Source	<1%
18	9pdf.net Internet Source	<1%
19	Herrero, E "Redox control and oxidative stress in yeast cells", BBA - General Subjects, 200811 Publication	<1%
20	journals.plos.org Internet Source	<1%
21	www.nature.com Internet Source	<1%
22	Pinto-de-Oliveira, A "Expression of HPV16 E6 oncoprotein increases resistance to several stress conditions in Saccharomyces cerevisiae", FEMS Yeast Research, 200505	<1%

ebin.pub
Internet Source

		<1%
24	"Iron-Sulfur Clusters in Chemistry and Biology", Walter de Gruyter GmbH, 2014 Publication	<1%
25	Chao-Wen Wang, Per E. Stromhaug, Emily J. Kauffman, Lois S. Weisman, Daniel J. Klionsky. "Yeast homotypic vacuole fusion requires the Ccz1–Mon1 complex during the tethering/docking stage", The Journal of Cell Biology, 2003 Publication	<1%
26	Submitted to University of Central Florida  Student Paper	<1%
27	core.ac.uk Internet Source	<1%
28	d.docksci.com Internet Source	<1%
29	www.frontiersin.org Internet Source	<1%
30	Jae-Hwan Lim, Katherine L West, Yaffa Rubinstein, Michael Bergel, Vuri V Postnikov	<1%

Jae-Hwan Lim, Katherine L West, Yaffa Rubinstein, Michael Bergel, Yuri V Postnikov, Michael Bustin. "Chromosomal protein HMGN1 enhances the acetylation of lysine 14 in histone H3", The EMBO Journal, 2005 Publication 31

Kipros Gabriel. "The Mitochondrial Machinery for Import of Precursor Proteins", Methods in Molecular Biology™, 2007

<1%

Publication

32

Priya Chaudhary, Pracheta Janmeda, Anca Oana Docea, Balakyz Yeskaliyeva et al. "Oxidative stress, free radicals and antioxidants: potential crosstalk in the pathophysiology of human diseases", Frontiers in Chemistry, 2023

<1%

**Publication** 

33

d-scholarship.pitt.edu

Internet Source

<1%

Exclude quotes On Exclude bibliography On

Exclude matches

< 14 words

Date of Registration: 04/08/2017 : 03/08/2025 Date of Expiry

#### UNIVERSITY OF HYDERABAD SCHOOL OF LIFE SCIENCES DEPARTMENT OF BIOCHEMISTRY

### PROFORMA FOR SUBMISSION OF THESIS/DISSERTATION

1. Name of the Candidate : ARPAN CHATTERTEE.

2. Roll No. : 17LBPH09

3. Year of Registration : 2017

UNRAVELING THE ROLE OF MXR2 IN REGULATING CVT PATHWAY AND NON-SELECTIVE MACRO-4. Topic

AUTOPHAGY PATHWAY IN SACCHAROMYCES CEREVISIA

5. Supervisor(s) and affiliations : PROF. NARESH BABUV, SEPURI, PROFESSOR

6. Whether extension/re-registration granted: (Specify below)

: 12/09/2024 7. Date of submission

Last class attended on (M.Phil/Pre-Ph.D): 20/66/2023 8.

Whether tuition fee for the current period Paid: Receipt No. & Dt: 220012305,30/6/2023 9.

Whether thesis submission fee paid: Receipt No & Dt: 07HPC 228679, 02/08/2024 10.

11. Whether hostel dues cleared : Receipt No & Dt: 240803192582621 03/08/2024

Whether a summary of the dissertation enclosed: YES 12.

Supervisor(s)

Signature:

Dept. of Biochemistry School of Life Science School of Life Scienced School of Hyderabad University of Hyderabad University of Hyderabad 500 046. T.S. संकाय अध्यक्ष / Dean

जीव विज्ञान संस्थाय (Sedoon of Life Sciences

हैदराबाद / Hyderabad-500 046.

S, v. Naum Signature of the Head of the

Department.

जीवरसायनविभाग / Department of Biochemistry जीवविज्ञान राज्य / School of Life Sciences दैवराबाद विश्वार असम् / University of Hyderabad

हैदराबाद / Hyderabad-500046. INDIA



# **DEBIT\_CARD**

#### FINANCE OFFICER UNIVERSITY OF HYDERABAD



invoice Customer was successful.

#### **Payment Details**

#### **Payer Details**

Pgamount	1200	Reference No	240803154934003
ictStCess	0	Submerchant Id	240803154934003
Late Fee	0	Application Number	17LBPH09
Early Fee	0	Name	ARPAN
Convenience Fee	0.00		CHATTERJEE
GST	0	Ps	PD
		Ss	ВС
		Paymenthead	P1102007
		Mobilenumber	8697607952

Contact Us

ibcmsdesk@icicibank.com

Please check the status of the payment by login to

https://www.eazypay.icicibank.com/Transaction Status/